

**Sun-1, a regulator of the nuclear shape in
*Dictyostelium discoideum***

INAUGURAL-DISSERTATION

Zur Erlangung des Doktorgrades der
mathematisch-naturwissenschaftlichen
Fakultät der Universität zu Köln



Vorgelegt von

Huajiang Xiong

aus Chang Chun, V.R. China

Köln, Februar 2007

This research work was carried out under the supervision of Prof. Dr. Angelika A. Noegel from April 2004 to December 2006, in the Institute for Biochemistry I, Medical Faculty, University of Cologne, Cologne, Germany.

Diese Arbeit wurde unter der Anleitung von Frau Prof. Dr. Angelika A. Noegel vom April 2004 bis Dezember 2006 im Institut für Biochemie I der Medizinischen Fakultät der Universität zu Köln, angefertigt.

Referees/Berichterstatter: Prof. Dr. Angelika A. Noegel
Prof. Dr. Siegfried Roth

Oral examination expected/

Mündliche Prüfung

vorraussichtlich: 24. April 2007

Danksagungen

Ich möchte mich ganz herzlichst bei Frau Prof. Dr. Noegel bedanken, daß sie mich in ihre Gruppe aufgenommen und mir die wunderbare Gelegenheit gegeben hat, an diesem spannenden Projekt zu arbeiten. Dank ihrem herausragenden Wissen und ihrer Unterstützung auf allen Gebieten wurde diese Arbeit so vielfältig gestaltet.

Ich danke den Herren Prof. Dr. Siegfried Roth und Prof. Dr. Jens Brüning für die freundliche Übernahme der jeweiligen Koreferate, außerdem der „International Graduate School for Genetics and Functional Genomics“ für die finanzielle Unterstützung und wissenschaftliche Förderungskurse.

Besonderer Dank gilt Dr. Francisco Rivero für die Hilfe bei allen Mikroskopieproblemen, die Bereitstellung der interaptin-Stämme, Schokolade, Süßigkeiten und Knaller in jeglichen Versteckmöglichkeiten...Du bist der Knaller.

Herzlichen Dank an das Labor 14, das Labor mit den Golden Girls, Anne (Tanz mir den Dicty!), Mary (Sushi?), Monika, Rosi (Falcon-Sekt hat Stil und Du solltest Klaus öfters mitbringen!), Julia, Tanja (schön mit dir die Bench zu teilen), Surayya und the best Indian dancer/dressman/white collar Subhanjan and the karaoke master, and Vivek (do more of the Oooouhs, good to have you guys in the lab, you are the balance for all the estrogens!).

Ich danke alle Mitarbeiter der Biochemie I, Wenshu (my favourite batch mate), Georgia (meine „Nachbarin“, ich drücke Dich so gern), Jianbo, Rui, Ludwig, Yvonne, Verena, Sascha, Akis, Ria, Martina, Jessica, Kristina, Eva-Maria, Rolf, Charles, Christoph, Christian, Maria, Dörte, Budi, Gudrun, Berthold, Claudia, Bärbel, Brigitte, Sonya, Oliver und Chrisitina, sowie Ursula Euteneuer für die herrlichen EM Aufnahmen und Annette Vogel für ihre Hilfe

Ein liebevoller Dank gilt meinen Eltern und Großeltern, die mich immer gefördert und unterstützt haben. Ich hoffe, die Arbeit gefällt Euch!

Für meine Eltern

Table of contents

1	Introduction	1
1.1	Organization of the nuclear envelope	1
1.2	Nuclear positioning	2
1.2.1	KASH domain proteins in the ONM	2
1.2.2	SUN domain proteins in the INM	7
1.3	The model system <i>Dictyostelium discoideum</i>	12
1.3.1	Aim of the study	13
2	Material and Methods.....	14
2.1	Materials.....	14
2.1.1	Kits	14
2.1.2	Enzymes, antibodies and antibiotics	14
2.2	Media and buffers	16
2.2.1	Media and buffers for <i>Dictyostelium</i> culture	16
2.2.2	Media for <i>Escherichia coli</i> culture	16
2.2.3	Buffers	16
2.2.4	Biological materials	17
2.2.5	Plasmids and constructs	17
2.2.6	Oligonucleotides	18
2.3	Methods	19
2.3.1	Generation of cDNA	19
2.3.2	Plasmid DNA and total RNA isolation	19
2.3.3	Constructs	19
2.4	Biochemical methods.....	20
2.4.1	Preparation of total lysates and intact nuclei	20
2.4.2	Gel electrophoresis and immunoblotting	21
2.4.3	Proteinase K protection assay	21
2.4.4	Chromatin immunoprecipitation (ChIP)	22
2.4.5	Preparation of GST fusion proteins	22
2.4.6	GST pull-down assay	23
2.4.7	<i>In vitro</i> cross-linking experiment	23
2.4.8	Indirect immunofluorescence microscopy	23
2.4.9	Electron microscopy	24
2.4.10	Metaphase arrest of cell division	24
2.5	Growth and development of <i>D. discoideum</i>	25
3	Results	26
3.1	SUN domain proteins in <i>Dictyostelium</i>	26
3.1.1	Sun-1 and Sun-2 in <i>Dictyostelium</i>	26
3.1.2	Domain architecture of Sun-1 and Sun-2	26
3.1.3	Multiple alignment of the SUN domains	29
3.2	Generation of Sun-1 monoclonal antibodies.....	30
3.3	Biochemical properties of Sun-1	34
3.3.1	Sun-1 is restricted to the nucleus	34
3.3.2	Sun-1 is an integral membrane protein	36
3.3.3	Sun-1 oligomerizes via the coiled-coil domains	37
3.3.4	Sun-1 may form dimers and trimers <i>in vivo</i>	40
3.3.5	Sun-1 is a type II transmembrane protein	42
3.3.6	Sun-1 associates with chromatin	44
3.4	Sun-1 and the KASH domain protein interaptin.....	46
3.4.1	The KASH domain protein homolog interaptin	46
3.4.2	Expression profile of Sun-1 and interaptin	49
3.4.3	Localization of Sun-1 and interaptin	50
3.4.4	The KASH motif of interaptin is required for nuclear membrane targeting	53
3.4.5	The KASH motif of interaptin competes with Sun-1 for the nuclear membrane localization	55
3.5	N-terminal truncation of Sun-1	57
3.5.1	Expression of GFP- Δ NSun-1 deforms the nucleus	57
3.5.2	GFP- Δ NSun-1 causes aneuploidy	58
3.5.3	GFP- Δ NSun-1 accumulated at the ONM	61

3.5.4 GFP- Δ NSun-1 cells formed protrusion to the centrosome	65
3.5.5 GFP- Δ NSun-1 disconnected the nucleus from centrosomes	67
3.5.6 GFP- Δ NSun-1 deformed the nucleus during intracellular movement	72
4 Disussion	75
4.1 SUN domain proteins in <i>D. discoideum</i>	75
4.2 Subcellular localization of Sun-1	77
4.3 Sun-1 forms dimers and trimers <i>in vitro</i>	78
4.4 Sun-1 is a type II nuclear envelope protein and associated with chromatin	80
4.5 Sun-1 and interaptin compete for the nuclear membrane localization	82
4.6 The N-terminus of Sun-1 confers INM localization	85
4.6.1 GFP- Δ NSun-1 affects the nuclear shape	86
4.6.2 GFP- Δ NSun-1 causes centrosome amplification	88
4.7 Proposed model for the function of Sun-1 in <i>D. discoideum</i>	91
5 Summary	93
6 Zusammenfassung	94
7 References	95
8 Table of figures	100
9 Appendix	I
General abbreviations	I
Eidesstattliche Erklärung	III
Curriculum vitae	IV
Lebenslauf	V



1 Introduction

1.1 Organization of the nuclear envelope

In eukaryotic cells, the interphase nucleus is surrounded by the nuclear envelope (NE) that functions as a barrier separating the nuclear and the cytoplasmic compartment. The NE is a highly specialized membrane system composed of the morphologically distinct outer and inner nuclear membrane (ONM, INM), the nuclear pore complexes (NPCs) and the nuclear lamina (Figure 1A). The ONM is contiguous with the rough endoplasmic reticulum that is decorated with ribosomes (Franke et al., 1981; Gerace and Burke, 1988; Newport and Forbes, 1987; Watson, 1955) and joins the INM at the sites of the nuclear pore membrane within the NPCs (Figure 1B). Further, the INM is supported by the nuclear lamina, a dense network consisting of the intermediate filaments lamins and lamin-associated proteins which confers mechanical stability to the nucleus and provides an anchor for integral proteins of the INM (Gruenbaum et al., 2005; Holmer and Worman, 2001).

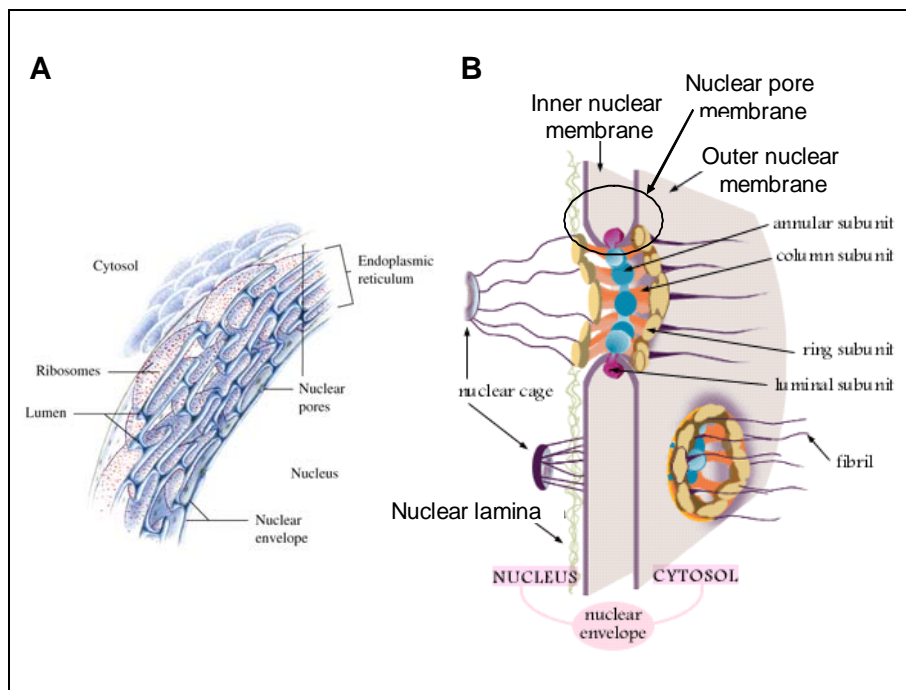


Figure 1: Composition of the nuclear envelope in eukaryotic cells. A. The nuclear envelope is a system of nuclear membranes continuous with the rough endoplasmic reticulum. B.



The inner nuclear envelope is supported by the nuclear lamina and joins the outer nuclear membrane at the sites of the nuclear pore complex (Horton et al., 2002).

1.2 Nuclear positioning

The well-defined position of the nucleus within a cell is essential for many processes such as mitosis, meiosis, fertilization as well as cell migration, differentiation and polarization which represent the repertoire of all eukaryotic cells (Morris, 2000). However, nuclear positioning and migration requires a concerted action of the cytoskeleton that includes the actin filaments (F-actin), microtubules (MTs) and intermediate filaments (IFs), to which the nucleus must be connected. In recent years, two conserved nuclear envelope protein families, the KASH domain proteins and the SUN domain proteins have been described as molecular linkers connecting the nuclear envelope and the cytoskeleton.

1.2.1 KASH domain proteins in the ONM

Although the ONM is contiguous with the tubular system of the rER and allows integral proteins to diffuse to both membranes (Ellenberg et al., 1997; Lippincott-Schwartz et al., 2000), they possess distinct protein compositions. A new protein family termed the KASH domain proteins is mainly localized in the ONM and has been proposed to connect the nucleus to the different cytoskeletal elements. These proteins can be divided into three groups based on their interaction with (1) F-actin: Anc-1 of *Caenorhabditis elegans* (Hedgecock and Thomson, 1982; Starr and Han, 2002), Msp-300/Nesprin in *Drosophila melanogaster* (Rosenberg-Hasson et al., 1996; Volk, 1992; Zhang et al., 2002), as well as Nesprin-1 and 2 (synonym Syne, Myne, Enaptin and NUANCE) in mammals (Apel et al., 2000; Padmakumar et al., 2005; Zhang et al., 2001; Zhen et al., 2002); (2) IFs: Nesprin-3 in mammals (Wilhelmsen et al., 2005); (3) centrosome and/or MTs: Zyg-12 (Fridkin et al.,



2004; Malone et al., 2003) and UNC-83 in worms (Malone et al., 1999; Reinsch and Gonczy, 1998) and Klarsicht in flies (Fischer-Vize and Mosley, 1994; Patterson et al., 2004).

All KASH domain proteins reported so far possess a highly conserved C-terminal region referred to as the Klarsicht/Anc-1/Syne-1 homology (KASH) domain harboring a single transmembrane domain and a short tail sequence of approximately 35 amino acids (Starr and Han, 2005; Wilhelmsen et al., 2006). Regardless of the KASH domain, the three groups of KASH domain proteins differ in their N-terminal domain organization that is specialized for the connection to the different cytoskeletal components (Figure 2).

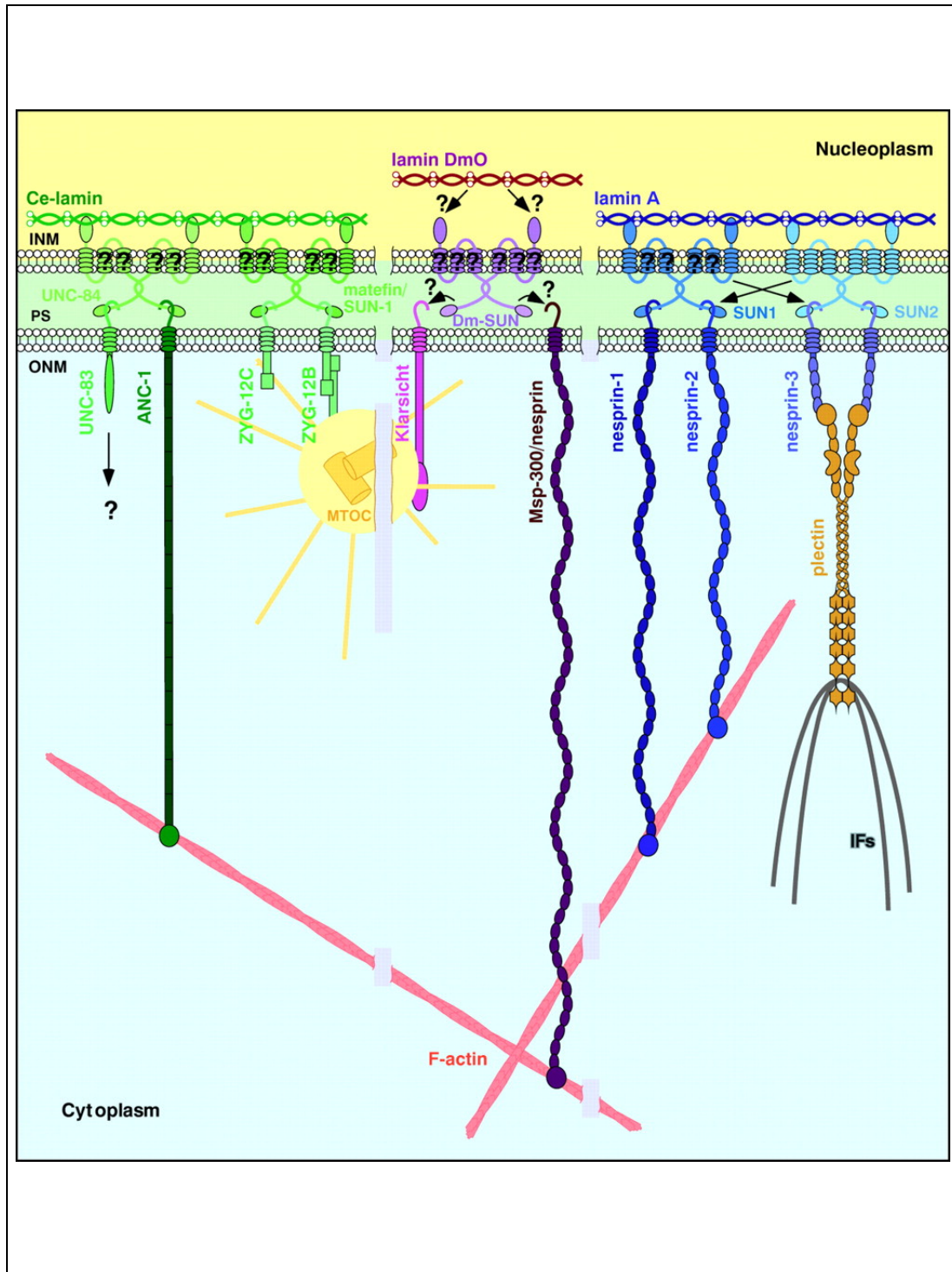


Figure 2: Proposed model for nuclear positioning and migration. SUN domain proteins, e.g. UNC-84, reside in the inner nuclear membrane (INM) by interaction with the nuclear lamina or lamin-binding proteins. The SUN domain of UNC-84 binds directly to the KASH domain proteins (UNC-83- or Nesprin-related protein), which are retained specifically in the outer nuclear membrane (ONM). UNC-83-related proteins connect the nucleus to microtubules, whereas Nesprin-related proteins link the nucleus to actin filaments (Wilhelmsen et al., 2006).



1.2.1.1 Nuclear positioning on F-actin and IFs

The F-actin binding KASH domain proteins contain two N-terminally located calponin-homology (CH) domains followed by a central stretch of spectrin-like repeats and the KASH domain, giving rise to the giant molecules of up to 1 MDa. Anc-1 is unique as it harbors six interspersed coiled-coil repeats in its elongated domain. Worms, carrying mutated *anc-1* (nuclear anchorage defective, expressed as a 950 kDa protein) failed to position the nuclei and mitochondria correctly and the nuclei floated freely in the cytoplasm (Hedgecock and Thomson, 1982; Starr and Han, 2002).

In agreement, flies generated with the germ-line specific *msp-300*^{SZ-75} allele for a mutated 300 kDa muscle-specific protein were observed with defective nuclear positioning during oogenesis (Yu et al., 2006). Moreover, binding of Msp-300/Nesprin to F-actin *in vivo* is essential for myogenesis in *Drosophila* embryos, as the lethal *msp-300*^{SZ-75} mutation caused defects in myotube migration, attachment and contraction (Rosenberg-Hasson et al., 1996; Volk, 1992).

In mammals, Nesprin-1 and 2 occur as diverse isoforms generated by alternative splicing, transcription initiation and termination of the genes *syne-1* and *syne-2* (Warren et al., 2005), whereas the giant Nesprin-1 and Nesprin-2 isoforms Enaptin and NUANCE (976 and 764 kDa) encompass completely the CH domains and the KASH domain and can potentially reach out 500 nm from the nuclear envelope into the cytoplasm (Starr and Han, 2005). Similar to Msp-300/Nesprin in flies, Nesprin-1 (Myne-1) was first found to position the postsynaptic nuclei at neuromuscular junctions and within myocytes, but is also expressed in other cell types (Apel et al., 2000; Mislow et al., 2002; Padmakumar et al., 2005; Zhang et al., 2001; Zhen et al., 2002). Nevertheless, Nesprin-1 may have other functions despite of nuclear positioning, e.g. when overexpressed in epithelial cells it acted as a dominant-negative inhibitor for the morphology of the Golgi apparatus that collapsed into a condensed structure near the centrosome (Gough et al., 2003).

Additionally, the mammalian Nesprin-3, a protein of 110 kDa, lacking a calponin homology domain interacts with plectin a protein that in turn is capable



to cross-link cytoplasmic intermediate filaments and F-actin as it also harbors an F-actin binding domain. This indicates that the small Nesprin isoform can also contribute to nuclear positioning (Wilhelmsen et al., 2005).

1.2.1.2 Nuclear positioning on centrosome and microtubules

Evidently, positioning and migration using F-actin and IFs may be assisted by the additional connection of the nucleus to the centrosomes and microtubules, a property attributed to the second group of KASH domain proteins including Zyg-12 and UNC-83 in *C. elegans* and Klarsicht in *D. melanogaster*.

In detail, worm embryos with the *zygote defective* (*zyg-12*) genetic background die owing to chromosome segregation defects caused by the nucleus-centrosome detachment (Malone et al., 2003). Notably, Zyg-12 binds to dynein and is a member of the Hook protein family that has been suggested to link membrane compartments and microtubules (Walenta et al., 2001). However, of the three Zyg-12 isoforms (A, B and C) derived from alternative splicing of a single gene the isoforms B and C are localized at the ONM, whereas A lacking a KASH domain is associated with the centrosome. In the proposed two-step model, all Zyg-12 isoforms migrate on microtubules in a dynein-dependent manner, but Zyg-12B and C are localized at the nuclear envelope and Zyg-12A is attached to the centrosome. Once the nucleus and centrosome are located in close proximity the connection is provided by heterodimerization of Zyg-12B and/or C with Zyg-12A (Malone et al., 2003).

Comparable to Zyg-12, Klarsicht of *D. melanogaster* participates in nuclear migration from the basal compartment to the apex of the imaginal disc during the compound eye development by attachment of the nucleus to the centrosome and microtubules (Fischer et al., 2004; Fischer-Vize and Mosley, 1994; Patterson et al., 2004). Distinctly different from Zyg-12, *Drosophila* embryos bearing a null mutation in the gene *klarsicht* are viable and fertile regardless of the misshapen photoreceptors.



UNC-83 is essential for the nuclear migration in certain tissues during embryonic development of the worm, such as the hypodermal cells and the intestine. Interestingly, though mutations in the *unc-83* gene abrogated nuclear migration, the nucleus-centrosome connection was not disrupted hinting at a putative function of UNC-83 in nuclear migration along microtubules, but not essential for the connection to centrosomes yet to be uncovered (Lee et al., 2002; Starr et al., 2001; Sulston and Horvitz, 1981). In summary, KASH domain proteins of the ONM engage in interactions with different cytoskeletal elements to allow the processes nuclear positioning and migration and are thus essential both for the embryonic development and the organization of the cytoplasm.

1.2.2 SUN domain proteins in the INM

As the integral proteins can diffuse laterally throughout the rER and the ONM, specific mechanisms are required to retain distinct proteins at the ONM. Studies on the KASH domain proteins revealed that they are recruited to the ONM by the SUN domain proteins, a new INM protein family.

The first SUN domain protein UNC-84 was identified in *C. elegans*. Mutants exhibiting an uncoordinated movement due to the defects in nuclear positioning and migration resulted from alterations in the gene *unc-84* (Horvitz and Sulston, 1980; Malone et al., 1999; Sulston and Horvitz, 1981). Interestingly, the phenotype of the *unc-84* mutation resembles that of the *unc-83* worms indicating that both proteins are involved in a common mechanism (Starr et al., 2001). The N-terminal domain of UNC-84 containing several putative transmembrane domains does not show sequence or domain similarities with any known proteins whereas a C-terminal region of approximately 120 amino acids shares a significant homology with the C-terminus of the spindle pole body protein Sad1 in *Schizosaccharomyces pombe* (Hagan and Yanagida, 1995). Therefore it was designated as the Sad1/UNC-84 (SUN) domain (Malone et al., 1999; McGee et al., 2006). As illustrated in Figure 3, further database searches discovered two SUN domain



proteins in *D. melanogaster* and *D. discoideum* (termed *Dd Sun-1* and *Dd Sun-2*) and four in mammals (Crisp et al., 2006; Dreger et al., 2001; Hasan et al., 2006; Jaspersen et al., 2006; Malone et al., 1999; Padmakumar et al., 2005). The presence of SUN domain proteins across many species and their propensities to interact with KASH domain proteins indicate a conserved mechanism for nuclear positioning and migration.



1.2.2.1 Domain architecture of SUN domain proteins

In metazoa, SUN domain proteins interact with the nuclear lamina, whereas the conserved C-terminal SUN domain is responsible for the binding to the KASH domain proteins. Despite of these characteristics, they exhibit great variabilities in their N-terminal domain architecture that appear to contain functionally related domains. In general, most of these proteins possess at least one transmembrane domain, e.g Sad1 and human Sun-3 (Crisp et al., 2006; Hagan and Yanagida, 1995), whereas some may have multiple transmembrane domains as nine hydrophobic domains were predicted for UNC-84 and three for human Sun-1 (Malone et al., 1999; McGee et al., 2006; Padmakumar et al., 2005). Extraordinarily, none of the two uncharacterized SUN domain proteins in *D. melanogaster* possess a transmembrane domain. A further feature of the SUN domain proteins is the presence of at least one coiled-coil domain that may promote dimerization or oligomerization (Crisp et al., 2006).

1.2.2.2 INM targeting of SUN domain proteins

In general, integral proteins of the INM are translated on the rER and diffuse along the ONM to the INM by passing the highly curved nuclear pore membrane of the NPCs which occurs in an ATP-dependent and temperature-sensitive manner (Ohba et al., 2004; Soullam and Worman, 1993; Soullam and Worman, 1995). According to the "Diffusion-Retention" model implying that INM proteins may be trapped in there by interaction with lamins or chromatin-binding proteins or both (Ellenberg et al., 1997; Ohba et al., 2004; Ostlund et al., 1999; Smith and Blobel, 1993; Worman and Courvalin, 2000), SUN domain proteins may be targeted to the INM and retained there by interaction with lamins, as *C. elegans* UNC-84 and matefin/Sun-1, mammalian Sun-1 and Sun-2 colocalize with lamins (Crisp et al., 2006; Fridkin et al., 2004; Hodzic et al., 2004; Lee et al., 2002; Padmakumar et al., 2005). Interestingly, the N-termini of matefin/Sun-1 and mammalian Sun-1 and Sun-2 bind to lamins *in vitro*, but this interaction is not essential *in vivo* since they localized to the INM in the



absence of lamins (Crisp et al., 2006; Fridkin et al., 2004; Haque et al., 2006; Hasan et al., 2006; Padmakumar et al., 2005). On the contrary, though UNC-84 does not bind to lamin, it is localized to the INM in a lamin-dependent fashion (Lee et al., 2002) suggesting that an alternate mechanism for INM retention may exist.

1.2.2.3 Interaction of the SUN with the KASH domain proteins

In the nuclear envelope, the SUN and the KASH domain proteins interact with each other by projection of their C-termini into the perinuclear space, connecting the nucleoskeleton with the cytoskeleton (Figure 2). The combination of the SUN domain proteins with various KASH domain proteins gives rise to a great repertoire linking the nucleus simultaneously to different cytoskeletal elements: (1) combinations of UNC-84 with Anc-1 or UNC-83 provide nuclear positioning on F-actin or migration along MTs (Lee et al., 2002; Starr and Han, 2002; Starr et al., 2001); (2) interaction of mammalian Sun-1 and Sun-2 with Nesprin-1/Nesprin-2 or Nesprin-3 contribute to the nuclear positioning on F-actin or lfs (Crisp et al., 2006; Haque et al., 2006; Padmakumar et al., 2005; Wilhelmsen et al., 2005); (3) the complex formed by matefin/Sun-1 and Zyg-12 is capable to transport the nucleus on MTs towards the centrosome and maintain their proximity (Fridkin et al., 2004; Malone et al., 2003). Likewise, interaction of Sad1 with Kms1, which is a KASH domain protein in *S. pombe*, is required for the localization of Sad1 at the spindle pole body, the centrosome equivalent of yeast (Niwa et al., 2000).

Based on their location and their interactions SUN domain proteins as linker proteins in the INM may transduce mechanical signals originating in the cytoplasm to the nucleus that responds with biochemical processes. Despite of the important role of the SUN domain proteins in nuclear positioning and migration, non-mechanical roles such as influencing the fat metabolism, germline cell proliferation/maintenance and telomere clustering has become evident (Fridkin et al., 2004; Greer and Brunet, 2005; Niwa et al., 2000).

1.3 The model system *Dictyostelium discoideum*

Dictyostelium discoideum is a haploid eukaryote with a simple but fast and well-defined life-cycle which facilitates genetic, biochemical and cell biological studies. The social amoebae feed on bacteria, and live as single cells that develop into multicellular organisms in response to starvation. During the development, cells migrate chemotactically following a central cAMP source to form aggregates (slugs) that induce the expression of cell-cell adhesion molecules establishing the mound structures. The mounds differentiate into the terminal fruiting bodies composed of a head filled with spores supported by a stalk of vacuolated cells (Figure 4).

D. discoideum shares several features with mammalian cells, thus it is a well-accepted model to study many processes such as chemotaxis, cell-cell adhesion and morphogenesis. As nuclear positioning and migration is important for the development of various tissues in worm, fly and mammals, we set out to examine the new field of nuclear envelope proteins in *D. discoideum*.

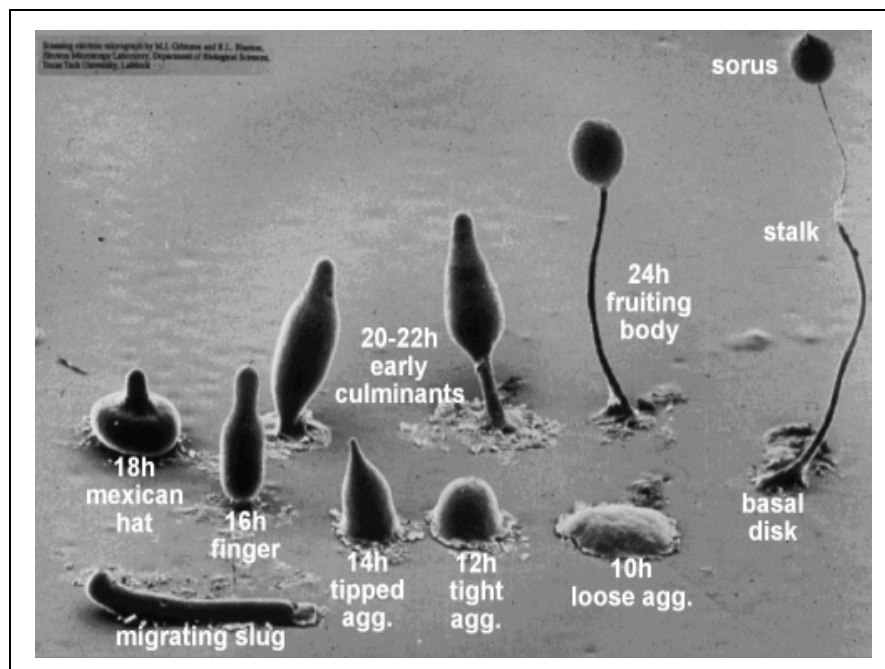


Figure 4: Development of *D. discoideum* from single-cell amoeba into the multicellular fruiting bodies (courtesy of M. Grimson, R. Blanton, Texas Tech University).



1.3.1 Aim of the study

To date, the organization and function of the nuclear envelope is not understood in *D. discoideum*, this challenged us to shed light onto these aspects. The first nuclear envelope protein described so far, interaptin (Rivero et al., 1998), may function as a KASH domain protein as suggested by the findings in higher eukaryotes.

The prediction of two SUN domain proteins (Sun-1 and Sun-2) in the *D. discoideum* proteom prompted us to investigate the function of the SUN domain proteins using biochemical and cell biological approaches. In this study, we focus on the proteins Sun-1 and interaptin. Particularly, we are interested in (1) whether Sun-1 is targeted to the inner nuclear membrane in the absence of lamins, as reported for other SUN domain proteins; (2) whether Sun-1 interacts with interaptin in a manner similar to mammalian SUN domain proteins and the Nesprins to connect the nucleus to the elements of the cytoskeleton; (3) whether these proteins have evolved other functions in the ameba.



2 Material and Methods

2.1 Materials

Standard laboratory reagents and materials were obtained from local suppliers, fine chemicals from Sigma if not otherwise indicated and instruments were supplied by the Departmental facility.

2.1.1 Kits

Nucleobond AX 100	Macherey Nagel
NucleoSpin Extraction Kit	Macherey Nagel
Qiagen RNeasy Mini Kit	Qiagen
pGEM-T easy Cloning Kit	Promega

2.1.2 Enzymes, antibodies and antibiotics

2.1.2.1 Enzymes for molecular biology purposes

Calf intestinal alkaline phosphatase (CIP)	Roche
Klenow fragment	Roche
Lysozyme	Sigma
M-MLV reverse transcriptase	Promega
Proteinase K	Merck
Restriction endonucleases	New England Biolabs
Ribonuclease A (RNase A)	Sigma
Ribonuclease H (RNase H)	Boehringer
T4 DNA ligase	Invitrogen
<i>Taq</i> polymerase	Amersham Pharmacia

2.1.2.2 Primary antibodies

Mouse monoclonal anti-actin antibody (Act1-7)	(Simpson <i>et al.</i> , 1984)
Mouse monoclonal anti-GFP antibody (K3-184-2)	(Noegel <i>et al.</i> , 2004)
Rabbit polyclonal anti-GFP antibody	Gift from M. Schleicher
Rabbit polyclonal anti-GST antibody	Unpublished



Mouse monoclonal anti-interaptin antibody (260-60-10)	(Rivero <i>et al.</i> , 1998)
Mouse monoclonal anti-PDI-1 antibody (221-135-1)	(Monnat <i>et al.</i> , 1997)
Mouse monoclonal anti-Sun-1 antibody (K55-432-2), western blot analysis	This study
Mouse monoclonal anti- Sun-1 antibody (K55-460-1 and K55-450-1), immunofluorescence, (chromatin) immunoprecipitation	This study
Mouse monoclonal anti-Spermatozopsis $\alpha\beta$ - tubulin antibody (<i>D. discoideum</i> centrosome) (K29-359-31)	Gift from K. Herkner
Mouse monoclonal anti- α -tubulin antibody (6-11B1)	(Piperno and Fuller, 1985) (Generous gift from Michael Koonce)
Rat monoclonal anti- α -tubulin antibody (YL1/2)	Kilmartin et al., 1982

2.1.2.3 Secondary antibodies

Goat anti-mouse IgG, peroxidase conjugated	Sigma
Goat anti-rabbit IgG, peroxidase conjugated	Sigma
Goat anti-mouse IgG, Cy3 conjugated	Sigma
Goat anti-mouse IgG, Cy5 conjugated	Sigma
Goat anti-mouse IgG, Alexa 568 conjugated	Molecular probes
Goat anti-rat IgG, Alexa 568 conjugated	Molecular probes

2.1.2.4 Antibiotics

Ampicillin	Gruenthal
Blasticidin S	ICN Biomedicals
G418	Sigma
Dihydrostreptomycinsulfate	Sigma
Tetracyclin	Sigma



2.2 Media and buffers

All media and buffers were prepared using deionized water, filtered through an ion-exchange unit (Membra Pure). All media and buffers were sterilized by autoclaving at 120°C; the antibiotics were added to the media after cooling to approx. 50°C. Agar plates were prepared using a semi-automatic plate-pouring machine (Technomat).

2.2.1 Media and buffers for *Dictyostelium* culture

AX2 medium, pH 6.7 (Claviez <i>et al.</i> , 1982)	7.15 g yeast extract 14.3 g peptone (proteose) 18.0 g maltose 0.486 g KH_2PO_4 0.616 g $\text{Na}_2\text{HPO}_4 \times 2\text{H}_2\text{O}$ ad 1 liter H_2O
Soerensen phosphate buffer, pH 6.0 (Malchow <i>et al.</i> , 1972)	2 mM Na_2HPO_4 , 14.6 mM KH_2PO_4
Phosphate agar plates, pH 6.0	9 g agar ad 1 liter Soerensen phosphate buffer
SM agar plates, pH 6.5 (Sussman, 1951)	9 g agar 10 g peptone 10 g glucose 1 g yeast extract 1 g $\text{MgSO}_4 \times 7\text{H}_2\text{O}$ 2.2 g KH_2PO_4 1 g K_2HPO_4 ad 1 liter H_2O

2.2.2 Media for *Escherichia coli* culture

LB medium, pH 7.4 (Sambrook *et al.*, 1989)
SOC medium, pH 7.0 (Sambrook *et al.*, 1989)

2.2.3 Buffers

10x MOPS (pH 7.0 or pH 8.0)	41.9 g MOPS 7 ml 3 M sodium acetate 20 ml 0.5 M EDTA
-----------------------------	--



	ad 1 liter H ₂ O
10x NCP (pH 8.0)	12.1 g Tris/HCl, pH 8.0 87.0 NaCl 5 ml Tween 20 ad 1 liter H ₂ O
1x PBS (pH 7.4)	8.0 g NaCl 0.2 g KH ₂ PO ₄ 1.15 g Na ₂ HPO ₄ 0.2 g KCl ad 1 liter H ₂ O
20x SSC (pH 7.0)	3 M NaCl 0.3 M sodium citrate
TE buffer (pH 8.0)	10 mM Tris/HCl, pH 8.0 1 mM EDTA
10x TAE buffer (pH 8.3)	27.22 g Tris 13.6 g sodium acetate 3.72 g EDTA ad 1 liter H ₂ O

2.2.4 Biological materials

Bacterial strains

<i>E. coli</i> DH5 α	(Hanahan, 1983)
<i>E. coli</i> XL1 Blue	Bullock <i>et al.</i> , 1987
<i>Klebsiella aerogenes</i>	(Williams and Newell, 1976)

D. discoideum strains

AX2-214, an axenically growing derivative of wild strain NC-4, commonly referred to as AX2	(Wallraff <i>et al.</i> , 1986)
<i>abpD</i> ⁻ (AX2 strain carrying a disrupted locus of interaptin)	(Rivero <i>et al.</i> , 1998)
<i>abpD</i> ⁺ (AX2 strain overexpressing interaptin)	(Rivero <i>et al.</i> , 1998)
MAD-GFP (AX2 overexpressing the C-terminal region of interaptin, referred to as GFP-IntCT in this study)	(Rivero <i>et al.</i> , 1998)

2.2.5 Plasmids and constructs

pGEM-T easy	Promega
pGEX-4T2	
pGEX-4T3	Clontech
pDEX-GFP79	
pGEX-4T2-SunCT1	Amino acid 411 to 572, overlapping the coiled-coil domains located between the



	transmembrane domain and the SUN domain (cloned into pGEX4T2 using <i>Xma</i> / <i>Xho</i>)
pGEX-4T2-SunCT2	Amino acid 700 to 905, overlapping the SUN domain (cloned into pGEX4T2 using <i>Xma</i> / <i>Xho</i>)
pDEX-GFP79- Δ NSun-1	Amino acid 283 to 905 overlapping the transmembrane domain, coiled-coil domains and SUN domain (cloned into pDEX-GFP-79 using <i>Clal</i>)

2.2.6 Oligonucleotides

SunCT1

Xma-SunCT1-For	5'- <u>CCCGGG</u> GCATCATCAAACATTTTACACAATAGAT TTAGTAATAGTA
Xho-SunCT1-Rev	5'- <u>CTCGAG</u> ACTACCATAATAAAAGTTTTTCCATGGG TCTC

SunCT2

Xma-SunCT2-For	5'- <u>CCCGGG</u> GCTACAAAT TGGATATCCCACAACCA AAA
SunCT2-Xho-Rev	5'- <u>CTCGAG</u> CTCTTGAATAATTTGTATTTGTTCTTGTT CTGGAT

GFP- Δ NSun-1

Clal- Δ NSun-1-For	5'- <u>ATCGAT</u> AAAGTTAATTTTAAACAAGCTATTTGGAT TTTC
Δ NSun-1-Clal-Rev	5'- <u>ATCGAT</u> ATCGATTTATAATTCATCAGATTGTTGTT G



2.3 Methods

Standard molecular biology techniques were performed as described in "A Laboratory Manual. Cold Spring Harbor Laboratory Press, NY, Vol 1-3 (Sambrook et al., 1989).

2.3.1 Generation of cDNA

For the generation of cDNA, 1-5 μ g of total RNA was incubated with the M-MLV reverse transcriptase in each reaction as recommended in the manufacturer's protocols.

2.3.2 Plasmid DNA and total RNA isolation

Plasmid DNA from bacteria and total RNA from vegetative AX2 cells (shaking culture) were extracted using Nucleobond AX 100 and Qiagen RNeasy, respectively, following the manufacturer's instructions. The plasmid DNA was used for transfection of AX2 cells; RNA samples were used in for reverse transcription and subsequent cDNA generation.

2.3.3 Constructs

2.3.3.1 GST-SunCT1 fusion vector

The two coiled-coil domains amino acid 412 to 571 is encoded in the cDNA position 1223 to 1710 bp. A PCR fragment extending from DNA position 1220 to 1713 (overlapping amino acid 411 to 572) was generated with a 5'-*Xma*I and a 3'-*Xho*I, the fragment was cloned as into the expression vector pGEX4T2 using *Xma*I/*Xho*I. The resulting vector GST-SunCT1 was expressed in the *E. coli* strain XL1 Blue.



2.3.3.2 GST-SunCT2 fusion vector

The SUN domain spans the amino acid 712 to 859 that corresponds to the position 2133 to 2877 in the cDNA. We have cloned the downstream coding region from position 1885 to 2718 bp including both the SUN domain and the ER retention signal (amino acid 608 to 905) *Xma*I/*Xho*I into the expression vector pGEX4T2. Expression of the recombinant fusion protein GST-SunCT2 was carried out in the *E. coli* strain XL1 Blue.

2.3.3.3 GFP- Δ NSun-1 fusion construct

A DNA fragment from position 853 to 2718 bp of the encoding region, corresponding to the amino acid position 283 to 905, was cloned into the vector pDEX-GFP79 using *Cla*I. After transfection of the construct lacking the N-terminus (GFP- Δ NSun-1) into AX2 cells, positive clones were obtained by addition of G418 (0.4 μ g/ml) as a selection drug.

2.4 Biochemical methods

2.4.1 Preparation of total lysates and intact nuclei

Total cell lysates were prepared from vegetative cells or at the indicated time points. After washing twice with Soerenen buffer, cells were resuspended in TMS buffer containing:

- 50 mM Tris/HCl pH 7.4
- 100 mM NaCl
- 5 mM MgCl₂
- 250 mM Sucrose
- 1 mM EDTA
- 1 mM EGTA
- 1 mM DTT
- 1 mM Benzamidine
- 1 mM PMSF



Total cell lysates were obtained by passing through Nuclepore membrane (5 μ m diameter, Whatman) and used in further experiments. Intact nuclei were isolated from vegetative cells. Nuclei were collected after lysis through Nuclepore membrane by spinning for 5 min at 4000 *g*.

2.4.2 Gel electrophoresis and immunoblotting

Cells were resuspended and lysed in TMS buffer in a concentration of 2x10⁶/ml. Protein samples were separated on 10% polyacrylamide gels (SDS-PAGE), then either stained with Coomassie Brilliant Blue, or transferred onto nitrocellulose membranes (Schleicher and Schuell) semi-dry and wet blotting transfer systems, respectively. After electro-transfer, the membranes were blocked with 5% (w/v) milk in 1x NCP prior to the appropriate antibody detections. The primary antibodies were detected using the according peroxidase-conjugated secondary antibodies and visualized by ECL (enzyme chemiluminescence) reactions. ECL reactions on the nitrocellulose membranes were documented on X-ray films.

2.4.3 Proteinase K protection assay

Intact nuclei were isolated from AX2 cells and incubated in proteinase K protection assay buffer (10mM Tris/HCl pH7.4, 250mM sucrose, 1 μ g/ml proteinase K) without and as a positive control for the enzyme activity with 0.5(v/v)% Triton X-100 on ice. Samples were collected from both reactions after 5, 10, 30, 45 min and the activity of proteinase K was immediately stopped by adding PMSF to a final concentration of 1mM and boiling (95°C, 5 min) in SDS sample buffer. The samples were further analyzed by SDS-PAGE and western blot.



2.4.4 Chromatin immunoprecipitation (ChIP)

Vegetative AX2 cells were harvested and lysed in TMS buffer in a density of 5×10^7 cells per ChIP reaction. To reduce the viscosity of genomic DNA and disrupt the nuclear envelope, total cell lysates were sonified (10 impulses, each of the twice repeated procedure was paused for 10 sec). The appropriate mAb was coupled to protein A-beads and PBS was used as a negative control (1hr, 4°C).

The beads were washed three times with PBS then incubated with sonified total cell lysate (2hrs on a vertical rotator, 4°C). Unspecific protein and DNA bindings were removed by five times washing with PBS and once with TE buffer and divided into two aliquotes.

One aliquote of the each ChIP reaction was used for elution of DNA by adding 100 μ l of TE buffer containing 1% SDS. After Phenol/Chloroform and ethanol precipitation DNA was resuspended in 50 μ l aqua bidest, 5 μ l of this DNA was subsequently used for PCR amplification to detect the presence or absence of coprecipitated DNA. To the second aliquote 20 μ l SDS sample buffer was added and subjected to SDS-PAGE and western blotting.

2.4.5 Preparation of GST fusion proteins

Recombinant GST-u84CT1 expression was induced in *E. coli* strain XL1-Blue by 0.3 mM IPTG for 5h at room temperature. Cells were harvested by centrifugation at 5000 g, 4°C for 15 min (Beckman) and resuspended in TM buffer (TMS without sucrose). After sonification the soluble fraction of the bacterial lysate was obtained by centrifugation at 13000 g, 4°C for 30 min. The GST-u84CT1 was isolated from the supernatant by incubating with glutathione agarose beads (4°C, 16 h). Glutathione agarose beads coupled with GST-u84CT1 was washed five times with PBS (500 g, 4°C, 10 min) before performing thrombin cleavage (4°C, 16 h) or incubating with AX2 total cell lysate.



2.4.6 GST pull-down assay

Total cell lysate of AX2 was prepared as described above. Glutathione agarose beads coupled with GST-SunCT1 (see above) were incubated with total cell lysate at 4°C for 5 h. The beads were washed three times with PBS (500 μ l, 4°C, 1min) and boiled in SDS sample buffer (95°C, 5 min). Samples were analyzed using 10% SDS polyacrylamide gels and stained with Coomassie Brilliant Blue. Protein bands of interest, when indicated, were excised from gels and subjected to peptide sequencing by MALDI.

2.4.7 *In vitro* cross-linking experiment

To address protein-protein interaction, the GST tag of the recombinant fusion proteins was removed by thrombin cleavage. 10 μ g of the protein of interest was incubated in the phosphate potassium buffer (pH7.4) containing 0.001(v/v)% glutaraldehyde at room temperature, samples were taken at the time points 5, 10 and 20 min. The reaction was stopped by quenching the cross-linker glutaraldehyde with glycine (added to a final concentration of 0.1M). All samples were subsequently investigated by SDS-PAGE and western blotting.

2.4.8 Indirect immunofluorescence microscopy

Approximately 1×10^6 cells were transferred onto each coverslip (10mm diameter) and allowed to adhere to the surface for 20 min at room temperature.

- Pre-incubation buffer: 1x PBS containing 25mM glycine
- Blocking solution: 1x PBS containing 0.5 (w/v)% BSA and 0.1 (v/v)% fish gelatine

If not mentioned otherwise, standard immunofluorescence stainings were carried out using ice-cold methanol as fixative (5 min, -20 °C) prior to incubation with the pre-incubation buffer (three times, 5 min, room temperature) and blocking solution (two times, 15 min, room temperature). The appropriate antibodies were diluted in the blocking solution to the



working concentration and applied for 1hr at room temperature; the excess of antibodies was removed by washing with the blocking solution prior to the 1hr of incubation with the according secondary antibodies. Nuclear DNA was stained with 4'-6-diamidino-2-phenylindole (DAPI) or ToPro-3 (Invitrogen).

For sequential digitonin/Triton X-100 permeabilization experiments, cells adhered on the coverslips were fixed by application of 4% (w/v) paraformaldehyde for 20 min. After three times washing with PBS, cells were first permeabilized by short incubation with prechilled 10 μ g/ml digitonin solution in PBS (5 min, on ice) and washed five times with PBS. Blocking reaction and incubation with the primary antibodies was performed as described above. After removal of excess of the primary antibodies (six washes with PBS), cells were permeabilized by application of 0.2% Triton X-100 in PBS (10 min, room temperature). The permeabilized nuclear envelope was blocked before probing with the second epitope-specific antibodies. The two specific primary antibodies were finally visualized by simultaneous incubation of the according secondary antibodies.

Confocal images were acquired with an inverted Leica LSM 410 laser-scanning microscope using 40x and 100x Neofluar oil immersion objectives.

2.4.9 Electron microscopy

Intact nuclei were isolated GFP- Δ NSun-1 cells following the procedure described above and fixed with 4% (w/v) formaldehyde prior to blocking and immunogold labeling using polyclonal rabbit anti-GFP antibodies for subsequent electron microscopy studies.

2.4.10 Metaphase arrest of cell division

Cells were placed on a culture dish covered with coverslips and allowed to attach to that for 2hrs before adding nocodazole to a final concentration of 33 μ m in the media. The incubation with nocodazole was maintained for 4hrs at room temperature that increased cells arrested in the metaphase of mitosis. Chromosome structures were then fixed on the



coverslips in ethanol/acetic acid (volume ratio 3/1) for 1hr on ice, followed by a change of fresh chromosome fixative for an additional 10 min on ice, before proceeding with DAPI staining.

2.5 Growth and development of *D. discoideum*

The strain AX2 was either grown in liquid media at 22°C and shaking at 160 rpm or on SM agar plates along with *Klebsiella aerogenes*. To allow development, AX2 cells grown to the density of 2×10^6 to 3×10^6 /ml and washed twice with Soerensen phosphate buffer (500 g, 4°C, 2 min). 1×10^8 cells were spread on one phosphate agar plate and incubated at 22°C during development.



3 Results

3.1 SUN domain proteins in *Dictyostelium*

3.1.1 Sun-1 and Sun-2 in *Dictyostelium*

In *D. discoideum*, two SUN domain proteins, Sun-1 (dictybase accession code DDB0219949) and Sun-2 (DDB0186751), are predicted in the database, each encoded by a single-copy gene in the genome.

The gene *sun-1* is located on chromosome 2 at the coordinates 2044015 to 2046802 overlapping 2788 bp of the Crick strand. The genomic locus of *sun-1* consists of two exons, the first spans 1075 bp which is intercalated by an intron of 69 bp from the second exon initiating from position 1146 encoding for a mRNA of 2718 bp, accordingly a protein of 905 amino acids.

The gene *sun-2* is located on chromosome 4 spanning the genomic coordinates 3835569 to 3839405 on the Watson strand and does not contain introns, resulting in a coding region of 3837 bp and a protein of 1278 amino acids.

3.1.2 Domain architecture of Sun-1 and Sun-2

In *D. discoideum*, Sun-1 comprises 905 amino acids giving rise to a protein of 105 kDa. Analysis of the domain structure using the program SMART revealed an N-terminal coiled-coil domain (amino acids 170 to 221), a single transmembrane domain (amino acids 291 to 313), followed by a pair of coiled-coil domains (amino acids 412 to 457 and 507 to 571). Additional analysis of the primary protein sequence with the program InterProScan revealed a C-terminal SUN domain (amino acid 712 to 859), which terminates with a putative ER retention signal SDEL (Figure 5A). The presence of an ER retention signal in *Dictyostelium* Sun-1 is unique for a



SUN domain protein, since ER retention signals were not found in SUN domain proteins from other species. Sun-1 resembles features found in different SUN domain protein homologues: (1) it shares the single transmembrane domain with the *C. elegans* UNC-84 and the *S. pombe* Sad1. (2) Like the mammalian SUN domain proteins, Sun-1 possesses coiled-coil domains, that are absent in *Ce* UNC-84 and *Sp* Sad1 (Hagan and Yanagida, 1995; Malone et al., 1999).

Sun-2 represents the second SUN domain protein in *D. discoideum* containing 1278 amino acids with a molecular weight of 146 kDa. The program SMART predicted an N-terminal transmembrane domain (amino acids 7 to 25), a long coiled-coil domain (amino acids 177 to 360) and a C-terminal histone deacetylase (HDAC) interaction domain at the amino acid position 842 to 914 of Sun-2 (Figure 5B). Further, the program InterProScan identified a centrally located SUN domain (amino acids 534 to 657). The domain architecture of Sun-2 is atypical compared to the common domain architecture of SUN domain proteins from other subfamilies. Thus proteins with a central SUN domain are termed as the SUN-like proteins (SLP), which are also present in the proteom of yeast and flies. Due to the central SUN domain Sun-2 represents rather a putative SUN-like protein than an orthologue of the mammalian Sun-2. The outstanding domain architecture of the SUN-like proteins demonstrates that this subfamily diverged from other SUN domain proteins early during evolution. However, SUN domain proteins, reported to be involved in nuclear positioning and migration, possess a C-terminal SUN domain. Hence, SUN-like proteins may function in other cellular mechanisms yet to be identified. One considerable functional aspect of Sun-2 in *D. discoideum* may be the regulation of gene expression or the modification of chromatin due to a putative HDAC interaction domain.

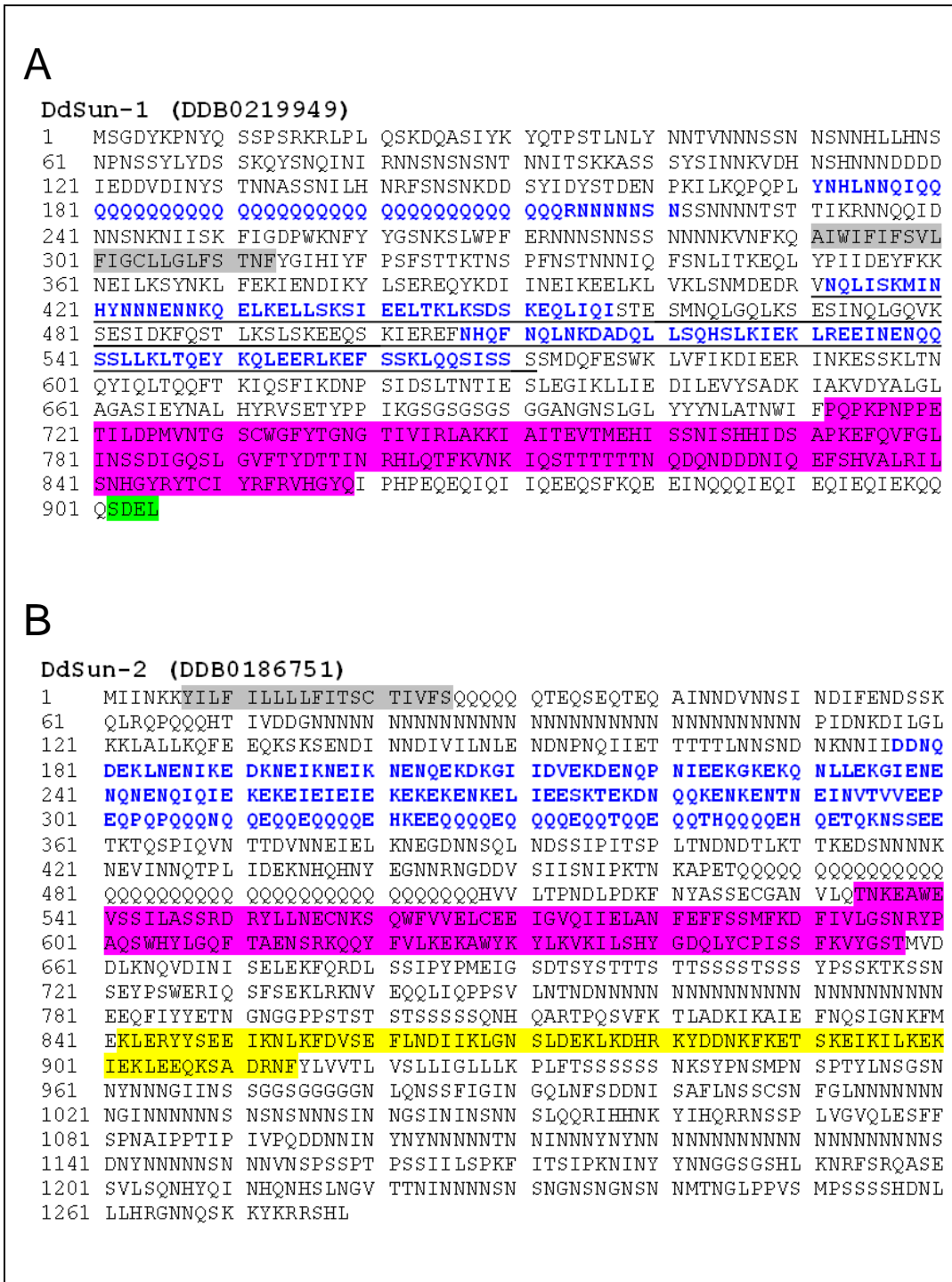


Figure 5: Primary structure of Sun-1 and Sun-2 in *D. discoideum*. The domain predictions were obtained using the programs SMART and InterProScan. The putative domains are highlighted: coiled-coil domains (blue), SUN domain (pink box) and transmembrane domain (grey box). **A.** Sun1 possesses an additional ER retention signal at the C-terminus (green box). Monoclonal antibodies were raised against the pair of coiled-coil domains (underlined). **B.** Sun-2 encompasses an N-terminal transmembrane domain, a putative coiled-coil domain, a centrally located SUN domain and a histone deacetylase (HDAC) interaction domain (yellow box).



3.1.3 Multiple alignment of the SUN domains

In *C. elegans*, *D. melanogaster* and mammals SUN domain proteins bind directly or indirectly to the KASH domain proteins forming a molecular bridge between the INM and the ONM. The SUN domain is of high biological relevance for the binding to KASH domain proteins. Thus, we analyzed the SUN domain of Sun-1 and Sun-2 in detail. The SUN domain of Sun-1 shares 28% homology with the SUN domain of *Ce* UNC-84 (Figure 6). Although *D. discoideum* is a lower eukaryote and diverged in the evolutionary tree before the fungi (Eichinger et al., 2005), the SUN domain of Sun-1 is closer related to human SUN proteins (39% identity to SUN-1, 38% identity to SUN-2) than to SUN proteins in yeast (27% identity) or worm (28% identity). In the evolution, *D. discoideum* represents an intermediate organism between yeast and mammals therefore proteins from *D. discoideum* show higher homology to mammalian proteins. With respect of the overall structure and sequence homology Sun-1 belongs to the subfamily of SUN3 proteins along with mouse and human Sun-3. Due to the domain architecture, Sun-1 may be involved in the organization of the nuclear envelope in *D. discoideum*.

The centrally located SUN domain of Sun-2 shared sequence homology with the SUN domains of SUN-like proteins found in *S. cerevisiae*, *S. pombe*, and *D. melanogaster*, demonstrating that Sun-2 belongs to the subfamily of the SUN-like proteins (Figure 6). However, the SUN domain sequences of SUN-like proteins are distinct from those of other SUN domain proteins, suggesting that the SUN-like proteins are specific for other conserved cellular processes than organization of the nuclear envelope



<i>DdSun1</i>	TNWIFPQPKNPPETILDP--MVNTGSGCFYTGNGTIVIRLAKKIAITTEVTMEHLSSN	763
<i>HsSun1</i>	LFGIPLWYFSQSPRVVIQP---DIYPGNCFKFKGSQGYLVVRLSMMIHPAAF TLEHLPKT	736
<i>SpSad1</i>	YFFDSLWVRGHEP SIALTP--NNVAMGFSFQGSEGLGSLSRPVYITNTIEHWQHK	404
<i>CeSun1</i>	FFYDEMSYFGTFQEGYALLDRIVLSPGEATCTYDKRATLTVRLARFVIPKSVSYQHWWS	356
<i>CeUNC84</i>	FWDIPIYYFHYSPRVVIQRNSKSLFPGEQCFKESRGYLAVELSHFDVSSISYEHIGSE	1025
<i>DdSun2</i>	NVLQTNKFAWEVSSITLASS-RDRYLLNEGNKS----QWEVVELCEETIGVQIIELANPEF-	583
<i>ScSlp1p</i>	TIVKSNPBAIGATSTLIES-KDKKLLNPKSAPQ---QFIVTELCEETLWEELEIANYDF-	253
<i>SpSlp1p</i>	AVIKTNPBAVGSSTLITEN-KDKYMLNKCSAEN---KFWVVELCEETIYVDIVQIANPEF-	257
<i>DmQ7YU09</i>	KILAHNSQSKHTEAVLTQS-TDEYMLSTCESR----IWFVVELCEETIQAQKVDVANYEL-	458
<i>OsQ8LJA6</i>	KVLAHNRBAKGAANDLGGD-KDRYLRNPKSADD---KFWVVELSEETLVRTIGLANLPH-	238
<i>DdSun1</i>	ISHH--IDSAPRFEQVFG---LINSDDIGQSLGVFTYD TTINR--HLCTEKVNKIQSTTT	816
<i>HsSun1</i>	LSPTGNISAPKDFAVYG--LENEYQEEGQLLGFVYDQDGES---LQMFQALKRPD---	788
<i>SpSad1</i>	IAHD--LSAPKDFELVW---QGMSSKMFVLLGKARYSLTEDS---LCTEFSESSNYI--	454
<i>CeSun1</i>	G---IVPNHAPFLYDVVAC-TDSCCTKWQPLVANCEYKERDGSYDEQEQFCVPTIQN-	410
<i>CeUNC84</i>	VAPEGNRSSAPKGVLYWY-KQIDDLNSRVLTGDYTYDLDGPP---LQEFQAKHKP----	1077
<i>DdSun2</i>	-----ESSMFKDFIVLGSNRYPAQS--MHWLGFVTAENSRK-----QCYEVLK-----	624
<i>ScSlp1p</i>	-----ESSIFKDFRVSVDRIKNEWTLLGDFEARNRE-----LQCFQIHN-----	297
<i>SpSlp1p</i>	-----ESSIFDFKVSVSGKYPKYESSMELGDFLALNLRT-----LQSFHLEN-----	301
<i>DmQ7YU09</i>	-----ESSSPKDFIVAVSKREP--TRDWSNVGDFEADKRT-----LQTEELH-----	499
<i>OsQ8LJA6</i>	-----YSSNFRDFELVGSPTSYPAPAEEMELLGDFEADNAKH---AQREVLPD-----	282
<i>DdSun1</i>	TTTNQDQNDDDNIQEFSHVALKILSNFGYR-YTCLYRFVWFGYQIP	861
<i>HsSun1</i>	-----DTAFQIQLRLRFSNFGHPBYTCLYRFVWFGEPVK	820
<i>SpSad1</i>	-----VAEPIQNVILKIKSNFGNPKYTCLYQVRFVWFGIVPN	487
<i>CeSun1</i>	-----HSPINHWQFRFRENFGDMPKTCANLIRVYGEFVD	442
<i>CeUNC84</i>	-----DFPVKFEVLEVTSTNYGAP-FTCLYRLRWFVWFGVYVQ	1199
<i>DdSun2</i>	-----EKAWYKYLKVKILSHYGDQLYCPTSSFFVYGGSTMV	657
<i>ScSlp1p</i>	-----PQIWA SYLKIETLSHYEDEFYCPISLIRVYGKSLM	330
<i>SpSlp1p</i>	-----PLIWA KYLKIETLHYGSEFYCPVSLIRVYGKTM	334
<i>DmQ7YU09</i>	-----PHLFGKFRVVDITSHYANEHFCPLSLFRVFGTSEY	532
<i>OsQ8LJA6</i>	-----PRWTRVLRRLRATHYGSFYCILSYLRYVYGDVAV	314

Figure 6: Sequence homology of SUN domains of *D. discoideum* Sun-1 (DDB0219949), human Sun-1 (NP 079430), *S. pombe* Sad1 (Q09825), *C. elegans* Sun-1 (Q20924) and UNC-84 (Q20745), *D. discoideum* Sun-2 (DDB0186751), *S. cerevisiae* Slp1p (Q12232), *S. pombe* Slp1p (O59729), *D. melanogaster* Q7YU09 and *O. sativa* Q8LJA6.

3.2 Generation of Sun-1 monoclonal antibodies

To address the biochemical and the functional aspects of Sun-1, we generated monoclonal antibodies against the amino acids 337 to 671 spanning the two coiled-coil domains (SunCT1) that are located between the transmembrane domain and the SUN domain. We targeted the coiled-coil domains of Sun-1 due to (1) the uniqueness of the protein sequence in the *D. discoideum* proteom and (2) the higher solubility during heterologous protein expression. The DNA sequence encoding the two coiled-coil domains (SunCT1) was cloned into the bacterial expression vector pGEX-4T2. The 65 kDa fusion protein GST-SunCT1 was purified from the

Escherichia coli strain XL1-Blue and the GST tag was subsequently removed by thrombin cleavage. After thrombin digestion the SunCT1 had an apparent molecular weight of 40 kDa (Figure 7A). Two naïve mice were immunized with 10 μ g of the purified SunCT1. After three weeks the mice were boosted twice with 10 μ g SunCT1 and the mouse with higher antiserum titer was sacrificed for isolation of spleen cells, which were fused to the myeloma cell lines AG8 and PAI, respectively (Figure 6B).

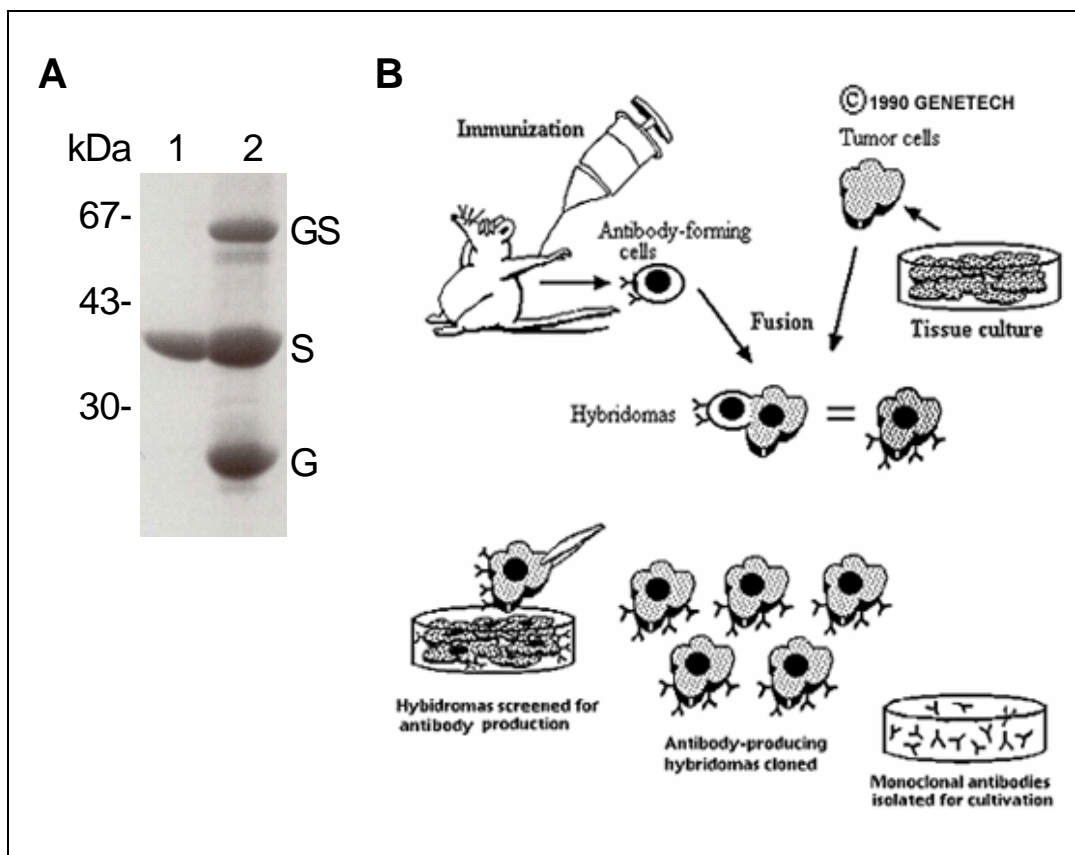


Figure 7: Generation of monoclonal antibodies against Sun-1. **A.** The fusion protein GST-SunCT1 (GS) was purified from bacterial cell lysate. The 40 kDa SunCT1 (S, lane 1) was cleaved from the GST moiety (G) prior to immunization of the mice. **B.** Scheme illustrating the process of monoclonal antibody generation (Genetech, 1999). Mice were immunized with purified SunCT1. Spleen cells from the mouse with the highest serum titer were isolated and fused to myeloma cells AG8 and PAI, respectively, giving rise to hybridoma clones. The immortalized hybridoma clones were screened for specificity to Sun-1 by ELISA and western blots.



Immunoreactivity of the hybridoma clones for SunCT1 was screened by ELISA assay and on western blot stripes. Promising clones were subjected to single-cell subcloning. In the screening experiments, three single-cell subclones were identified to be specific for biochemical or cell biological studies, i.e. K55-432-2, K55-450-1 and K55-460-1. Each of the single-cell clones recognized specifically the endogenous Sun-1 in western blot screening experiments. Further screenings of these clones by immunofluorescence and immunoprecipitation assays revealed that the clones K55-450-1 and K55-460-1 were suitable for immunolocalization and immunoprecipitation studies of Sun-1.

The monoclonal antibody (mAb) K55-432-2 detected Sun-1 in the AX2 total cell lysate with the expected molecular mass of 105 kDa. In a crude fractionation experiment, K55-432-2 localized the endogenous Sun-1 specifically to the nuclear fraction but not to the cytoplasmic fraction (Figure 8A), indicating that Sun-1 is a protein associated with the nuclear compartment. To monitor the efficiency of the fractionation procedure, the samples were probed with monoclonal antibodies against α -tubulin (mAb 6-11B1, Piperno and Fuller, 1985, a kind gift from Michael Koonce). The 51 kDa protein α -tubulin was found both in the total cell lysate and in the cytoplasmic fraction (Figure 8A). However, low amount of α -tubulin was also detected in the nuclear fraction, which may be derived from the microtubule (MT) tips associated with the microtubule organization center (MTOC) at the centrosome. Since the mAb K55-432-2 displayed the highest immunoreactivity in western blot analysis, this clone was used for all biochemical studies.

In cell biological screening, the mAb K55-432-2 failed to stain Sun-1 by indirect immunofluorescence. The inability of mAb K55-432-2 to detect Sun-1 in AX2 cells may be due to the specificity of mAb K55-432-2 for denatured Sun-1 protein. In further immunofluorescence screenings, a second mAb clone, K55-460-1, localized the endogenous Sun-1 to the nuclear envelope and some cytoplasmic compartments in AX2 cells (Figure 8B). To confirm the nuclear envelope localization, nuclei of AX2 cells were stained with ToPro-3 to visualize the DNA. In a merged image, Sun-1



surrounded the nucleus in a rim-like pattern, demonstrating that mAb K55-460-1 recognizes specifically the native epitope of Sun-1 *in vivo*. Subsequently, mAb K55-460-1 was used for all cell biological analyses.

Interaptin has been reported to be a nuclear envelope protein in *D. discoideum* (Rivero, *et al.*, 1998). Thus, the localization pattern of the endogenous Sun-1 was compared to that of interaptin. The mAb 260-60-10 localized interaptin predominantly to the nuclear envelope but also to further cytoplasmic compartments, most likely the peripheral ER. However, the cytoplasmic staining of Sun-1 *in vivo* may be derived from unspecific antibody binding, since endogenous Sun-1 was not distributed to the cytoplasmic fraction as shown in the crude AX2 cell lysate fractionation experiment (Figure 8A).

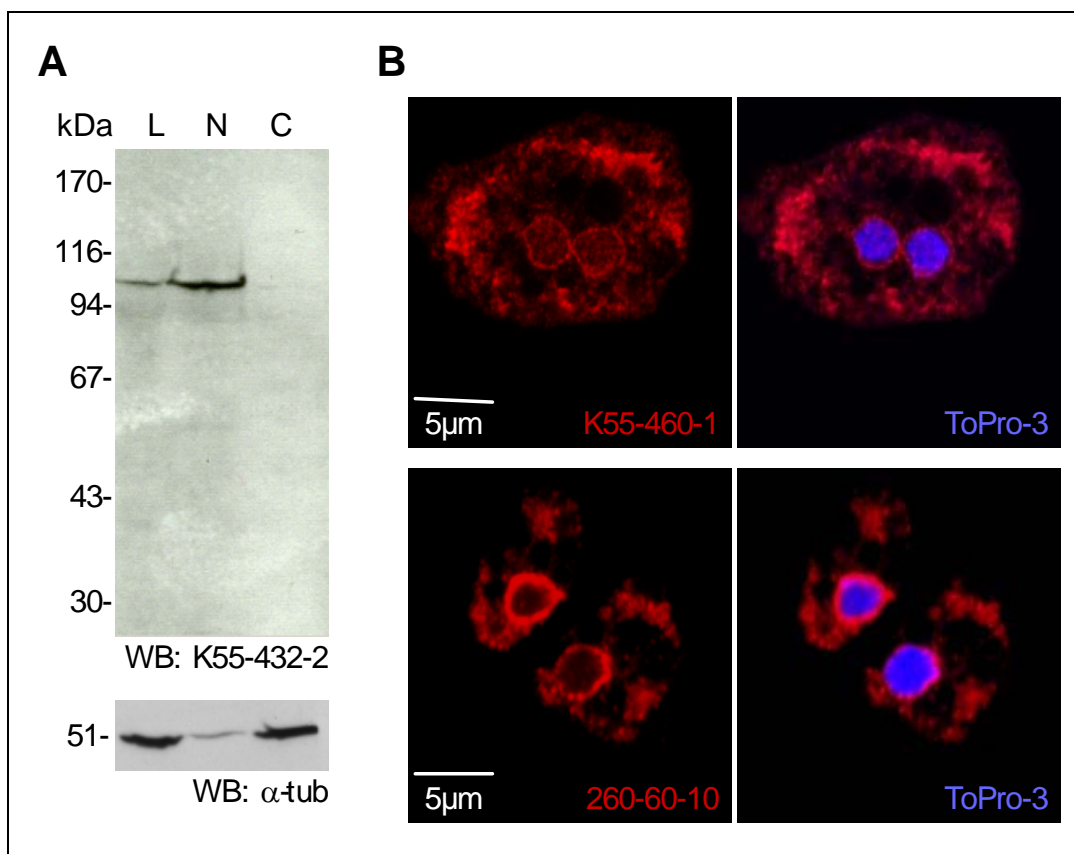


Figure 8: Screenings of monoclonal antibodies against Sun-1. **A.** The mAb K55-432-2 detected endogenous Sun-1 in the AX2 total cell lysate (L) and in the nuclear fraction (N) but not in the cytoplasmic fraction (C). The mAb 6-11B1 (Piperno and Fuller, 1985), a kindly gift from Michael Koonce, monitored α -tubulin in the AX2 total cell lysate (L). In the crude fractionation experiment, α -tubulin was associated with the nuclear fraction to some extent (N), but enriched in the cytoplasmic fraction (C). **B.** The mAb K55-460-1 localized the endogenous Sun-1 to the nuclear



envelope and some cytoplasmic compartments. The mAb 260-60-10 stained interaptin at the nuclear envelope, as well as some cytoplasmic compartments. Indirect immunofluorescence (Cy3 conjugated anti mouse IgG, red), DNA was visualized by ToPro-3 (blue).

3.3 Biochemical properties of Sun-1

3.3.1 Sun-1 is restricted to the nucleus

To examine the subcellular localization of endogenous Sun-1 in more detail, cellular components were isolated by ultracentrifugation on discontinuous sucrose gradients. In brief, 5×10^8 AX2 cells were lysed in 5ml TMKS buffer by passing through a Nucleopore filter (5 μ m pore diameter, Whatman). To reduce the loading volume from 5ml to 1ml, the total cell lysate was spun for 30 min at 15000 *g*. After centrifugation, the pellet containing all cellular organelles was resuspended in 1ml of TMKS buffer and was separated on a discontinuous sucrose gradient ranging from 0.85M to 2.49M of sucrose. Samples were analyzed on western blots.

To test the accuracy of the fractionation procedure, the samples from all gradients were probed with antibodies against interaptin (mAb 260-60-10) and protein disulfide isomerase 1 (PDI-1, mAb 221-135-1), respectively. To some extent, interaptin was localized with the ER marker, PDI-1, to the low-density sucrose gradient fractions two and three confirming that interaptin is partially targeted to the peripheral ER (Figure 9, fractions 2 and 3). As a nuclear envelope protein, the majority of endogenous interaptin was predominantly localized to the high-density sucrose fractions corresponding to the nuclear fractions (Figure 9, fractions, 9 to 11). However, PDI-1 was also found in high-density fractions, correlating to the rough ER, which is contiguous with the nuclear envelope (Figure 9, fractions 7 to 11). Comparable to the nuclear envelope marker interaptin and the ER marker PDI-1, Sun-1 was recovered in the high-density sucrose fractions representing the nuclear fractions (Figure 9, fractions 8 to 11). Distinct from the localization pattern of interaptin and PDI-



1, the endogenous Sun-1 was exclusively found in the nuclear fractions and was absent from the peripheral ER. These data indicate that the distribution of Sun-1 is limited to the nuclear envelope. Thus we conclude that the cytoplasmic staining observed in the immunofluorescence experiment may be derived from non-specific interaction of mAb K55-460-1.

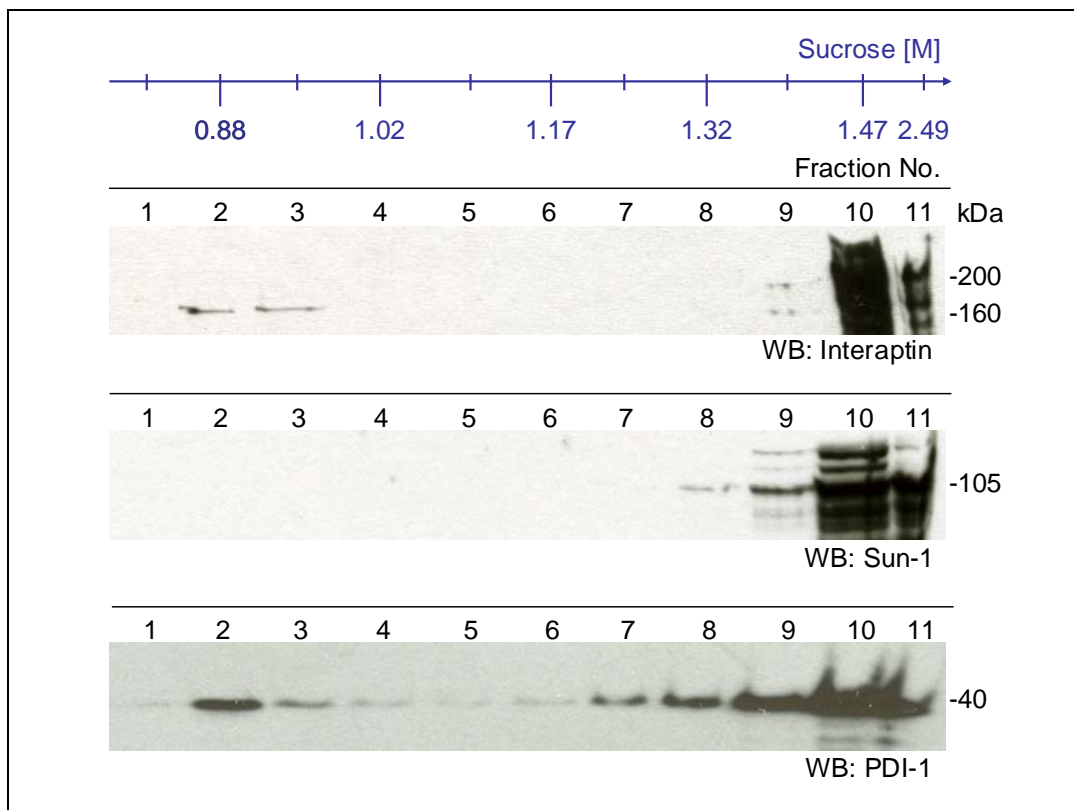


Figure 9: Localization of Sun-1 to the nuclear compartment. Total cell lysate of AX2 was separated on a discontinuous sucrose gradient. Interaptin is localized to peripheral ER (Fraction 2 and 3) and to the nuclear compartment (Fraction 9 to 11) overlapping with the distribution pattern of PDI (mAb 221-135-1). Colocalizing with the nuclear envelope marker interaptin, Sun-1 is limited to the high-density fractions representing the nuclear fractions (Fraction 8 to 11).



3.3.2 Sun-1 is an integral membrane protein

Analysis of the Sun-1 primary protein sequence using the program SMART revealed one putative transmembrane domain. To examine, whether Sun-1 exhibits properties of a transmembrane protein, extraction experiments were carried out. Application of alkali (0.1M NaOH) or high salt (1M KCl) extracts peripheral membrane proteins from cytoplasmic and nuclear membranes. Wildtype AX2 cell lysates were obtained by filtration of cells through Nucleopore membranes (5 μ m pore diameter, Whatman). Intact nuclei were isolated from the cell lysate by 10 min spinning at 3000 *g*.

Addition of alkali (0.1M NaOH) or high salt (1M KCl) to the nuclei led to some degradation of Sun-1. However, Sun-1 was not extracted from the nuclear membrane fraction by alkali or high salt indicating that Sun-1 is not peripherally anchored on the surface of nuclear membranes. Moreover, Sun-1 was only partially solubilized from the nuclear membranes in the presence of 1% Triton X-100 or 8M Urea or a combination of both reagents, demonstrating that Sun-1 is highly hydrophobic (Figure 10B). Hydrophobicity and nuclear membrane association of Sun-1 agreed with the properties observed for interaptin (Rivero *et al.*, 1998), thus Sun-1 is a putative integral protein of the nuclear membranes in *D. discoideum*.

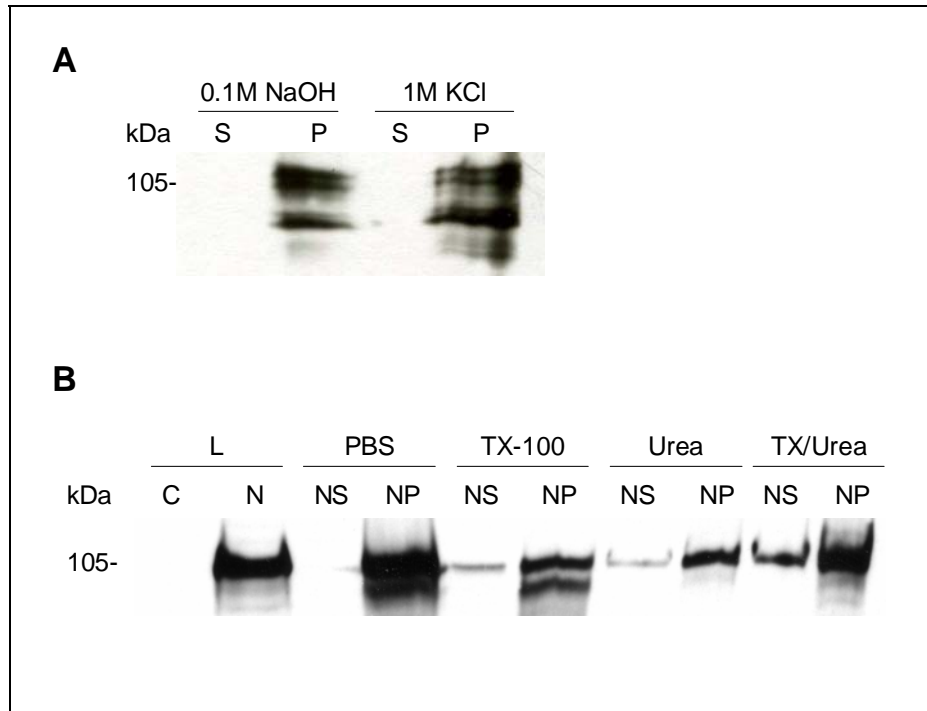


Figure 10: Sun-1 is a putative integral nuclear membrane protein. AX2 cells were lysed by filtration through Nucleopore membrane (5 μ m pore diameter, Whatman). Intact nuclei were isolated from the cell lysate by centrifugation for 10 min at 3000 *g*. **A.** Sun-1 was resistant to extraction with alkali (0.1M NaOH) or high salt (1M KCl) and remained membrane-associated. The endogenous Sun-1 was partially degraded due to alkali or high salt extraction. **B.** The intact nuclei (N), obtained after filtration through Nucleopore membrane (5 μ m pore diameter, Whatman), were used for further extractions. Sun-1 was partially solubilized from nuclear membranes by addition of 1% Triton X-100 (NS and NP), 8M Urea (NS and NP) or a combination of both reagents (NS and NP). Western blots were probed with mAb K55-432-2.

3.3.3 Sun-1 oligomerizes via the coiled-coil domains

As mentioned above, two putative coiled-coil domains were predicted between the transmembrane domain and the SUN domain of Sun-1 by the program SMART. The first coiled-coil domain spans the amino acids 412 to 457, whereas the second coiled-coil domain extends from amino acid 507 to 571 (Figure 11A). As coiled-coil domains represent oligomerization motives, we tested whether the coiled-coil domains of Sun-1 are capable to oligomerize. For this purpose, recombinant SunCT1 overlapping the amino acid 419 to 578 bearing the two coiled-coil domains was expressed as GST fusion protein and purified from *E. coli* using GST-Sepharose beads (Amersham). To eliminate the chance of unspecific



protein dimerization via the GST moiety, GST was removed from SunCT1 by thrombin cleavage.

The native protein, SunCT1, occurs as a monomer of approximately 40 kDa. Notably, low amount of dimeric (80 kDa) and trimeric (120 kDa) SunCT1 was not dissociated into monomers under denaturing and reducing conditions (Figure 11A). The presence of dimeric and trimeric SunCT1 after addition of 1% SDS and 0.1% β -Mercaptoethanol to the sample buffer indicate a strong affinity within the dimers and trimers. The strong affinity within the dimers and trimers may result from covalent bonds given by intermolecular disulfide bridges, thus we sought for cysteine residues within the protein sequence of the coiled-coil domains. Unlike mouse Sun-1 (unpublished data from our lab), *Dictyostelium* Sun-1 does not harbor any cysteine residue in these coiled-coil domains. Thus, the dimers and trimers were not stabilized by disulfide bonds, which can be reduced in presence of β -Mercaptoethanol. The affinity between the subunits of a dimer or a trimer may be a consequence of strong association of intermolecular hydrogen bonds, salt bridges, aromatic and/or hydrophobic interactions inducing conformational changes within the coiled-coil domains that were not taken apart by denaturation, i.e. boiling in 1% SDS containing sample buffer.

The amount of dimers and trimers observed in SDS polyacrylamide gels were enriched by incubation of 5 μ g purified SunCT1 with the cross-linker glutaraldehyde that stabilizes oligomers by creating covalent bonds between the interacting subunits. In a time-dependent fashion, an increase of SunCT1 dimers, trimers, tetramer and pentamer was observed 20 min after addition of 0.001% glutaraldehyde to the native SunCT1 (Figure 11B). The stabilized SunCT1 dimers and trimers resembled with respect to their migration behaviour those detected in the absence of glutaraldehyde hinting to a specific cross-linking of SunCT1 dimers and trimers (Figure 11B).

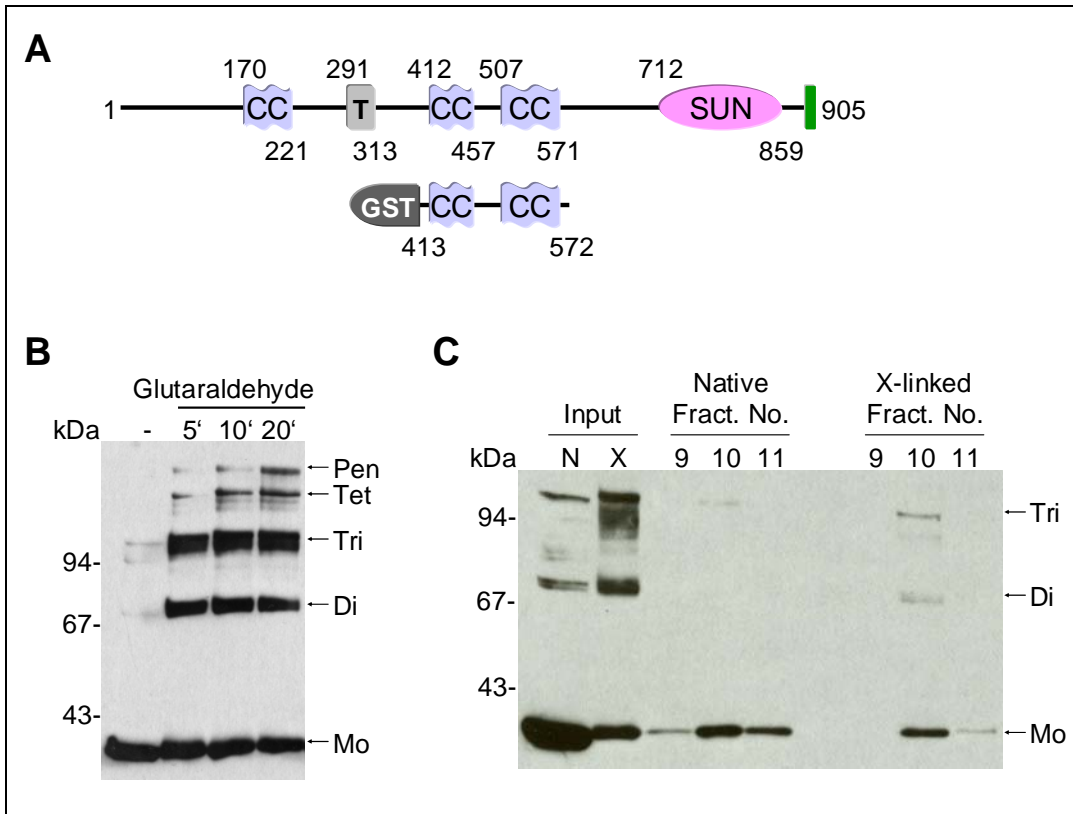


Figure 11: Recombinant SunCT1 forms oligomers *in vitro*. **A.** The recombinant GST-SunCT1 harbors the two predicted coiled-coil domains (amino acids 419 to 578). **B.** The native SunCT1 occurs as a 40 kDa monomer (Mo), whereas low amounts of dimers (80 kDa, Di) and trimers (120 kDa, Tri) were detected under denaturing and reducing conditions. 5 μ g of SunCT1 was incubated with 0.001% glutaraldehyde. At the indicated time points, the cross-linking reaction was stopped by addition of 1M glycine to a final concentration of 0.1M. The amount of dimers, trimers, tetramers (160 kDa, Tet) and pentamers (200 kDa, Pen) were increased 20 min after addition of glutaraldehyde. **C.** Gel filtration of native SunCT1 (N) and cross-linked SunCT1 (X). 10 μ g of native or cross-linked SunCT1 were analyzed by size-exclusion chromatography using a Sephadex G75 column. The native SunCT1 trimers (Fraction 9), dimers (Fraction 10) and monomers (Fraction 11) were eluted from the column. Cross-linked SunCT1 trimers and dimers were recovered in fraction 10, whereas the monomeric SunCT1 was found in fraction 11. Western blots were probed with mAb K55-432-2.

To confirm the presence of SunCT1 oligomers under native conditions, 10 μ g of native and cross-linked SunCT1 protein was also subjected to gel filtration chromatography on a size-exclusion column. On a size-exclusion column, high-molecular-weight proteins pass through the Sepharose beads faster than low-molecular-weight proteins, since the diffusion of low-molecular-weight proteins is retarded. Due to the high molecular mass of the SunCT1 trimers, the complex was eluted in fraction 9,



whereas fraction 10 contained dimeric and trimeric forms (Figure 11C, crosslinked material) and fraction 11 the monomer. A comparison of the elution behaviour of the native and the crosslinked material shows that in both cases the majority of the protein elutes in a fraction which contains dimers and trimers (Figure 11C). Remarkably, a certain amount of high affinity SunCT1 trimers resistant to the denaturing and reducing conditions was observed in the fraction 10, whereas high affinity dimers were not detected. These observations suggest that the trimeric complex may exhibit higher affinity and stability. Taken together, recombinant native SunCT1 occurs as dimers and trimers *in vitro*. Further, the majority of the dimers and trimers can be disassembled into monomers under denaturing and reducing conditions.

Analysis of the cross-linked SunCT1 on a size-exclusion column revealed a reduction of monomeric SunCT1 (Figure 11C, right panel, fraction 11) due to the increase of the dimeric and trimeric complexes. Unfortunately, the cross-linked SunCT1 trimers were present in the same fraction as the dimers owing to the limited resolution capacity of the gel matrix, which failed to separate the cross-linked trimers from the dimers accurately.

3.3.4 Sun-1 may form dimers and trimers *in vivo*

Given the evidence that the coiled-coil domains mediate the dimerization and trimerization of Sun-1, the recombinant GST-SunCT1 may also interact with the endogenous Sun-1 from *D. discoideum*. In a pulldown experiment, GST-SunCT1 was immobilized on Glutathione-Sepharose beads and incubated with AX2 total cell lysate. A 200 kDa protein band precipitated by GST-SunCT1 was subjected to MALDI mass spectrometry (Figure 12A). The peptide sequences of the precipitated protein matched significantly to the protein sequence of Sun-1, indicating an interaction of the recombinant SunCT1 with the endogenous Sun-1 (Figure 12B). Interestingly, the precipitated Sun-1 was found at the position of about 200 kDa, whereas



the molecular mass of the monomeric Sun-1 protein is 105 kDa. Further, we have identified the amino acid residues arginine, tyrosine, phenylalanine, histidine and methionine within the pair of coiled-coil domains which are reported as conserved residues to promote strong protein-protein interactions (Bogan and Thorn, 1998; Brinda and Vishveshwara, 2005). Additionally, the cluster of amino acids contributing to the strong affinities was supported by further cluster of leucines and isoleucines that forms weak protein-protein interactions (Brinda and Vishveshwara, 2005). By combination of the amino acid clusters for strong and weak intermolecular dimerization in the coiled-coil domains, the 200 kDa band may be derived from a stable dimer that was not disassembled under the denaturing and reducing conditions during SDS-PAGE. The fact that a Sun-1 dimer was precipitated by the recombinant SunCT1 indicates that Sun-1 may also form higher oligomers.

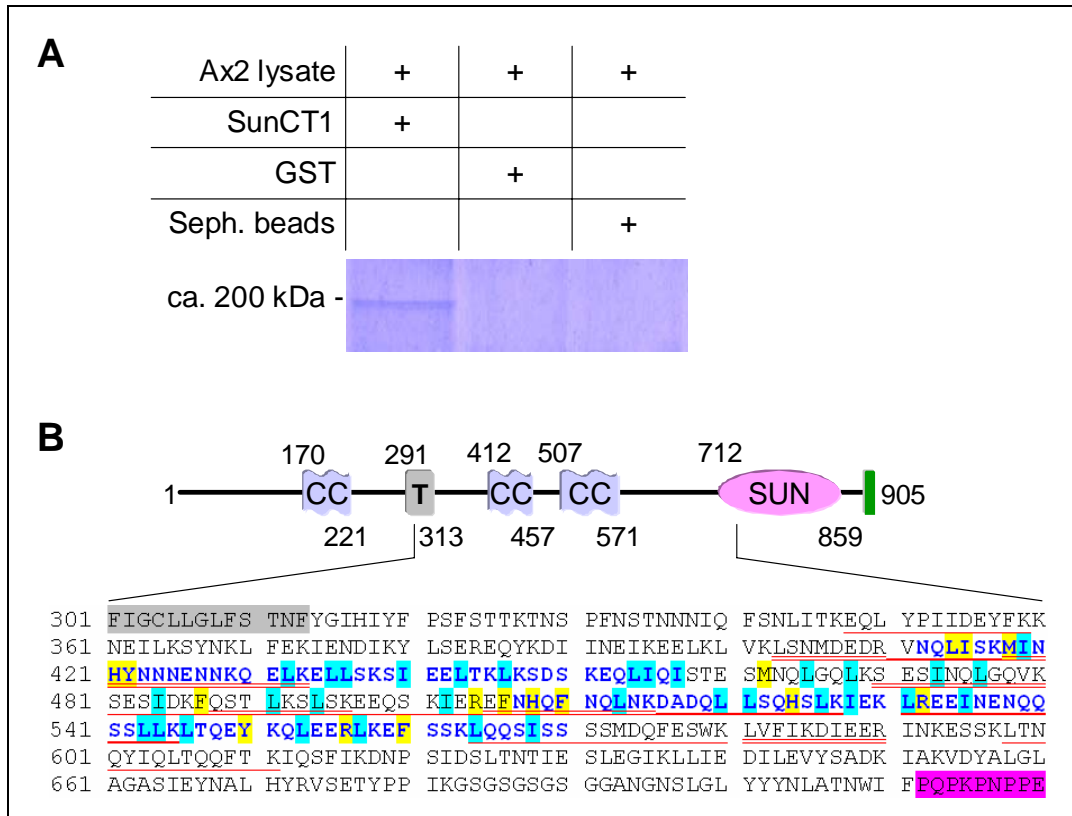


Figure 12: Pulldown experiment using GST-SunCT1. **A.** Recombinant GST-SunCT1 was immobilized on GST-Sepharose and incubated with AX2 total cell lysate. In control reactions, AX2 total cell lysate was incubated with GST immobilized on GST-Sepharose beads and GST-Sepharose beads alone. The samples were subjected to SDS-PAGE (10% acrylamide) and the gel was stained with Coomassie Brilliant blue. **B.** The scheme of Sun-1 depicts the region that matched the peptide sequences obtained from MALDI. Single peptide matches are underlined (red), overlapping peptide matches are double underlined (red). The amino acids within the coiled-coil domains conferring strong and weak dimer interactions are highlighted in yellow and blue. Partially shown the transmembrane domain sequence is highlighted by grey box and the initiation of the SUN domain by the pink box,

3.3.5 Sun-1 is a type II transmembrane protein

Transmembrane proteins are grouped into four classes due to their membrane topology: (1) Type I transmembrane proteins possess an N-terminal signal peptide, targeting the protein to ER or Golgi. Thus the N-terminus is located in the lumen of the ER/Golgi or on the extracellular surface, whereas the C-terminus of the protein is exposed to the cytoplasm. (2) Type II proteins exhibit the C-terminus to the lumen of ER/Golgi or the extracellular surface and the N-terminus to the cytoplasm. (3) The N-



terminus of type III membrane proteins faces the lumen of ER/Golgi or the extracellular surface, comparable to the type I membrane proteins, with the exception, that a signal peptide is absent in type III proteins. (4) Type IV comprises the seven-transmembrane proteins with a cytoplasmic C-terminus.

To determine the topology of Sun-1 in the nuclear envelope, intact nuclei were isolated from AX2 and treated with proteinase K, which is an unspecific proteinase. On a western blot, mAb K55-432-2 detected a protein of 70 kDa in the proteinase K treated nuclei, correlating with the molecular mass derived for the amino acids 291 to 905 extending from the transmembrane domain to the C-terminus of Sun-1 (Figure 13A and B), suggesting that this part projects into the perinuclear space (PNS) between the inner and outer nuclear membrane (INM and ONM) and is protected from proteolysis. Moreover, finding a 70 kDa protein fragment after exposure of the intact nuclei to proteinase K confirmed that Sun-1 possesses a single transmembrane domain. Unfortunately, this experiment does not indicate whether the N-terminal domain of Sun-1 faces the cytoplasm or the nucleoplasm, as proteinase K (24 kDa) is capable to diffuse through the nucleopores into the nucleoplasm and degrade protein epitopes within the nucleoplasm. The fact that the C-terminal moiety of Sun-1 was protected from the proteinase K digestion suggests that the C-terminus of Sun-1 projects into the perinuclear space (PNS) between the INM and ONM. Conversely, the N-terminus was degraded by the proteinase K implying that the N-terminus of Sun-1 faces the cytoplasm and/or the nucleoplasm. In conclusion, Sun-1 is a single-pass nuclear membrane protein and adopts the membrane topology of the type II transmembrane proteins.

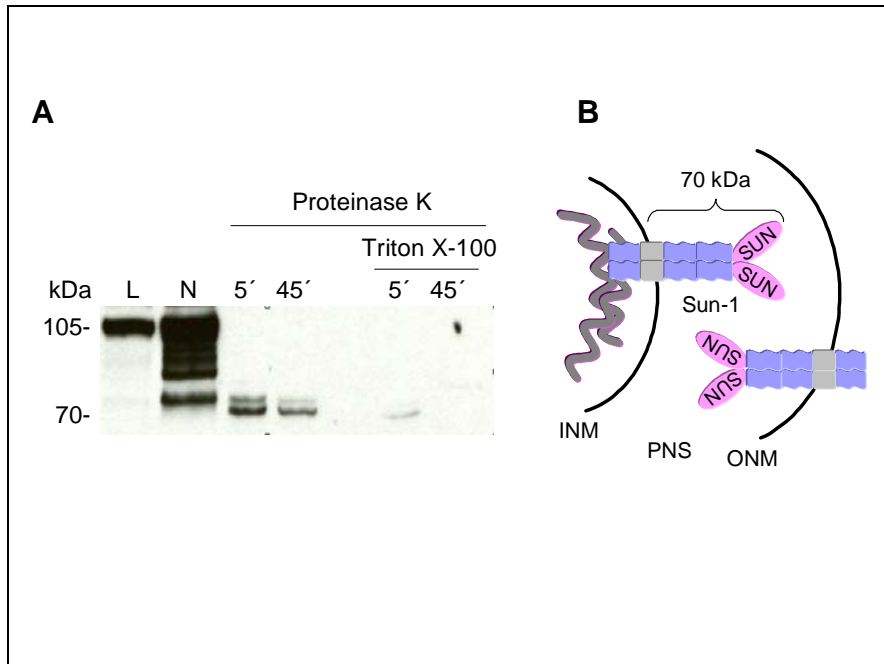


Figure 13: The C-terminus of Sun-1 is located in the perinuclear space (PNS). **A.** Intact nuclei from AX2 cells were treated with 1 μ g proteinase K for 5 or 45 min, giving rise to a protein fragment of 70 kDa. Addition of the membrane detergent Triton X-100 led to complete degradation of Sun-1. **B.** The protein fragment (amino acid 291 to 905) including the transmembrane domain and the whole C-terminus has an expected molecular mass of 70 kDa. Combining the data from the cross-linking experiment and the proteinase K protection assay, Sun-1 may reside in both the inner and/or the outer nuclear membrane (INM, ONM) whereas the C-termini of the dimers are located in the perinuclear space (PNS).

3.3.6 Sun-1 associates with chromatin

In *C. elegans*, *D. melanogaster* and mammals, SUN domain proteins are targeted to the INM. By binding of the SUN domain proteins to nuclear lamins and KASH domain proteins the nuclear skeleton is connected to the cytoskeleton.

We are motivated to examine the localization of Sun-1 specifically to the INM and/or the ONM. To distinguish the INM from the ONM localization of Sun-1, additional INM and ONM markers were required for colocalization studies. Since the research on the nuclear envelope proteins is a new field in *D. discoideum*, nuclear envelope markers are not available. So far, interaptin is the only nuclear envelope protein described in *D. discoideum*, but the localization to either the INM or the ONM was not



determined (Rivero *et al.*, 1998). Further on, *Dictyostelium* lacks nuclear lamins, leading to the most interesting question which nuclear component interacts with Sun-1. Given the evidence from the proteinase K protection assay, Sun-1 may expose the N-terminus both to the cytoplasm and the nucleoplasm. We hypothesize, if Sun-1 is targeted to the INM, then it may be capable to interact with chromatin.

To test our hypothesis, chromatin immunoprecipitation (ChIP) experiments were carried out. For each ChIP reaction, AX2 cells (2×10^8) were resuspended in the chromatin immunoprecipitation buffer and lysed by addition of Triton X-100 to the final concentration of 0.1%. Owing to the high viscosity of chromatin as such, it can be attached unspecifically to the protein A-Sepharose beads during the immunoprecipitation reaction. Thus, the chromatin in the AX2 lysate was fragmented by sonification prior to immunoprecipitation using antibodies against Sun-1 (K55-460-1), α -tubulin (6-11B1, Piperno and Fuller, 1985; a kind gift from Michael Koonce) and protein A-Sepharose beads only. Immunoprecipitated Sun-1 was analyzed by western blotting; chromatin fragments were eluted from the protein A-Sepharose beads in presence of 1%SDS. Subsequently, the presence or absence of chromatin was examined by PCR amplification of a housekeeping gene such as *actin-8*. Strikingly, chromatin was coprecipitated with the endogenous Sun-1, whereas the α -tubulin antibody or the protein A-Sepharose beads were not associated with chromatin (Figure 14). These data support our hypothesis that Sun-1 is targeted to the INM and associates with chromatin or chromatin-binding proteins. By extension, chromatin or chromatin-binding proteins may compensate for the lack of nuclear lamins for anchoring Sun-1 to the INM of *D. discoideum*.

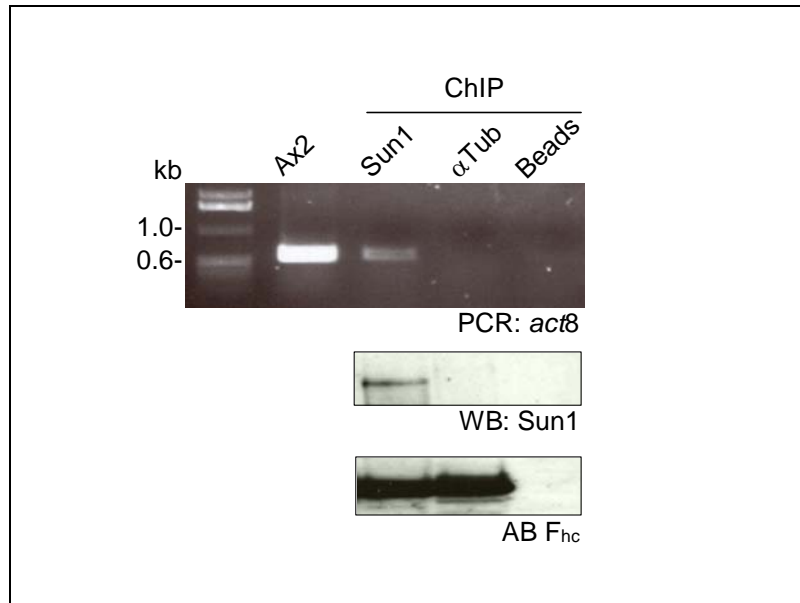


Figure 14: Chromatin immunoprecipitation (ChIP). Genomic DNA isolated from AX2 was used as positive control for PCR of the *act8* gene. Chromatin immunoprecipitation was carried out using antibodies for Sun-1 (K55-460-1) or α -tubulin (6-11B1, Piperno and Fuller, 1985; a kind gift from Michael Koonce). Protein A-sepharose beads were used as a negative control. The endogenous Sun-1 was precipitated the by the Sun-1 antibody (western blot). Antibody heavy chain (AB F_{hc}) was displayed as a loading control.

3.4 Sun-1 and the KASH domain protein interaptin

3.4.1 The KASH domain protein homolog interaptin

In worm, flies and mammals, the nucleus is connected to the cytoskeleton by interaction of the SUN domain proteins with a family of giant ONM proteins, referred to as the KASH domain proteins (Hodzic et al., 2004; Padmakumar et al., 2005; Crisp et al., 2006).

The first giant ONM proteins reported to provide a connection of the nucleus to the cytoskeleton are *C. elegans* Anc-1, *D. melanogaster* Klarsicht and human Syne1 and 2 (synonym Nesprin, Myne, Enaptin and NUANCE). The domain architecture of these giant proteins is conserved in all species and consists of three functional domains: (1) An N-terminal actin-binding



domain (Calponin homology domain) for F-actin-binding. (2) A central stretch of multiple coiled-coil domains (*C. elegans* Anc-1) or spectrin repeats (mammalian Nesprins). (3) A C-terminal domain resuming a single transmembrane domain and a short peptide tail. Functional and homology studies on these proteins revealed that the highly conserved transmembrane domain and the peptide tail is essential for the ONM targeting, subsequently termed as the KASH (Klarsicht-Anc1-Syne-Homology) domain. Once targeted to the ONM, the KASH domain proteins expose their N-terminus to the cytoplasm, whereas the C-terminal tail is located in the PNS. Within the C-terminal tail of the KASH domain of mammalian Nesprin-1 and 2 and Dm Nesprin, the final amino acid consensus motif G-P-P-P-(T/L) promote the interaction with the SUN domain proteins. Here, the G-P-P-P-(T/L) motif is referred to as the KASH motif. Distinct from the mammalian KASH domain proteins, *Ce* Anc-1 possesses a KASH motif terminating with a phenylalanine (G-P-P-P-F).

In *D. discoideum* interaptin may represent a candidate KASH domain protein. Interaptin encompasses 1737 amino acids resulting in a protein of 200 kDa (Rivero et al., 1998). The domain architecture of interaptin is similar to that of other KASH domain proteins: It possesses an N-terminal calponin homology domain and a central stretch of coiled-coil repeats, whereas the C-terminal domain harbors a single transmembrane domain and a 16 amino acids short tail.

As the C-terminal KASH domain is involved in the interaction with SUN domain proteins, we analyzed the C-terminal domain of interaptin from the transmembrane domain to the tail. Owing to the short sequence of the transmembrane domain (12 amino acids) and the C-terminus tail (16 amino acids), the software ClustalW failed to align the sequence of interaptin to the KASH domains of other species. Thus, we compared the C-terminal tail of interaptin with those of *C. elegans* Anc-1, *D. melanogaster* Msp-300/Nesprin, mammalian Nesprin-1 and 2 (Figure 15A). The C-terminal tail of interaptin shares higher homology with Anc-1 (12%) and Msp-300/Nesprin (12%) than with mammalian Nesprins (6%) (Figure 15B). However, the C-terminal tail of interaptin does not contain the complete KASH motif G-P-P-P-(T/L) though



the final pair of amino acids P-T of interaptin resembles the final amino acids P-T of human and mouse Nesprin-2 (Figure 15A). With respect to the extremely short C-terminus of interaptin, we propose that the final two amino acids P-T may be sufficient to function as a KASH motif in *D. discoideum*.

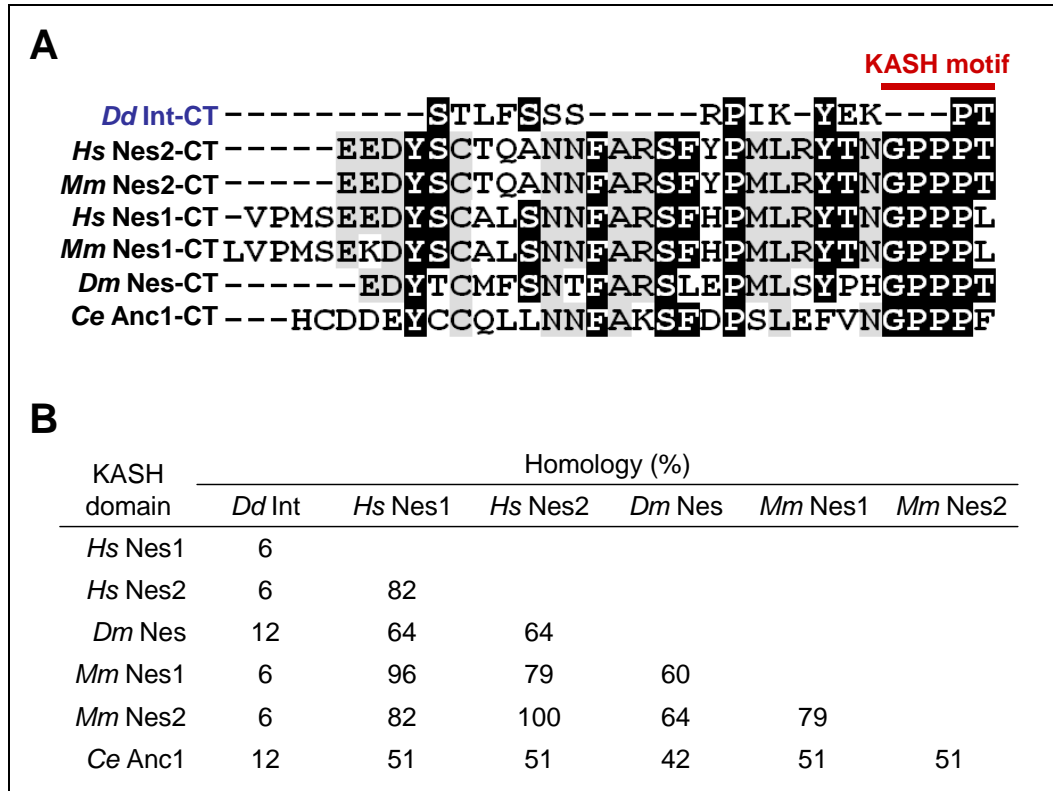


Figure 15: Multiple alignments of C-terminal tail sequences of interaptin and KASH domain proteins of human Nesprin-1 and -2, *D. melanogaster* Nesprin, mouse Nesprin-1 and -2, and *C. elegans* Anc-1. **A.** KASH domain proteins from mammals and flies possess a highly conserved KASH motif G-P-P-P-(T/L) at the C-termini (red bar), whereas *C. elegans* Anc-1 contains a KASH motif ending with a phenylalanine. The C-terminal tail of interaptin containing 16 amino acids terminated with the amino acids P-T, which represent a putative KASH motif. **B.** Percentage of homology between the KASH domains is summarized in the table. The C-terminal tail of interaptin shares higher homology with *D. melanogaster* Nesprin and *C. elegans* Anc-1 than with mammalian Nesprins.



3.4.2 Expression profile of Sun-1 and interaptin

To investigate the regulation of gene expression for Sun-1 and interaptin, we first focused on their expression profile during the development of *D. discoideum*. Sun-1 was expressed constitutively in all stages of development, with a slight increase in the expression level after 8 hr (t8) of starvation and a drop at the end of development when fruiting bodies were formed (Figure 16A). However, interaptin occurs in two isoforms, a 160 kDa and an approximately 200 kDa molecule due to alternate mRNA splicing. The domain structure of the 160 kDa isoform is not defined. Rivero *et al.* (1998) speculate that the alternative splice acceptor site may be located to the 5' end of the mRNA, thus it may lack the N-terminal actin-binding domain either completely or partially, whereas the C-terminus is intact. In *D. discoideum*, the 160 kDa isoform is expressed constitutively, whereas the 200 kDa isoform is developmentally regulated. The expression of the large isoform of interaptin is induced 8 hr (t8) after entering development (Figure 16A).

Next we compared the expression profile of Sun-1 to that of interaptin, to examine whether Sun-1 might influence the expression pattern of interaptin or vice versa. We noted an increase of Sun-1 expression at time point t8 coinciding with the onset of the expression of the large isoform of interaptin, indicating that interaptin may influence the expression level of Sun-1. Therefore, we monitored the Sun-1 protein expression in an interaptin-overexpressing and an interaptin-deficient mutant (Rivero *et al.*, 1998). In the interaptin-overexpressing or interaptin-deficient mutant, the expression level of Sun-1 remained unaffected, demonstrating that both proteins are independently regulated (Figure 16B).

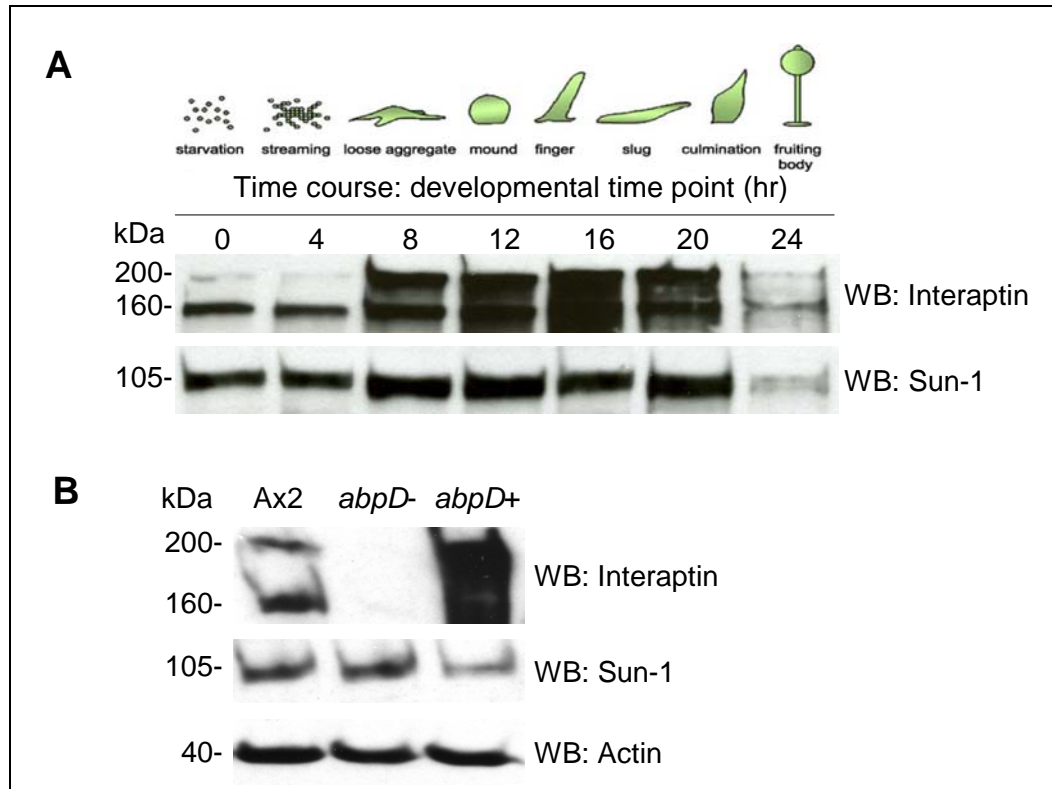


Figure 16: Sun-1 and interaptin are independently expressed in AX2. Protein samples were separated on 10% SDS-polyacrylamide gels. A. Expression profile of endogenous Sun-1 and interaptin in AX2 cells during development (Scheme, (Siu et al., 2004)). AX2 cells were starved on phosphate agar plates to induce the development. AX2 cells were harvested at the indicated time points of development by resuspending the cells in phosphate buffer. Interaptin was detected by mAb 260-60-10. Sun-1 was probed for mAb K55-432-2. During the development of AX2, Sun-1 and the small isoform of interaptin (160 kDa) were constitutively expressed. The large isoform of interaptin was upregulated 8 hrs after the onset of development. B. Sun-1 expression was not affected upon alteration of the expression level of interaptin. As a loading control actin is displayed using mAb Act1-7.

3.4.3 Localization of Sun-1 and interaptin

To study the *in vivo* localization of endogenous Sun-1 and interaptin, an immunofluorescence analysis was carried out. In AX2 cells, interaptin localized to the nuclear envelope in a rim-like pattern as reported by Rivero *et al.* (1998) (Figure 17A and A'). Distinct from the localization of interaptin, Sun-1 was not only localized to the nuclear envelope, but also inside the nuclei (Figure 17B). Additionally, Sun-1 accumulated at one pole of the nuclei (Figure 17B and B', arrows), suggesting an association of Sun-1 with



organelles attached to the nucleus such as the centrosome or the Golgi apparatus.

We observed that alteration of the interaptin expression level did not affect the expression of Sun-1. Subsequently, we addressed the question, whether alteration in the interaptin expression level affects the localization of the endogenous Sun-1 *in vivo*. In the absence of interaptin (Figure 17C and C'), Sun-1 was localized properly to the nuclear envelope and accumulated at one pole of the nuclei (Figure 17D and D', arrows). When compared to the wildtype AX2, Sun-1 seems to be enriched in the nuclear membranes as well as in cytoplasmic membranes, probably ER membranes of the interaptin-deficient cells. The nuclear membrane localization of Sun-1 in the interaptin-deficient mutant is comparable to that of AX2 cells, demonstrating that interaptin was not required for the nuclear membrane targeting of Sun-1. However, overexpression of interaptin led to an accumulation of the protein in the nuclear and ER membranes (Figure 17E and E'). As a consequence of the interaptin overexpression, Sun-1 was displaced from the nuclear membranes and was redistributed to cytoplasmic compartments, most likely to the ER membranes (Figure 17F and F'). In stark contrast to the mammalian model, implying the essential role of SUN-1 for recruiting Nesprin-2 to the ONM (Padmakumar *et al.*, 2005), our findings indicate a competition between Sun-1 and interaptin for the localization to the nuclear membranes in *D. discoideum*.

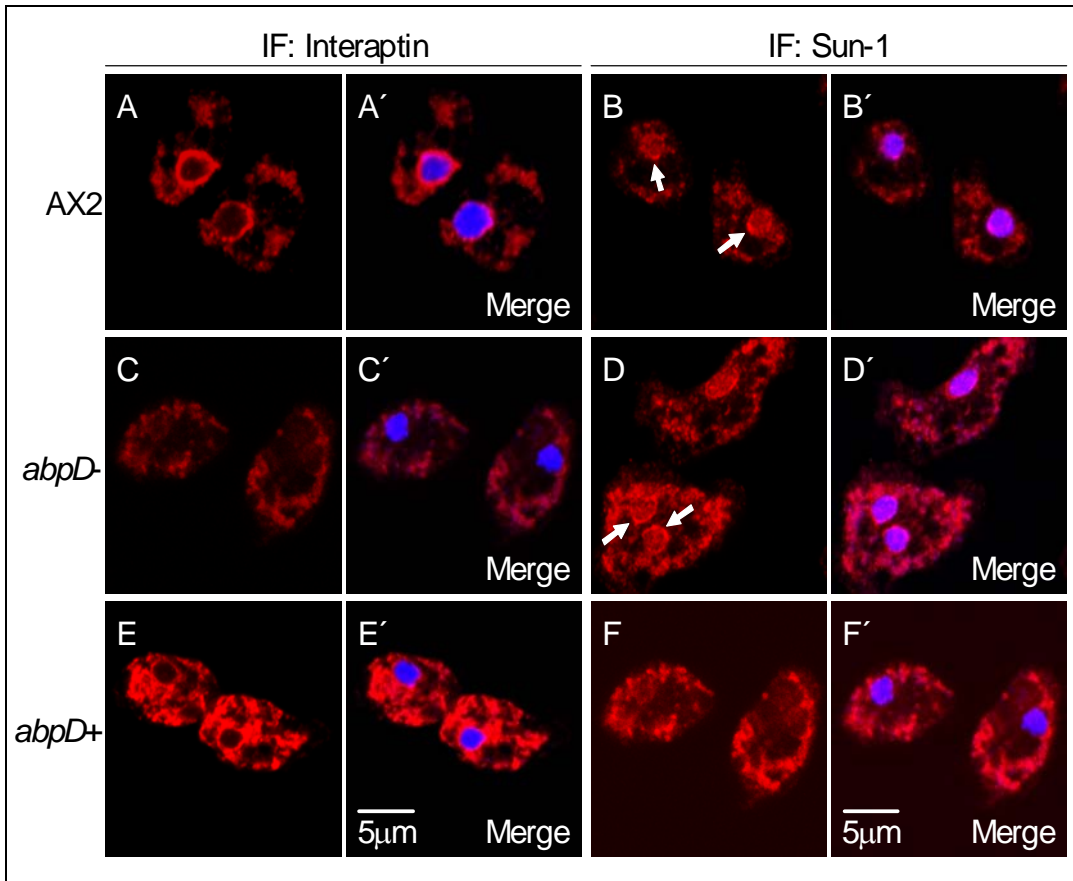


Figure 17: Subcellular localization of Sun-1 in AX2 cells, interaptin over-expressing (*abpD+*) and interaptin knockout (*abpD-*) strains using mAb K55-460-1 against Sun-1 or mAb 260-60-10 against interaptin (red). The secondary antibodies, goat-anti-mouseIgG, were conjugated with Cy3 (red). Nuclear DNA was visualized by DAPI staining (blue). **A and A'**: In AX2 cells, interaptin was predominantly localized to the nuclear envelope. **B and B'**: Sun-1 was localized to the nuclear envelope and also to the nucleoplasm. At distinct sites, Sun-1 accumulated at one pole of the nuclear envelope (arrows). **C and C'**: In the interaptin deficient strain, the protein was absent from the nuclear membranes. **D and D'**: Nuclear envelope localization of Sun-1 was unaffected in the absence of interaptin. To some extent, Sun-1 appeared to be enriched in the nuclear envelope compared to that observed in AX2. The accumulation of Sun-1 to a pole in the nuclear envelope was also observed (arrows). **E and E'**: Due to the overexpression, interaptin was accumulated both in the nuclear and ER membranes. **F and F'**: In interaptin overexpressing cells, Sun-1 was displaced from the nuclear membranes and accumulated in peripheral ER membranes.



3.4.4 The KASH motif of interaptin is required for nuclear membrane targeting

In previous studies, the C-terminal domain (amino acid 1441 to 1737) spanning the transmembrane domain and the C-terminal tail of interaptin has been demonstrated to be sufficient for nuclear envelope targeting (Rivero *et al.*, 1998) which is in line with the fact that KASH domain proteins are targeted to the nuclear envelope by their KASH domains. Particularly, the conserved KASH motif G-P-P-P-(T/L) interacts with SUN domain proteins thus is important for nuclear envelope targeting of the KASH domain proteins. Comparison of the interaptin C-terminal tail with those from *C. elegans* Anc-1, *D. melanogaster* Msp-300/Nesprin and mammalian Nesprin-1 and 2 revealed that the terminal two amino acids P-T may represent a putative KASH motif in interaptin. To address the putative KASH motif of interaptin, two peptides were expressed in AX2 cells (Figure 18A): (1) GFP tagged C-terminal tail lacking the final amino acids P-T, designated as GFP-IntCT- Δ PT. (2) GFP tagged C-terminal tail bearing an amino acid exchange of proline (1736) to alanine, termed GFP-IntCT-P/A.

The terminal amino acids PT play an important role in the nuclear envelope targeting of interaptin, as both GFP-IntCT- Δ PT and GFP-IntCT-P/A failed to localize to the nuclear envelope and accumulated in cytoplasmic compartments such as the peripheral ER and Golgi apparatus (Figure 18B, middle and bottom panel). Conversely, the endogenous interaptin bearing the functional KASH motif as well as the wildtype C-terminal domain, GFP-IntCT (Rivero *et al.*, 1998) were recruited to the nuclear envelope (Figure 18B, top and middle panel). Thus, we conclude that the proline 1736 is involved in nuclear envelope targeting of interaptin. Furthermore, expression of GFP-IntCT-P/A may have mild effects on the targeting of the endogenous interaptin, since the latter was localized in the nuclear envelope in a punctuated fashion and some amount of the protein was observed in the peripheral ER and Golgi apparatus.

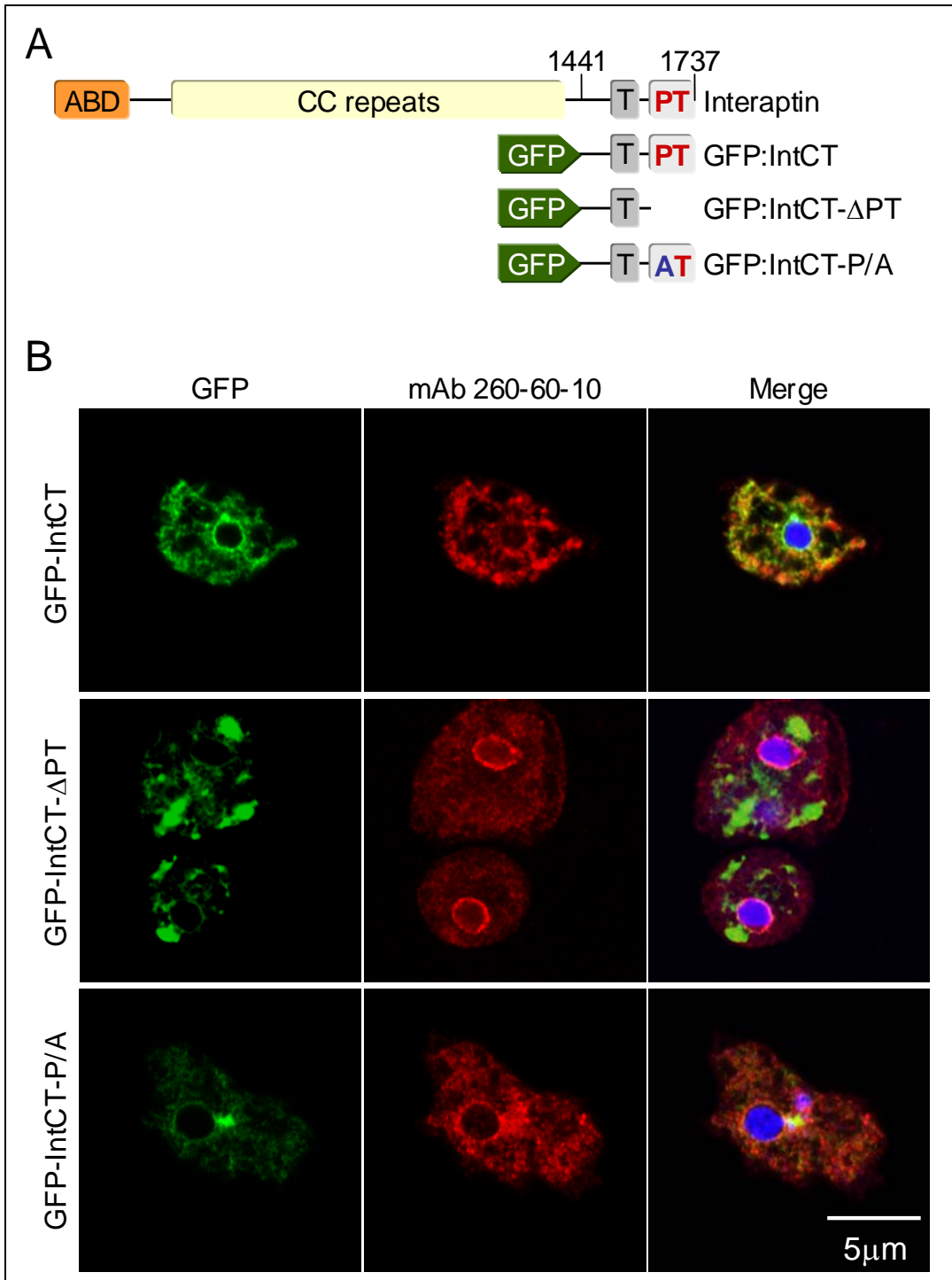


Figure 18: Localization of KASH motif mutants in AX2 cells. **A.** GFP tagged KASH domain of interaptin (GFP-Interaptin, Rivero et al., 1998). GFP tagged KASH domain lacking the KASH motif P-T (GFP-Interaptin-ΔPT). GFP tagged KASH domain with an amino acid exchange of proline 1736 to alanine (GFP-Interaptin-P/A). **B.** GFP-Interaptin was localized to the nuclear envelope displacing the endogenous interaptin from there. GFP-Interaptin-ΔPT mislocalized to peripheral ER and Golgi apparatus and did not interfere with the nuclear envelope localization of the endogenous interaptin. GFP-Interaptin-P/A was retained in the Golgi apparatus. To some extent, GFP-Interaptin-P/A affected the localization of endogenous interaptin that was found in the Golgi apparatus and stained in a punctuated fashion in the nuclear envelope. DNA was stained with DAPI.



3.4.5 The KASH motif of interaptin competes with Sun-1 for the nuclear membrane localization

In stark contrast to the models proposed for *C. elegans*, *D. melanogaster* and mammals, interaptin competes with Sun-1 for the nuclear envelope localization in *D. discoideum*. Probably, interaptin and Sun-1 bind competitively to a common unknown binding partner. To investigate whether the C-terminal KASH motif P-T of interaptin is involved in the competition with Sun-1, localization of endogenous Sun-1 was studied in AX2 cells expressing GFP-IntCT, GFP-IntCT- Δ PT and GFP-IntCT-P/A using immunofluorescence.

However, mislocalization of Sun-1 in cells expressing GFP-IntCT correlated with the increase in the expression level of GFP-IntCT: In cells overexpressing GFP-IntCT, Sun-1 was partially displaced from the nuclear envelope contrasting with proper nuclear envelope localization Sun-1 when GFP-IntCT was expressed at a reduced level indicates that the C-terminal domain of interaptin competes with Sun-1. (Figure 19A-D, arrow). Remarkably, the KASH motif P-T is involved in the competition between interaptin and Sun-1, since Sun-1 was found in the nuclear envelope if GFP-IntCT- Δ PT and GFP-IntCT-P/A were mislocalized to the peripheral ER and Golgi apparatus (Figure 19E-H and I-L). Additionally, in some cells expressing GFP-IntCT- Δ PT and GFP-IntCT-P/A Sun-1 was localized to the nuclear envelope though punctuated (Figure 19B, F and J, arrowheads), but exhibited a rim-like pattern (Figure 19B, arrows). The punctuated nuclear envelope staining of Sun-1 in GFP-IntCT- Δ PT and GFP-IntCT-P/A expressing cells may be explained by the presence of the endogenous interaptin in the nuclear envelope. Due to the competition of the endogenous interaptin or GFP-IntCT with Sun-1, it failed to localize to the nuclear envelope in a rim-like fashion.

Taken together, these observations demonstrate (1) that the interaptin C-terminus exert a dominant-negative effect on the nuclear envelope localization of Sun-1 and (2) that the KASH motif of is involved in this competition of interaptin and Sun-1 for a common binding partner.

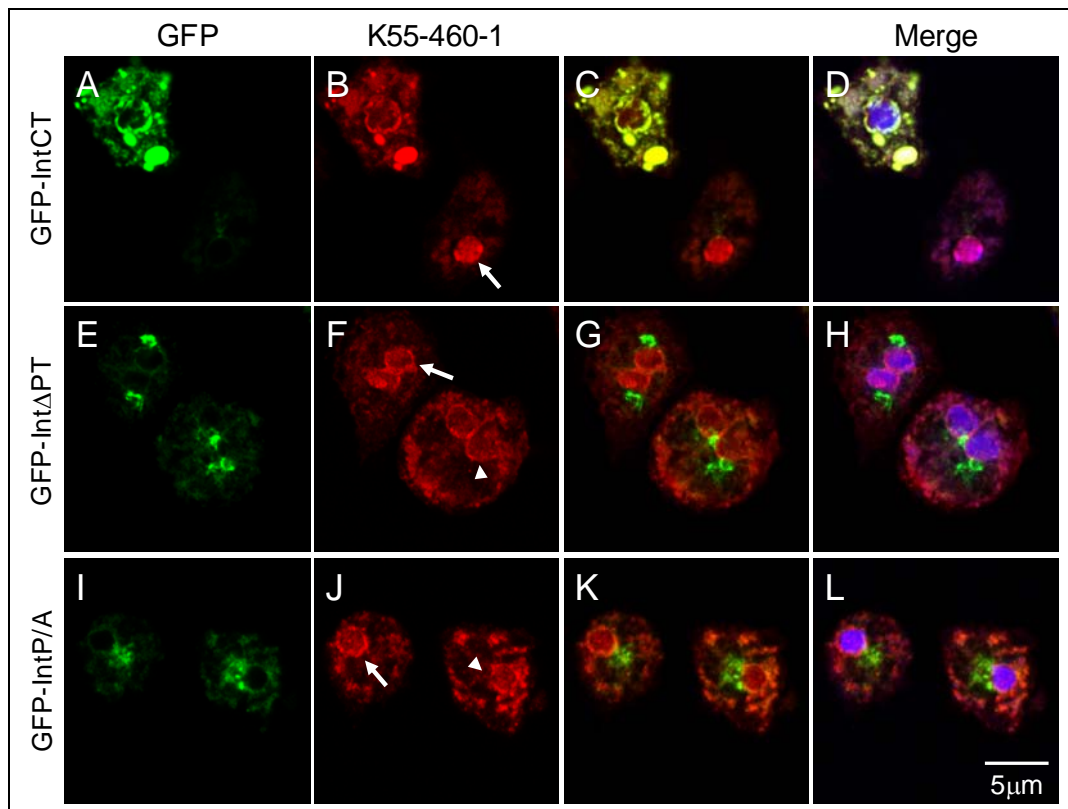


Figure 19: KASH domain of interaptin is capable to displace the endogenous Sun-1 from the nuclear envelope. **A.** GFP-IntCT containing the interaptin C-terminal transmembrane domain and the KASH motif localized to the nuclear envelope. **B.** Overexpression of GFP-IntCT displaced the endogenous Sun-1 from the nuclear envelope, whereas Sun-1 was not mislocalized in cells expressing low amounts of GFP-IntCT (arrow). **C.** Merged image of GFP-IntCT and Sun-1 staining. **D.** DNA was stained with DAPI (blue). **E.** GFP-Int Δ PT truncated in the C-terminal KASH motif accumulated in the peripheral ER and Golgi apparatus. **F.** Sun-1 was localized in a rim-like pattern to the nuclear envelope in GFP-IntCT- Δ PT (arrow). In some cells, Sun-1 was also found in a punctuated pattern (arrowheads). **G.** Merged image of GFP-IntCT- Δ PT and Sun-1 staining. **H.** DNA was stained with DAPI. **I.** GFP-IntCT-P/A, carrying an amino acid exchange P 1736 to A, was restricted to the Golgi apparatus. **J.** Sun-1 was detected both in a rim-like pattern (arrow) and in a punctuated pattern (arrowheads) in the nuclear envelope of GFP-IntCT-P/A cells. **K.** Merged image of GFP-IntCT-P/A and Sun-1 staining. **L.** DNA was stained with DAPI. Indirect immunofluorescence was carried out using K55-460-1, secondary antibodies goat-anti-mIgG was conjugated with Cy3. Images were acquired using confocal microscopy.



3.5 N-terminal truncation of Sun-1

3.5.1 Expression of GFP- Δ NSun-1 deforms the nucleus

Evidences from proteinase K protection assay demonstrated that the endogenous Sun-1 adopts the membrane topology of type II transmembrane proteins, exposing the N-terminus to the nucleoplasm. Combining the results from the proteinase K protection assay with that obtained from the chromatin immunoprecipitation assay, it is likely that chromatin association of the N-terminus may be required for the INM targeting of Sun-1 in *D. discoideum*. To validate the function of the N-terminus of Sun-1 in nuclear envelope targeting, a construct, encoding an N-terminal truncation (GFP- Δ NSun-1), was expressed in AX2 cells.

However, truncation of the N-terminus did not abrogate the nuclear envelope localization of GFP- Δ NSun-1 (Figure 20D-F) that is comparable to the endogenous Sun-1 in wildtype AX2 cells (Figure 20A-C), demonstrating that the N-terminus is dispensable for the nuclear envelope targeting of Sun-1. In parallel, this finding suggests that the C-terminal ER retention signal (SDEL) may be sufficient to target GFP- Δ NSun-1 to the rough ER from which GFP- Δ NSun-1 was further distributed to the nuclear envelope. Intriguingly, we observed frequently membrane blebs in the nuclear envelope, which did not contain DNA, hinting at deformations caused by GFP- Δ NSun-1 expression (Figure 20D and F, arrows). Additionally, a small population of GFP- Δ NSun-1 expressing cells (ca. 10% cells) exhibited increased cell size due to enlargement of the nuclear volume and cytoplasm suggesting that GFP- Δ NSun-1 cells suffer from cytokinesis defects that led to chromosome aberrations.

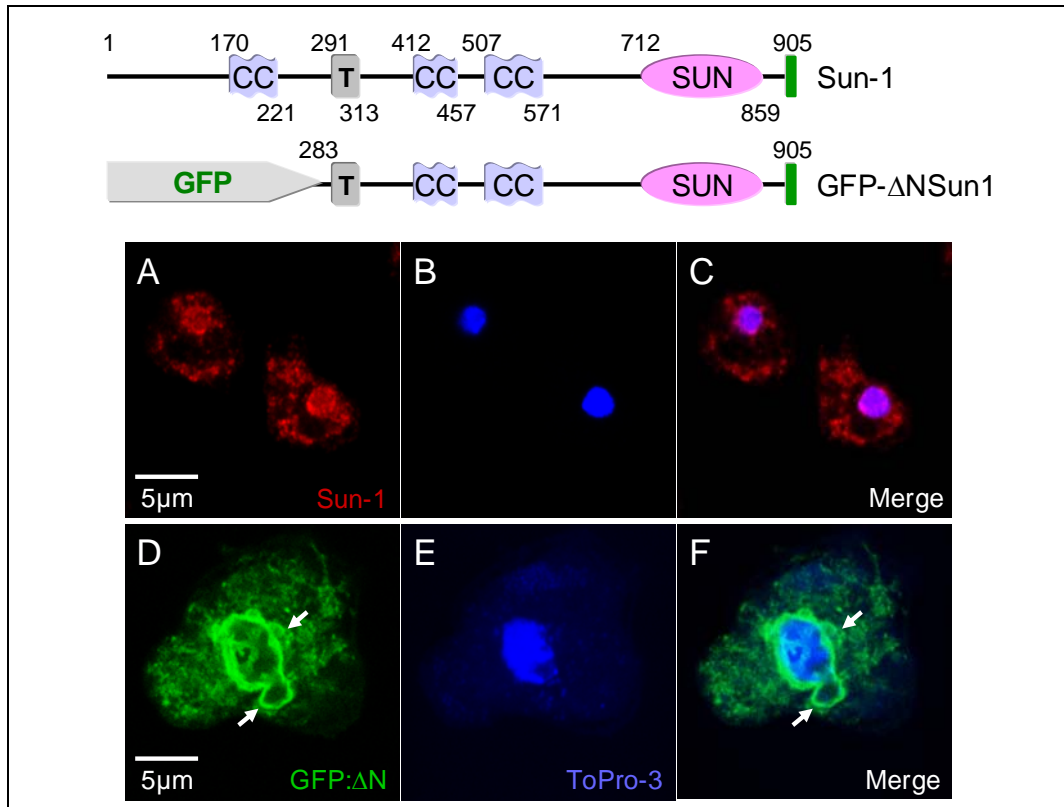


Figure 20: GFP- Δ NSun-1 caused nuclear envelope deformations. **A.** In wildtype AX2 cells, Sun-1 is localized to the envelope (mAb K55-460-1, red). **B.** DNA stained by ToPro-3 (blue). **C.** Merged image of Sun-1 (red) and DNA (blue). **D.** GFP- Δ NSun1 is targeted to the nuclear envelope (green). Expression GFP- Δ NSun1 caused nuclear envelope deformations (arrows) and an increase of the nuclear volume. **E.** DNA stained by ToPro-3 (blue). **F.** DNA was absent from the nuclear envelope blebs (arrows).

3.5.2 GFP- Δ NSun-1 causes aneuploidy

The GFP- Δ NSun-1 expressing cells may suffer from cytokinesis defects that led to formation of huge nuclei, indicating a tendency for polyploidy. To evaluate the karyotype, condensed chromosomes were arrested in the metaphase by addition of the mitotic spindle depolymerizing drug nocodazole (Figure 21A). The karyotype of wildtype AX2 cells and GFP- Δ NSun-1 expressing cells was evaluated for 400 nuclei; the evaluation was repeated in three individual experiments.

The haploid genome of wildtype AX2 cells is constituted by six chromosomes per nucleus (Figure 21A, circles), which was found in 83% of



the cells though occasionally, seven chromosomes were observed that encodes the ribosomal DNA (rDNA) (Figure 21B). In GFP- Δ NSun-1 expressing cells, the ratio of the nuclei displaying the wildtype karyotype of six chromosomes (Figure 21A, boxes) was reduced to 30% of the nuclei (Figure 21B). Accordingly, nuclei containing five (Figure 21A, circle), four and three chromosomes were found in 25%, 20% and 10% of the nuclei (Figure 21B). The increased amount of nuclei containing less than six chromosomes indicate, that GFP- Δ NSun-1 expressing cells exhibited a tendency for aneuploidy but not polyploidy. The observation of aneuploidy due to GFP- Δ NSun-1 expression is surprising, since enlargement of the nuclei hint at polyploidy. Hence, GFP- Δ NSun-1 expression may lead to a loss of the tension in the nuclear envelope that caused nuclear deformations and also expansion of the nuclear volume, which was not compensated by the endogenous Sun-1.

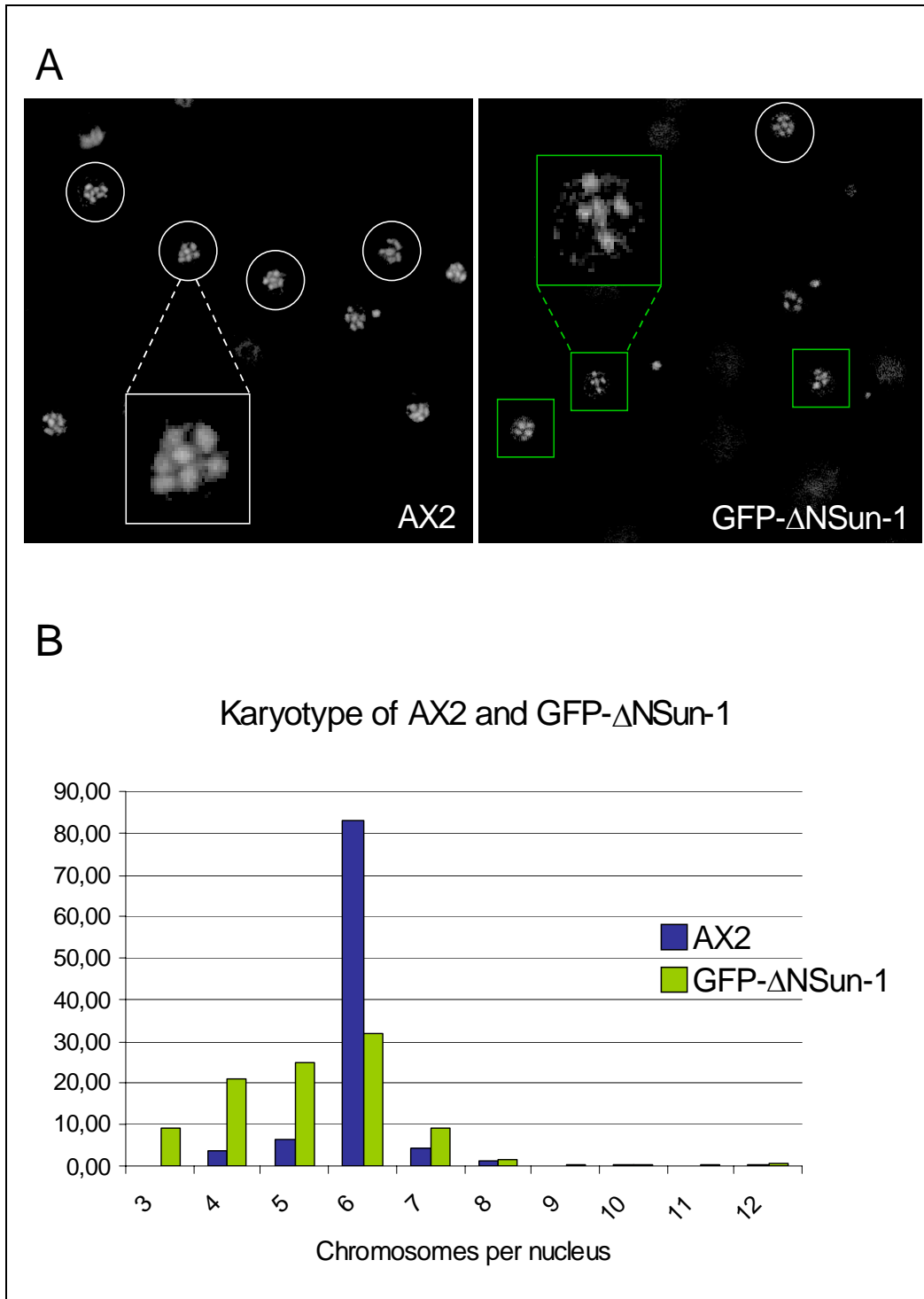


Figure 21: GFP- Δ NSun-1 cells exhibited aneuploidy. The percentage of chromosomes per nuclei was calculated from 400 nuclei each in three independent evaluations. **A.** AX2 and GFP- Δ NSun-1 cells were treated with 10 μ g/ml nocodazole to visualize the chromosomes, stained using DAPI. The haploid genome of AX2 cells constituted by six chromosomes and an additional chromosome encoding rDNA (circles, enlarged white box), whereas some cells expressing GFP- Δ NSun-1 displayed a tendency for aneuploidy with five chromosomes (boxes, enlarged green box). **B.** Evaluation of the karyotypes in AX2 cells and GFP- Δ NSun-1 cells. The majority of nuclei in AX2 cells contained six chromosomes (83%, blue). In GFP- Δ NSun-1 cells,



the karyotype varied from three to six chromosomes (10%, 20%, 25% and 30%), indicating a tendency for aneuploidy (green).

3.5.3 GFP- Δ NSun-1 accumulated at the ONM

To address the mechanism underlying the effect of aneuploidy in GFP- Δ NSun-1 cells, we set out to determine the topology and the localization of GFP- Δ NSun-1 in the nuclear envelope taking advantage of two available epitopes on GFP- Δ NSun-1: (1) GFP at the N-terminus and (2) coiled-coil domains located C-terminal to the transmembrane domain.

For this purpose, GFP- Δ NSun-1 cells were permeabilized sequentially using digitonin and Triton X-100 prior to immunofluorescence staining (Figure 22). Upon digitonin treatment, only the plasma membrane was permeabilized, the anti GFP-specific polyclonal rabbit antibody (pAb GFP) detected GFP- Δ NSun-1 demonstrating that GFP- Δ NSun-1 was localized in the ONM exposing the N-terminus to the cytoplasm (Figure 22B). Conversely, mAb K55-460-1 failed to detect the coiled-coil domains of GFP- Δ NSun-1 and the endogenous Sun-1 after digitonin treatment, as the nuclear envelope was intact and the C-terminal epitope was inaccessible (Figure 22F). The absence of mAb K55-460-1 staining after digitonin application was in line with the findings from the proteinase K protection assay, confirming that both Sun-1 and GFP- Δ NSun-1 projects the C-terminus into the perinuclear space thus both possess the identical membrane topology. Moreover, the conserved membrane topology of GFP- Δ NSun-1 and the endogenous Sun-1 underline the potential of the C-terminal ER retention signal S-D-E-L for nuclear envelope targeting.

However, both GFP- Δ NSun-1 and the endogenous Sun-1 possess the pair of coiled-coil domains, to which the mAb K55-460-1 is targeted. Thus, after Triton X-100 permeabilization, the distribution pattern of GFP- Δ NSun-1 and the endogenous Sun-1 in the nuclear envelope was indistinguishable by immunofluorescence staining using mAb K55-460-1 (Figure 22C). Nevertheless, merging the images obtained from pAb GFP



staining after digitonin treatment with those from mAb K55-460-1 after Triton X-100 enabled a discrimination of the INM and the ONM.

At the sites of nuclear envelope blebs, the endogenous Sun-1 was targeted to the INM and was also enriched in the nucleoplasm in the cells expressing GFP- Δ NSun-1 (Figure 22D, arrow); whereas GFP- Δ NSun-1 accumulated at the ONM (Figure 22D, arrowhead). As a control, the pAb GFP predominantly localized the GFP- Δ NSun-1 in the nuclear envelope after Triton X-100 permeabilization (Figure 22G and H). However, to some extent GFP- Δ NSun-1 was also found within the nucleoplasm, which may be translocated there as a heterodimeric/oligomeric complex with the endogenous Sun-1. The reduced localization of GFP- Δ NSun-1 within the nucleoplasm when compared to that of the endogenous Sun-1 implies that GFP- Δ NSun-1 was accumulated in the ONM.

In conclusion, the N-terminus of Sun-1 may be required for the INM targeting by binding to chromatin, chromatin-associated proteins or other nucleoplasmic proteins. Although the N-terminus is dispensable for nuclear envelope localization of GFP- Δ NSun-1, which may probably be engaged by the C-terminal ER retention signal, the majority of the protein failed to localize to the INM and accumulated in the ONM.

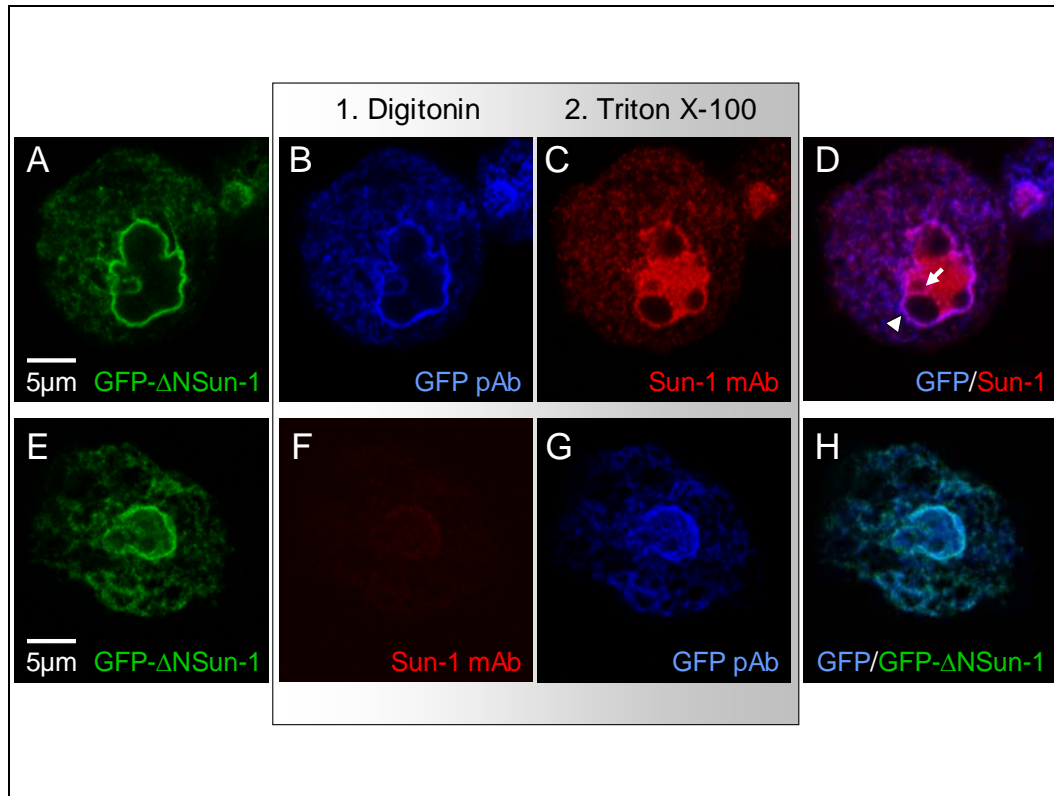


Figure 22: GFP- Δ NSun-1 was accumulated in the ONM. Sequential Digitonin/Triton X-100 permeabilization of cellular membranes was carried out prior to immunofluorescence. GFP- Δ NSun-1 was localized to the nuclear envelope (**A and E**). The N-terminal GFP tag was exposed to the cytoplasm that was proved by the staining using pAb for GFP (**B**). As digitonin does not permeabilize the nuclear envelope the mAb K55-460-1 failed to detect the coiled-coil domains of GFP- Δ NSun-1 and the endogenous Sun-1 in the perinuclear space (**F**). Finally, the nuclear envelope was permeabilized by application of Triton X-100. Consequently, both the pAb GFP antibody and the mAb K55-460-1 detected GFP- Δ NSun-1 and the endogenous Sun-1 (**C and G**). The endogenous Sun-1 is targeted to the INM (**D**, arrow), whereas GFP- Δ NSun-1 is accumulated in the ONM (**D**, arrowhead).

To further confirm the ONM localization of GFP- Δ NSun-1, nuclei were isolated from cells expressing GFP- Δ NSun-1 and stained with gold-labeled pAb GFP (Figure 23). Strikingly, GFP- Δ NSun-1 accumulated at distinct sites of the ONM, whereas the INM was not decorated with gold particles (Figure 23, bows). This supports the proposal that the N-terminus of Sun-1 may participate in the INM targeting by interaction with chromatin or chromatin-associated proteins. Interestingly, at some sites a separation of the INM and ONM was observed that may represent the nuclear envelope blebs as described above. However, those blebs were also found in nuclei



isolated from AX2 cells (data not shown), thus future statistical evaluations are required to exclude the probability of experimental artifacts. In addition to that, condensed chromatin structures were frequently found within the nuclei from GFP- Δ NSun-1 cells (Figure 23, asterisks), of which the nature is not clear yet.

Notably, finding gold-labeled pAb GFP in the INM strengthened our hypothesis that GFP- Δ NSun-1 may be translocated to the INM in a complex along with the endogenous Sun-1 (Figure 23, arrowheads). Finally, we speculate that the heterogeneous complex (composed of GFP- Δ NSun-1 and Sun-1) is functional to bridge the INM and the ONM as nuclear envelope blebs were limited to some sites. In contrast to the endogenous Sun-1, GFP- Δ NSun-1 may be unable to interact with chromatin or chromatin-associated proteins due to the truncation of the N-terminus, thus contributing to an expansion of the nuclear volume.

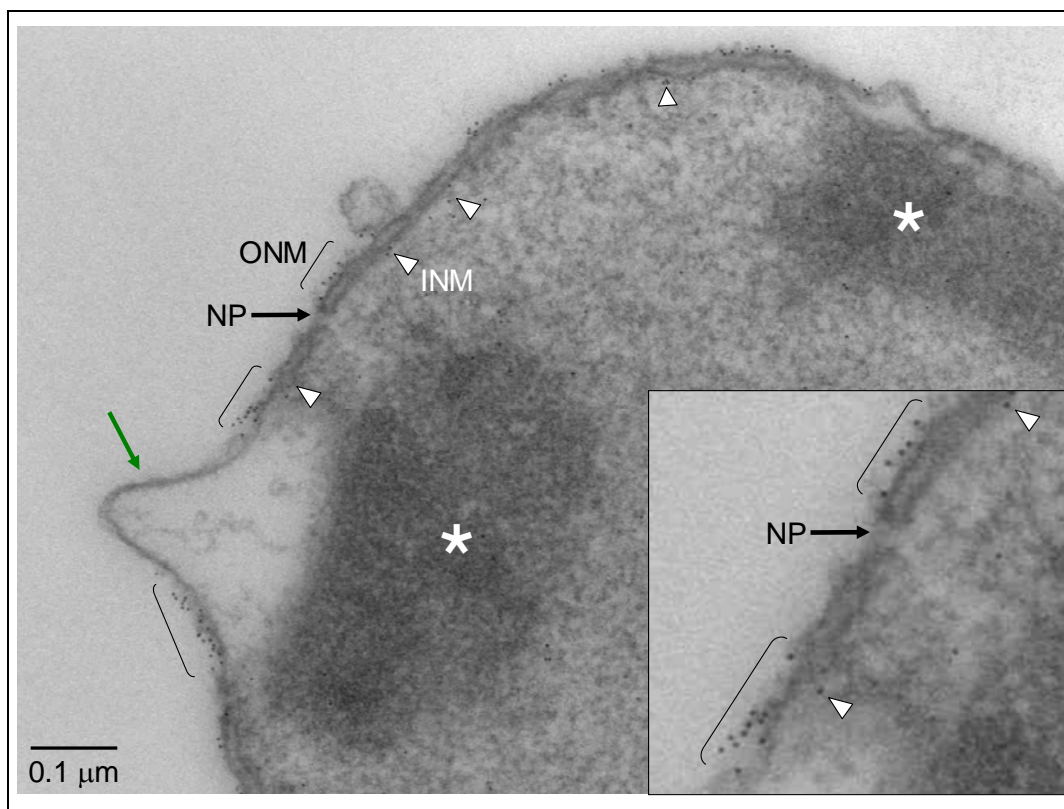


Figure 23: Electron micrograph of a nucleus isolated from GFP- Δ NSun1 expressing cells. GFP- Δ NSun-1 was labeled with gold conjugated pAb against GFP. At distinct sites, GFP- Δ NSun1 accumulated in the ONM (bows), whereas reduced amounts were also detected at the INM (arrowheads) that may be recruited to the INM by



dimerization with the endogenous Sun-1. Within the nucleoplasm, some subdomains contained condensed chromatin (asterisks). On occasion, nuclear envelope protrusions were observed to emerge from the ONM of the GFP- Δ NSun-1 cells (green arrow). The nuclear envelope near the nuclear pore (NP, black arrow) is shown in detail in the inserted box.

3.5.4 GFP- Δ NSun-1 cells formed protrusion to the centrosome

To address the nuclear envelope protrusion seen in the electron micrograph (Figure 23, green arrow), we screened the GFP- Δ NSun-1 cells for protrusions and investigated whether the endogenous Sun-1 is recruited to these sites.

To our surprise, GFP- Δ NSun-1 and/or the endogenous Sun-1 were not detected at the tip region of the protrusions using the mAb K55-460-1 (Figure 24A-D, arrowheads and magnified box). Given the evidence that the mAb K55-460-1 detected GFP- Δ NSun-1 in the proximal region of the nuclear envelope from which the protrusion emerged (Figure 24A-D, magnified box) we suggest that the tip of the protrusion may be decorated with an amount of GFP- Δ NSun-1 that was beyond the detection limit of the mAb K55-460-1. Alternatively, GFP- Δ NSun-1 may undergo dramatic conformational changes when localized to the nuclear envelope protrusion and thereby masking the epitope for the antibodies.

From the immunofluorescence experiments in interaptin mutants we suggested a competitive localization of Sun-1 and interaptin in the nuclear envelope. In concordance to that, overexpression of GFP- Δ NSun-1 displaced the endogenous interaptin from the nuclear envelope (Figure 24E-H). Furthermore, the dose-dependent competition between Sun-1 and interaptin became more evident as when GFP- Δ NSun-1 was expressed at low levels interaptin was localized to the nuclear envelope comparable to that in wildtype AX2 cells (Figure 24F, arrow), but overexpression of GFP- Δ NSun-1 caused the absence or a punctuated pattern of interaptin in the



nuclear envelope. Further, interaptin was apparently absent from the nuclear envelope protrusions (Figure 24A-D, arrowheads).

Taking into account that SUN domain proteins also interact with microtubule-associated KASH domain proteins to connect the nucleus to centrosomes, GFP- Δ NSun-1 may nuclear envelope protrusions to provide a connection to the centrosomes. Strikingly, in 90% of GFP- Δ NSun-1 cells the centrosomes were located far away from the nuclei and when protrusions were observed, they were attached to the centrosomes (Figure 24, I-L). Regarding the absence of these protrusions in wildtype AX2 cells and the interaptin mutants, these structures may specifically enable the GFP- Δ NSun-1 expressing cells to connect their nuclei to the centrosomes, though the distance between the two organelles was dramatically increased. Notably, GFP- Δ NSun-1 was not localized within the centrosome body (Figure 24K, magnified boxes), but was attached to the periphery of the centrosomes hinting at a putative protein complex in which GFP- Δ NSun-1 is involved to connect the nuclear envelope protrusion to the centrosome.

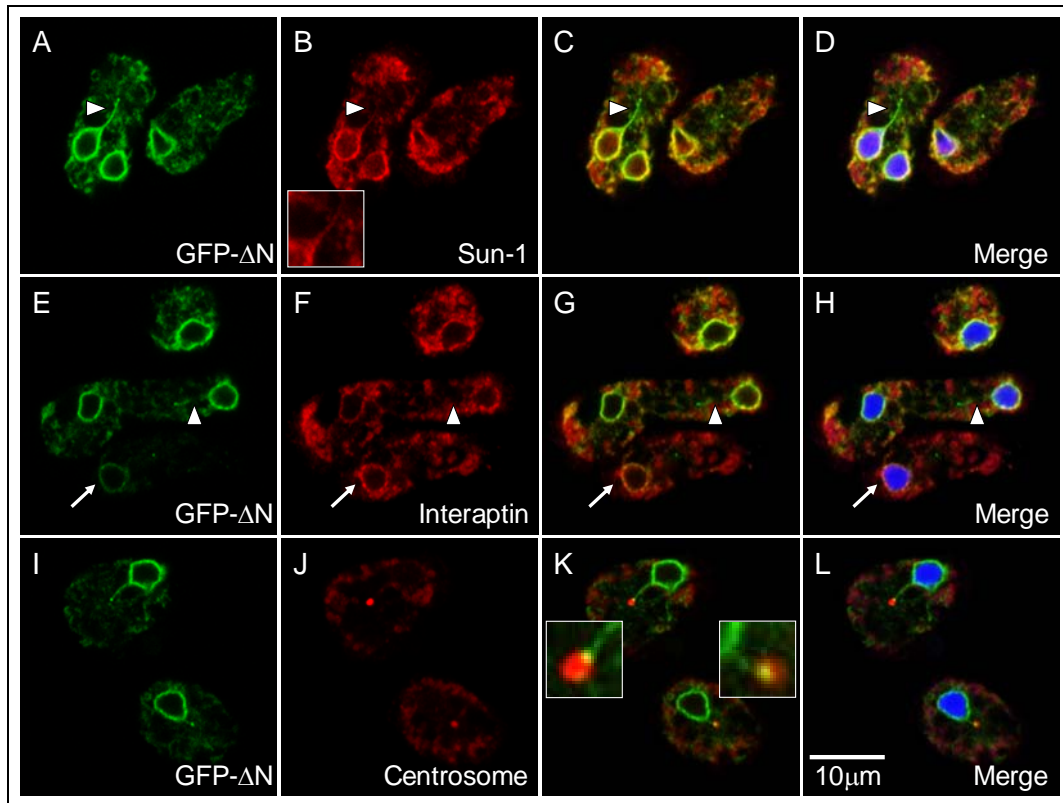


Figure 24: GFP- Δ NSun-1 cells form nuclear envelope protrusions disassociating the nucleus-centrosome proximity. DNA was visualized by DAPI (**D**, **H** and **L**). **A-D**. GFP- Δ NSun-1 was partially recognized in the proximal region of the nuclear envelope by mAb K55-460-1. At the tip of the protrusions, mAb K55-460-1 failed to detect GFP- Δ NSun-1, probably due to limited antibody sensitivities or epitope inaccessibility (arrowheads and box). **E-H**. Mislocalization of interaptin by GFP- Δ NSun-1 occurred in a dose-dependent fashion; overexpression of GFP- Δ NSun-1 displaced interaptin from the nuclear envelope, whereas basal expression of GFP- Δ NSun-1 did not (arrows). Notably, interaptin was not localized to the nuclear envelope protrusion (arrowheads). **I-L**. The nuclear membrane protrusion in GFP- Δ NSun-1 cells was connected to the centrosomes with an dramatically increased distance (mAb K29-359-31).

3.5.5 GFP- Δ NSun-1 disconnected the nucleus from centrosomes

As described before, a subpopulation of GFP- Δ NSun-1 cells (10%) exhibited severely enlarged and deformed nuclei we addressed the centrosome connection in these cells and compared to the phenotype in wildtype AX2 cells in which each nucleus was located in close proximity of



one centrosome during the interphase (Figure 25A-C) and nuclear envelope protrusions were absent..

In regular-sized GFP- Δ NSun-1 cells, the centrosomes were maintained in a central position within the cytoplasm and the nucleus number correlated with that of the centrosome (Figure 25D-F), which is comparable to the phenotype in AX2 cells. In sharp contrast, all huge cells with enlarged and deformed nuclei were disassociated even from closely located centrosomes (Figure 25D-F, magnified box) which were mislocated in the cell periphery and accompanied by an amplification of the centrosome number that did not correlate with the nuclear number (Figure 25D-F). Regardless of the cell and nucleus volume, these data clearly demonstrate that truncation of the Sun-1 N-terminus drives the centrosomes away from the nucleus and that Sun-1 may confer the proximity between the nucleus and the centrosome that probably determine the proper position of both organelles.

In correlation with the previous findings, GFP- Δ NSun-1 remained in the ONM and may bypass the bridge between the endogenous Sun-1 and a centrosome-linker leading to the formation of nuclear envelope protrusions. Probably, these protrusions were unable to withstand the mechanical force between the nucleus and the centrosome, thereby disconnecting the nucleus and centrosome in some cells, which led to the peripheral disposition of the centrosome. Consequently, division of the nucleus and centrosome occurred uncoordinated, resulting in an imbalance of the nucleus-centrosome ratio. In addition, centrosome amplification may impair the nuclear division, causing an enlargement of the nucleus. Taken together, these data indicate that (1) Sun-1 is involved in bridging the INM to a centrosome-linker in the ONM and (2) the connection of the nucleus to the centrosome is required for the accuracy of centrosome duplication in *D. discoideum*.

In contrast to other eukaryotic systems, *D. discoideum* undergoes a so-called closed mitosis, i.e. the duplicated chromosomes are segregated within the nucleoplasm that does not require a classical mitotic spindle formation within the cytoplasm. Nevertheless, the proximity between the



nucleus and the centrosome seemed important as GFP- Δ NSun-1 cells displayed a retarded growth rate when compared to AX2 cells (data not shown).

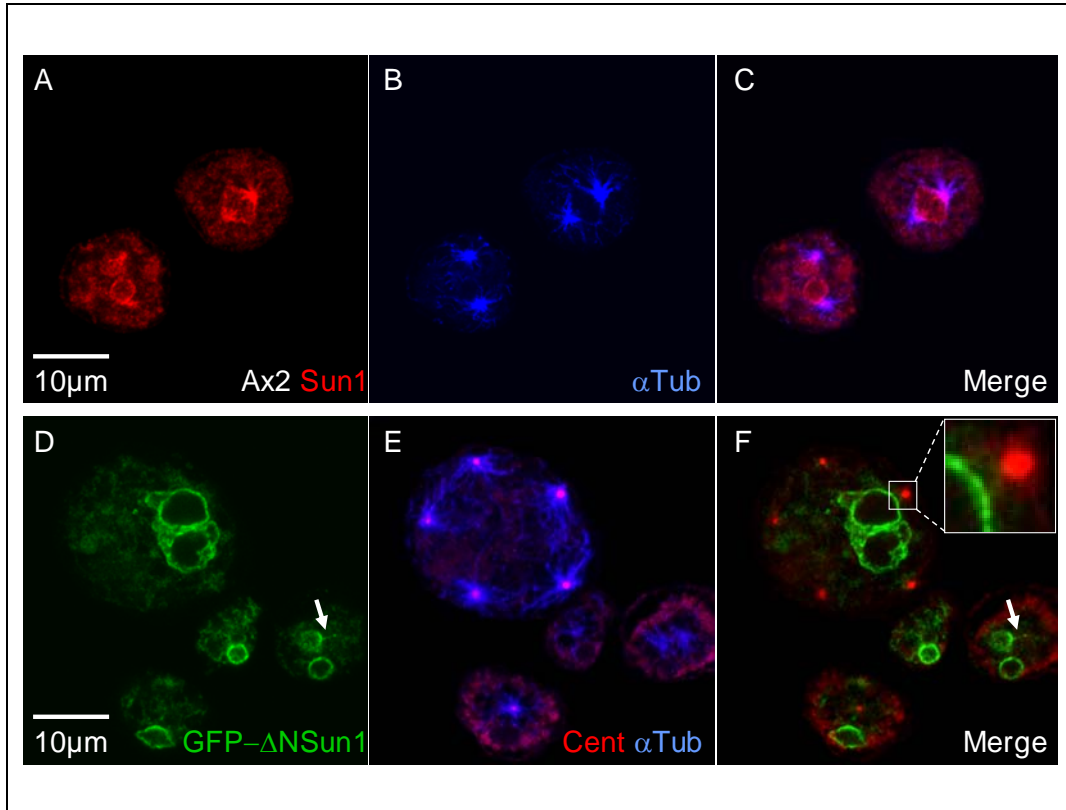


Figure 25: GFP- Δ NSun-1 expression abrogated the proximity between the nucleus and centrosome. Sun-1 was detected by mAb K55-460-1; α -tubulin was stained using rat monoclonal antibodies YL1/2 and centrosomes using mAb K29-359-31. Secondary antibodies goat-anti-mouse IgG were conjugated with Cy3 and goat-anti-rat IgG was coupled with Cy5. **A.** In wildtype AX2 cells, Sun-1 was localized to the nuclear envelope. **B.** α -tubulin staining displayed the central position of the microtubule organization center (MTOC) in wildtype AX2 cells. **C.** Merged image of Sun-1 and α -tubulin staining depicts that each nucleus was located in close proximity to one centrosome. **D.** A small population of GFP- Δ NSun-1 cells (10%) exhibited increased nuclear and cellular volume with nuclear envelope deformations. **E.** The centrosomes colocalized with the MTOC in GFP- Δ NSun-1 cells. **F.** Merged image of centrosome staining and GFP- Δ NSun-1 demonstrating that regular-sized nuclei were connected to the centrally positioned centrosome by nuclear envelope protrusions (arrow) whereas the huge nuclei were disconnected even from closely located centrosomes (magnified box). Enlargement of the nuclear and cell volume was accompanied by multiple centrosomes located in the cell periphery.



To validate the imbalance in the nucleus-centrosome ratio in GFP- Δ NSun-1 cells, approximately 400 cells were counted in three independent experiments. The average of all counting experiments was plotted in a diagram (Figure 26).

In wildtype AX2 cells, the majority of cells contained one (60.9%) or two (31.9%) nuclei whereas some were found with three (5.7%) or four (1.5%) nuclei. Independent from the total nucleus number per cell, each nucleus was associated with one centrosome in AX2 cells, demonstrating that the nucleus number correlated with the centrosome number (Figure 26B). In general, the majority of GFP- Δ NSun-1 expressing cells was represented by a population of single (total 63.7%), double (total 29.9%), triple (4.8%) and quadruple (2.0%) nucleated cells. The nucleus number in GFP- Δ NSun-1 cells is comparable to that in the wildtype cells, albeit various combinations of the nucleus and centrosome number were only found in GFP- Δ NSun-1 cells. In rare cases, cells with one nucleus contained up to eight centrosomes due to GFP- Δ NSun-1 expression (Figure 26B). In conclusion, loss of the proximity between the nucleus and centrosome in GFP- Δ NSun-1 cells caused an imbalance of the nucleus and centrosome ratio.

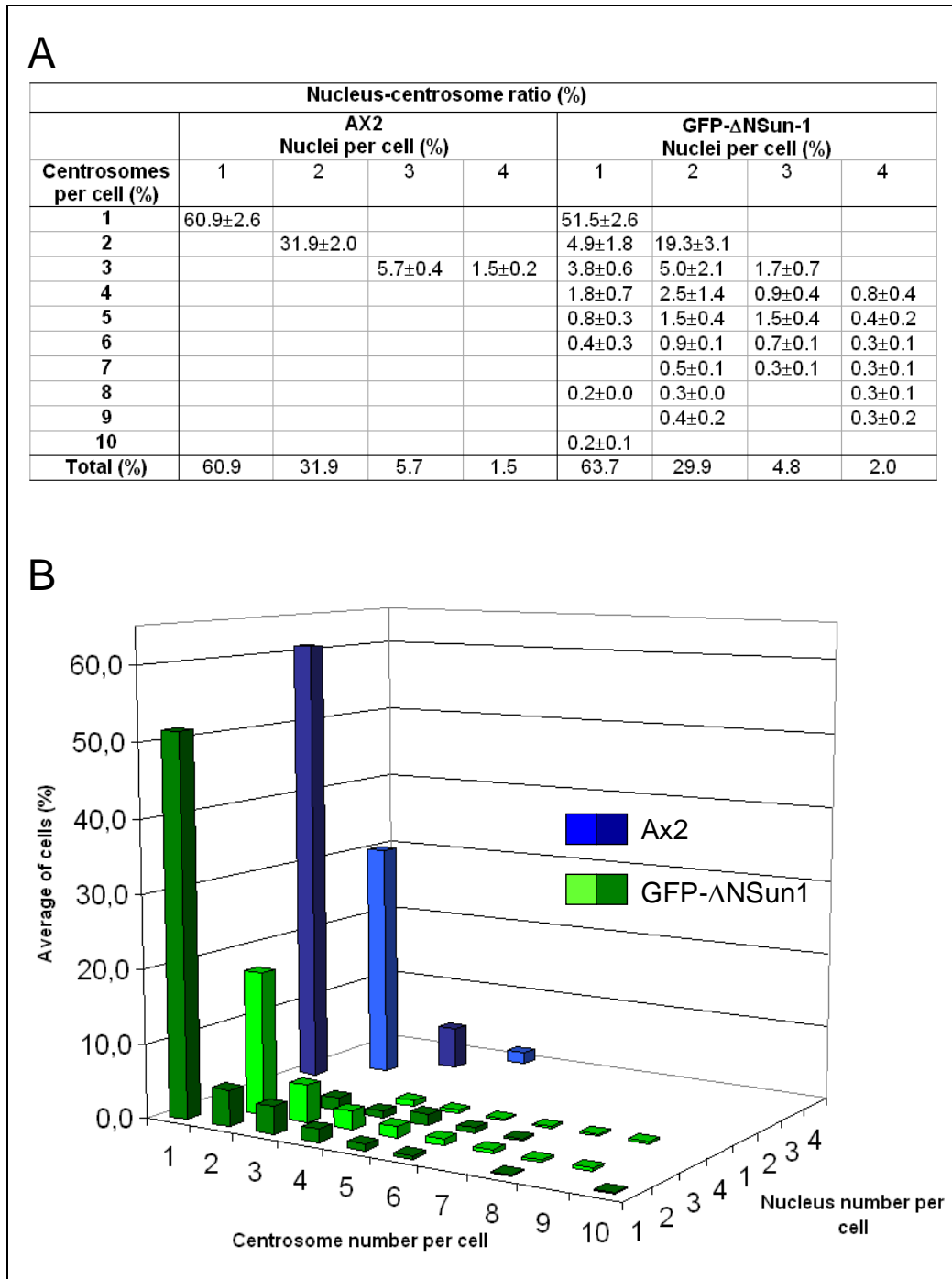


Figure 26: Imbalance of nucleus and centrosome ratio. **A.** The table summarizes the average percentage of nucleus and centrosome number in 400 cells, evaluated in three independent experiments including standard deviations. **B.** The average percentage of nuclei and centrosomes per cell was plotted in a three dimensional diagram. The ratio of nucleus and centrosome per cell correlates in wildtype AX2 (light and dark blue). In GFP- Δ NSun-1 cells, the distribution of nuclei and centrosomes displayed various combinations, e.g. some single-nucleated cells contained up to ten centrosomes (light and dark green).



3.5.6 GFP- Δ NSun-1 deformed the nucleus during intracellular movement

In *C. elegans*, mutations in the SUN domain protein UNC-84 or in the KASH domain protein Anc-1 lead to uncoordinated nuclear movement. To study the motility of the deformed nuclei, live-cell imaging experiments were performed.

The nuclear motility in GFP-intCT cells was not affected by the absence of the endogenous interaptin in the nuclear envelope and maintained a rounded shape during nuclear movement (Figure 27). This indicates that interaptin is not essential for the nuclear movement. According to the model proposed by Starr and Han (2002), interaptin bearing an actin-binding domain may be involved in nuclear positioning, a mechanism independent from nuclear movement that requires a connection of KASH domain proteins to microtubules.

Comparable to the GFP-IntCT cells, nuclei in GFP- Δ NSun-1 cells were capable to move within the cells, which may be compensated by the presence of the endogenous Sun-1 in GFP- Δ NSun-1 cells. Notably, the nuclei of GFP- Δ NSun-1 cells were dramatically deformed during nuclear movement, e.g. the nuclear envelope was stretched and squeezed to a high extent (Figure 28, arrowheads) indicating that the nuclei in GFP- Δ NSun-1 cells are exposed to higher physical stress during the nuclear movement which may be attributed to the accumulation of GFP- Δ NSun-1 in the ONM. Further on, the nuclear envelope formed temporary protrusions in GFP- Δ NSun-1 cells that may hint at a connection to the centrosomes at distinct sites (Figure 28, arrows). However, such protrusions were not observed in GFP-IntCT expressing cells, indicating that the endogenous Sun-1 and GFP- Δ NSun-1 may provide a link to microtubules or centrosomes in which interaptin is not required.

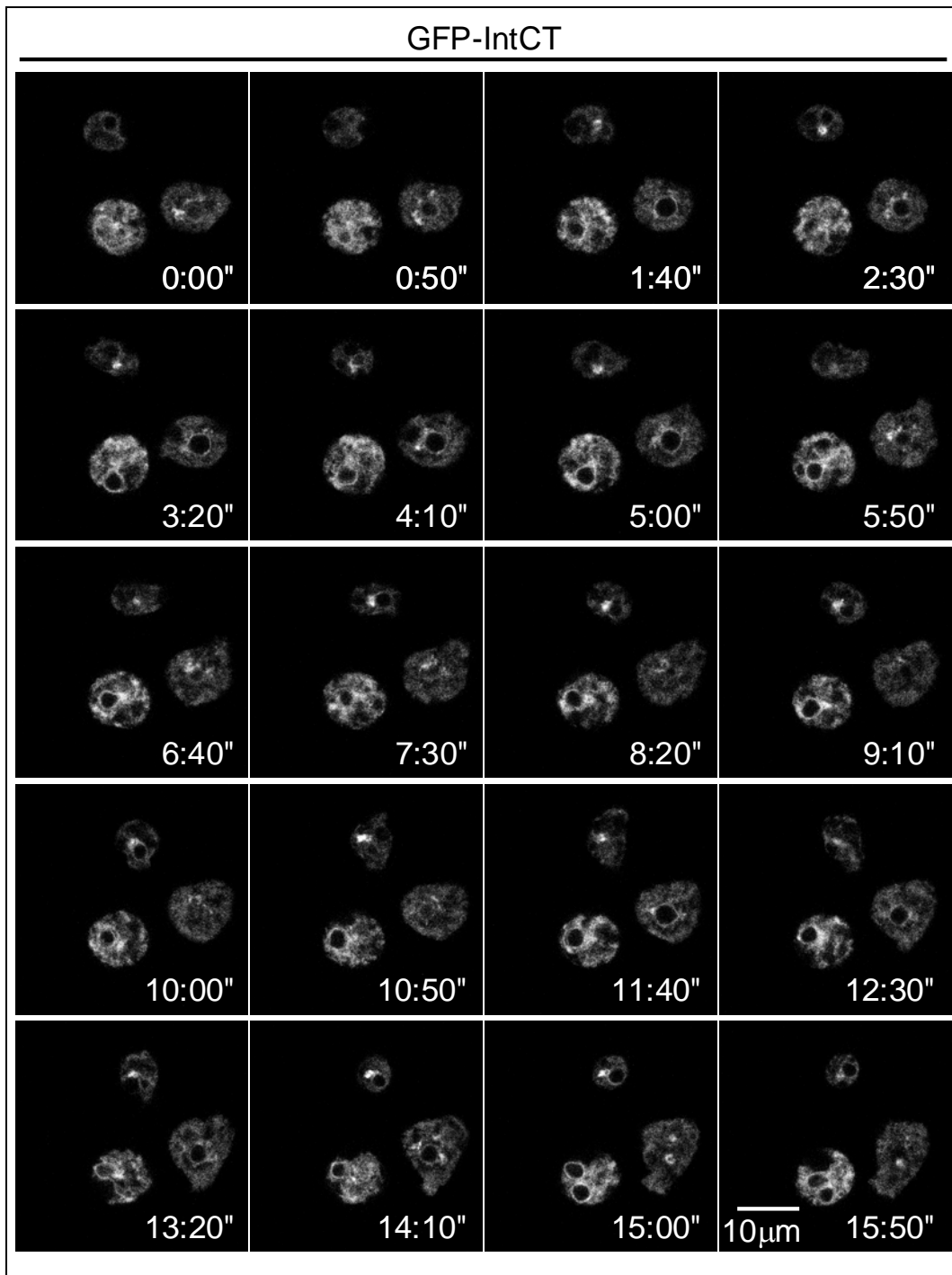


Figure 27: Live-cell imaging of GFP-IntCT expressing cells. Images were acquired every 10 sec over a time period of 15 min and 50 sec. To summarize the time period, images with a time lapse of 50 sec were displayed. The nuclei of GFP-IntCT cells were motile within the cytoplasm and maintained a rounded shape during the nuclear movement.

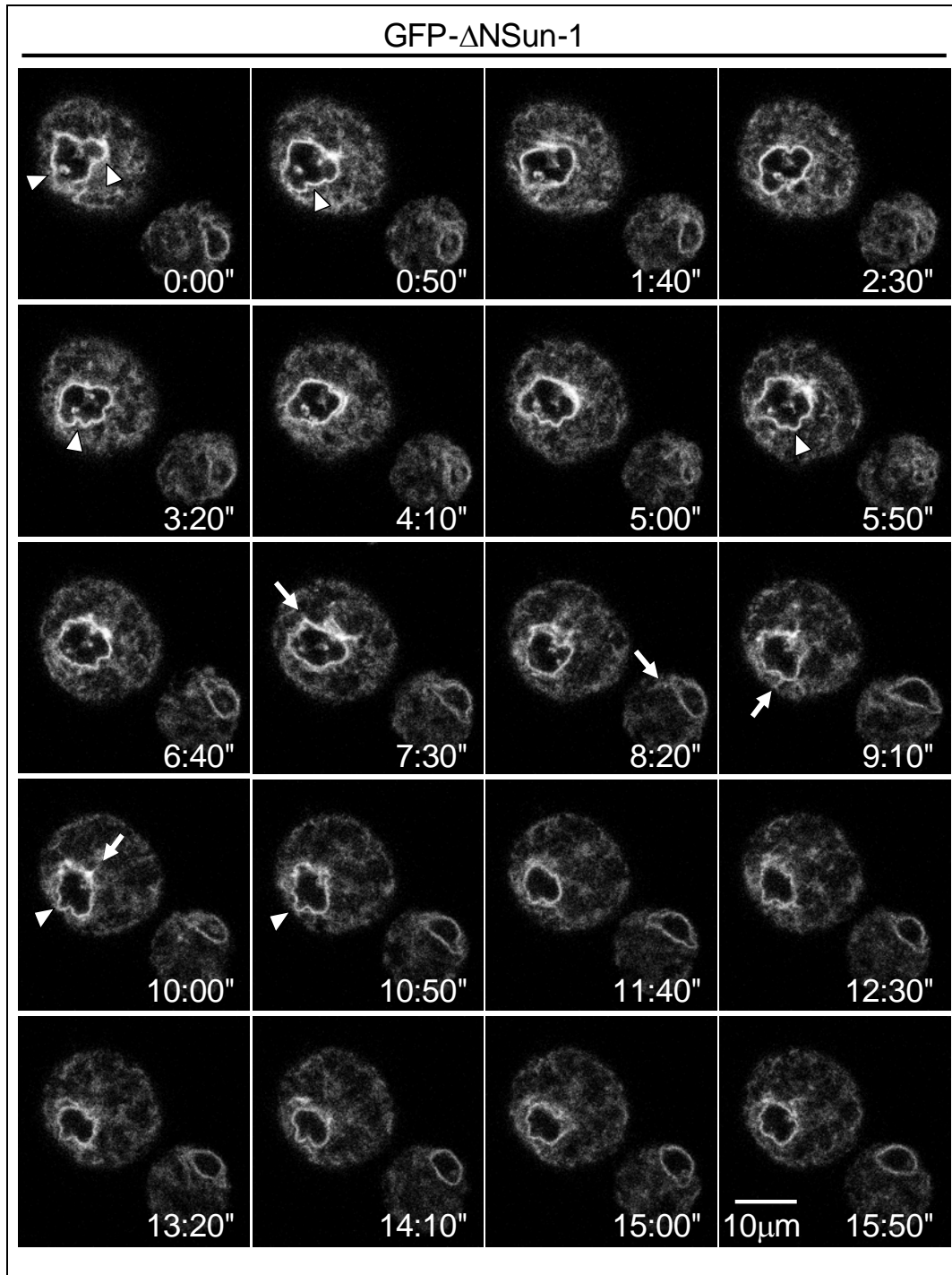


Figure 28: Nuclei in GFP- Δ NSun-1 cells experience higher mechanical stress during the intracellular movement. Live-cell images were acquired every 10 sec for a total time of 15 min 50 sec. Representative images with a 50 sec time lapse were displayed. In GFP- Δ NSun-1 expression did not affect the nuclear motility but the nuclei were deformed to a high extent when moving within the cells (arrowheads). Moreover, the nuclear membrane formed distinct protrusions (arrows), probably a connection to centrosomes.



4 Discussion

4.1 SUN domain proteins in *D. discoideum*

Analysis of the genome revealed the presence of two single-copy genes located on chromosome 2 and 4, respectively, encoding for the putative SUN domain proteins in the *D. discoideum* proteome, termed Sun-1 and Sun-2. To gain insight into the domain architecture of Sun-1 and Sun-2, the protein sequences were analyzed using the programs SMART and InterProScan.

Sun-1 contained an N-terminal coiled-coil domain, one transmembrane domain, a further pair of coiled-coil domains followed by a C-terminal SUN domain (Figure 5A). Based on the homology in the SUN domains, SUN domain proteins form three major groups: SUN domain proteins, SUN-like proteins and HECD1. Sun-1 of *D. discoideum* shares high homology with *C. elegans* UNC-84, mammalian Sun-1 and Sun-2 and is thus included in the group of the classical SUN domain proteins. Remarkably, the final amino acids S-D-E-L at the C-terminus of Sun-1 represent an ER retention signal, which was not found in SUN domain proteins from other eukaryotes and is therefore unique for Sun-1 of *D. discoideum*. In worm and mammals, the N-terminal domain of SUN domain proteins appears to be responsible for the INM targeting and interacts with lamins, which form the major component of the nucleoskeleton (Crisp et al., 2006; Grady et al., 2005; Haque et al., 2006; Malone et al., 1999; Padmakumar et al., 2005). Contrasting the higher eukaryotes, *D. discoideum* lacks lamins. Thus, the presence of an ER retention signal in the C-terminus of Sun-1 may be required for ER targeting from which integral proteins are supposed to diffuse into the nuclear envelope (Soullam and Worman, 1995). Further, in the absence of lamins, Sun-1 may interact with lamin-like nucleoskeleton components yet to be elucidated. Alternatively, Sun-1 may also be an ER resident protein as some SUN domain proteins, such as human Sun-3, appeared to be targeted predominantly to the ER, though an ER retention



signal was absent (Crisp *et al.*, 2006). So far, the function of the ER-associated SUN domain proteins remains unclear, but may be distinct from that of the classical SUN domain proteins UNC-84 and matefin/Sun-1 (Malone *et al.*, 1999; Fridkin *et al.*, 2004), mammalian Sun-1 and 2 (Crisp *et al.*, 2006; Haque *et al.*, 2006; Padmakumar *et al.*, 2005).

The overall structure Sun-2 in *D. discoideum* is constituted of an N-terminal transmembrane domain, a coiled-coil domain, a central SUN domain and a C-terminal histone-deacetylase (HDAC) interaction domain (Figure 5B). Although SUN domain proteins display great varieties in their domain structure, the majority possesses a C-terminally located SUN domain. However, proteins containing a centrally located SUN domain are not only found in *D. discoideum* but also in *S. pombe*, *S. cerevisiae*, *D. melanogaster* and *O. sativa*. Due to the unusual domain architecture, these proteins are designated as the SUN-like proteins (SLP). Further, the putative HDAC interaction domain in Sun-2 is a unique and interesting feature suggesting a function in gene regulation. Recently, (Tzur *et al.*, 2006) proposed new non-mechanical roles for the SUN domain proteins: Apart from the function as a mechanical nuclear envelope receptor connecting the nucleoskeleton to the cytoskeleton, SUN domain proteins may play a role in germline cell proliferation, germ-cell maintenance (Fridkin *et al.*, 2004) and activation of the apoptotic pathways (Tzur and Gruenbaum, unpublished observations). By extension of this speculation, Sun-2 may modulate the gene expression as an integral nuclear envelope protein in *D. discoideum* transducing cytoplasmic signals into the nucleoplasm and vice versa.



4.2 Subcellular localization of Sun-1

To study the Sun-1 in *D. discoideum*, mouse monoclonal antibodies were raised against the two coiled-coil domains located between the transmembrane domain and the SUN domain. The endogenous Sun-1 was localized in the nuclear envelope both in biochemical experiments (crude and discontinuous sucrose gradient fractionation assays) and in indirect immunofluorescence staining in wildtype AX2 cells (Figure 8 and Figure 9). However, the endogenous Sun-1 was not predominantly localized in the ER as reported for human Sun-3 (Crisp *et al.*, 2006), but was detected in the nuclear envelope of *D. discoideum* which was comparable to that observed for UNC-84 and matefin/Sun-1 in *C. elegans*, as well as mammalian Sun-1 and Sun-2 (Malone *et al.*, 1999; Fridkin *et al.*, 2004; Padmakumar *et al.*, 2005; Crisp *et al.*, 2006).

To confirm that Sun-1 is a transmembrane protein of the nuclear envelope, intact nuclei were isolated from wildtype AX2 cells and subjected to several extraction experiments. As shown in Figure 10, the endogenous Sun-1 was resistant to alkali (0.1M NaOH) and high salt (1M KCl) extraction indicating that Sun-1 is not peripherally anchored to the nuclear envelope. Similarly, interaptin, the first identified nuclear envelope protein in *D. discoideum* was also reported to be resistant to alkali and high salt extraction (Rivero *et al.*, 1998). Further on, when isolated nuclei were treated with Triton X-100 or urea, only small amounts of Sun-1 were extracted from the nuclear membranes, whereas a combination of the detergent and urea increased the amount of extracted Sun-1 to some extent. The strong hydrophobicity of Sun-1 is comparable to the biochemical properties of human Sun-2, which was only extracted from the nuclear envelope in the presence of both detergent and urea indicating that the insolubility was due to the direct binding to the nuclear lamina, a stable network composed of lamin A/C (Hodzic *et al.*, 2004). Nevertheless, alternative mechanisms to immobilize the SUN domain proteins in the INM are considerable, as *C. elegans* matefin/Sun-1 mammalian Sun-1 and Sun-2 can localize to the



nuclear INM in the absence of lamins (Crisp et al., 2006; Fridkin et al., 2004; Haque et al., 2006; Padmakumar et al., 2005). In this aspect, elucidating the mechanism for the nuclear envelope localization of the *D. discoideum* Sun-1 may uncover an alternate retention of the SUN domain proteins in the INM.

4.3 Sun-1 forms dimers and trimers *in vitro*

By the fact that coiled-coil domains are likely motifs to mediate oligomerization, we studied the two coiled-coil domains located between the transmembrane domain and the SUN domain of Sun-1. Our data obtained from cross-linking experiments using glutaraldehyde demonstrated that these coiled-coil domains of Sun-1 formed homodimers and homotrimers *in vitro* (Figure 11B). Moreover, when the recombinant coiled-coil domains SunCT1 was analyzed by SDS-PAGE under denaturing conditions, low amounts of stable dimers and trimers were observed in western blots suggesting that dimers and trimers exhibited a high affinity. To verify the presence of SunCT1 dimers and trimers, untreated and and chemically cross-linked SunCT1 were analyzed by liquid chromatography on a gel filtration column (Figure 11C). The fraction eluted from the column contained trimers, dimers and monomers in both the untreated and the cross-linked samples SunCT1 demonstrating that these two coiled-coil domains are capable to promote dimerization and trimerization. In addition, we addressed the question whether the recombinant SunCT1 is able to interact with the endogenous Sun-1 from AX2 total cell lysate using GST pull-down experiments. Surprisingly, the peptide sequences of a 200 kDa band coprecipitated with GST-SunCT1 matched significantly the sequence of Sun-1 (Figure 12). As a monomeric Sun-1 polypeptide is 105 kDa, we conclude that the protein of 200 kDa represents an endogenous Sun-1 dimer. Apparently, the endogenous Sun-1 formed dimers with high affinity, which were not disassembled under the denaturing and reducing conditions of the SDS polyacrylamide gel.



The strong affinity between the endogenous Sun-1 dimers was not derived from covalent disulfide bonds, since the coiled-coil domains do not harbor any cysteine residues. Instead, we identified clusters containing arginine, tryptophane, tyrosine, phenyl alanine, histidine and methionine in the coiled-coil domains which are conserved amino acid residues promoting high affinity interface association during dimerization (Bogan and Thorn, 1998; Brinda and Vishveshwara, 2005). Furthermore, these above-mentioned residues, were interspersed by several leucines and isoleucines. Though promoting weak interface association, they may trigger the strength of the dimeric and trimeric complexes along with the residues for the high affinity interactions.

Given the evidences that the recombinant SunCT1 may interact with an endogenous dimer, we suggest that Sun-1 may form functional homodimers and/or homotrimers *in vivo*. The formation of functional dimers or trimers may indicate a further feature of SUN proteins, as both mammalian Sun-1 and Sun-2 containing putative coiled-coil domains between the transmembrane domain and the SUN domain are proposed to occur as homodimers or heterodimers *in vivo* (Crisp *et al.*, 2006) which is in line with our findings. However, the affinity of the mammalian Sun-1 and Sun-2 dimers was not determined yet, but mammalian Sun-1 is likely to form stable dimers due to the presence of four cysteine residues within the coiled-coil domains (unpublished data from our laboratory). The common feature of the SUN domain proteins to dimerize and/or trimerize may provide multiple binding sites for the KASH domain proteins, thereby enhance the efficient transmission of the mechanical force to the nucleus during nuclear positioning and migration.



4.4 Sun-1 is a type II nuclear envelope protein and associated with chromatin

So far, most of the INM localized SUN domain proteins, such as *C. elegans* matefin/Sun-1, mammalian Sun-1 and Sun-2, bind with their N-terminus to Ce-lamin and lamin A, respectively, *in vitro* suggesting an INM retention mechanism which requires a common membrane topology of a nucleoplasmic N-terminus and a luminal SUN domain (Fridkin et al., 2004; Padmakumar et al., 2005; Crisp et al., 2006; Haque et al., 2006). Nevertheless, lamins may assist other players or vice versa to constitute the INM retention of the SUN domain proteins *in vivo*, as *C. elegans* UNC-84 though not binding to the Ce-lamin requires that for the nuclear envelope localization (Lee et al., 2002). Alternatively, a lamin-independent mechanism of INM retention may also be considered for the SUN domain proteins since *C. elegans* matefin/Sun-1 localized to the nuclear envelope in the absence of Ce-lamin as well as mammalian Sun-1 and Sun-2 when simultaneously depleted of lamin A, C and B1 (Fridkin et al., 2004; Padmakumar et al., 2005; Crisp et al., 2006; Hasan et al., 2006).

Contrasting the higher eukaryotes, *D. discoideum* does not contain lamins hence we were curious about the membrane topology of the endogenous Sun-1. The data obtained from the proteinase K protection assays using intact nuclei from wildtype AX2 demonstrate that C-terminus of Sun-1 is located in the perinuclear space, thereby was protected from proteinase K (Figure 13). Hence, the endogenous Sun-1 is a type II integral protein of the nuclear envelope and adopts the identical topology of *C. elegans* matefin, mammalian Sun-1 and Sun-2. Considering that the N-terminal domains of all SUN domain proteins protein do not share any sequence homology, this consistent membrane topology of *D. discoideum* Sun-1, *C. elegans* matefin, mammalian Sun-1 and Sun-2 may be a common feature of the SUN domain proteins. Owing to the capability of proteinase K to diffuse through the NPCs and digest nucleoplasmic proteins, we were unable to distinguish whether Sun-1 is predominantly located in the INM or ONM or in both membranes.



To shed light into the localization of the endogenous Sun-1 in the INM and/or ONM, we needed to overcome the unavailability of markers for these subdomains of the nuclear envelope in *D. discoideum*. Inspired by the observation that the N-terminus of *C. elegans* matefin/Sun-1 may be associated with chromatin and that downregulation of the corresponding gene *mtf-1* by RNAi led to abnormally condensed chromatin (Fridkin et al., 2004), we addressed whether Sun-1 is an INM protein that interacts with chromatin and whether this interaction is an alternate lamin-independent mechanism for INM retention in *D. discoideum*. Indeed, genomic DNA was coprecipitated with the endogenous Sun-1 by the mAb K55-460-1 in chromatin immunoprecipitation (ChIP) experiments (Figure 14). Remarkably, a putative histone-deacetylase (HDAC) interaction domain was found in the C-terminus of Sun-2 whereas binding motifs for DNA or chromatin-associated proteins were not predicted for Sun-1. However, the interaction of Sun-1 with chromatin appeared to be specific as chromatin was not coprecipitated with α -tubulin specific antibodies or the protein A-Sepharose beads. Thus, the N-terminus of Sun-1 may harbor a cryptic domain for the interaction chromatin or chromatin-associated proteins that needs to be uncovered in the future.

With respect to the evidences from the proteinase K experiments Sun-1 is likely localized in the INM with its N-terminus facing the nucleoplasm, which allows an interaction with chromatin. Moreover, we hypothesize that Sun-1 may not have preferences for specific DNA sequences in the chromatin, since this interaction may confer an alternate lamin-independent mechanism for the retention of Sun-1 in the INM of *D. discoideum*. Speculatively, the conserved membrane topology of *D. discoideum* Sun-1, *C. elegans* matefin/Sun-1, mammalian Sun-1 and Sun-2 suggests that SUN domain proteins of higher eukaryotes may also have the propensity to interact with chromatin or chromatin-associated proteins.



4.5 Sun-1 and interaptin compete for the nuclear membrane localization

In eukaryotic cells, positioning and migration of the nucleus on the cytoskeleton is proposed to occur by the interaction of the INM SUN domain proteins with the giant ONM KASH domain proteins (Starr and Han, 2002). This conserved interaction involves a binding of the C-terminal SUN domain (worm) or a region upstream to that (mammals) with the KASH motif G-P-P-P-(T/L) in the short C-terminal tail of the KASH domain proteins (Malone et al., 1999; Padmakumar et al., 2005).

In *D. discoideum*, interaptin has been reported to be a nuclear envelope protein of 200 kDa composed of an N-terminal actin-binding domain, centrally located coiled-coil domains and a C-terminal transmembrane domain including a rather short peptide tail of 16 amino acids (Rivero et al., 1998). The overall domain architecture of interaptin resembles that of the KASH domain proteins found in *C. elegans*, *D. melanogaster* and mammals leading to the hypothesis that interaptin represents a candidate KASH domain protein in *D. discoideum*. Further, the dominant-negative effect of the interaptin C-terminal transmembrane domain including the tail sequence to localize to the nuclear envelope and displace the endogenous interaptin is in line with the features of the KASH domain of the *C. elegans* Anc-1 and UNC-83, *D. melanogaster* Klarsicht, and murine giant Nesprin-1 (Grady et al., 2005; Guo et al., 2005; McGee et al., 2006; Rivero et al., 1998; Starr and Han, 2002; Zhang et al., 2001). The analysis the interaptin C-terminal tail revealed that the final two amino acids P-T resemble the final amino acids in the KASH motif of *D. melanogaster* Msp-300/Nesprin, mouse and human Nesprin-2 indicating that these two amino acids P-T may function as a KASH motif in interaptin, though not containing the complete C-terminal amino acids G-P-P-P-T. Given the similar domain architecture and a putative KASH motif, interaptin represents a potential binding partner of Sun-1 to connect the nucleus with F-actin.

As Anc-1 is a downstream partner of UNC-84 in *C. elegans*, mutations in the gene *anc-1* do not affect the expression or the localization



of the UNC-84 (Lee et al., 2002), therefore we analyzed the effect of interaptin on the expression and the localization of Sun-1 in *D. discoideum* by comparison of (1) the expression profile of interaptin with that of Sun-1 during the development and (2) the cellular localization of Sun-1 upon the alteration of the interaptin expression level. The two interaptin isoforms (160 and 200 kDa) derived from the single copy gene *abpD* through alternate mRNA splicing are expressed differently during the development (Rivero et al., 1998). Although the small interaptin isoform and Sun-1 were expressed constitutively, the upregulation of the large interaptin isoform 8 hr after initiation of the development coinciding with a minor increase of Sun-1 hinted at a role of the large interaptin in the regulation of the Sun-1 expression (Figure 16). Thus, we addressed the Sun-1 protein level in an interaptin-deficient and an overexpressing mutant. To some extent, the amount of Sun-1 was increased in the interaptin-deficient strain when compared to that in the interaptin-overexpressing mutant suggesting that the absence of interaptin may enhance the Sun-1 expression. As overexpression of interaptin did not deplete Sun-1 we suggest that interaptin does not strictly affect the Sun-1 expression *per se* but may modulate the level.

Further, we investigated the subcellular localization of Sun-1 upon alteration of the interaptin expression level (Figure 17). In wildtype AX2 cells, both Sun-1 and interaptin were localized in the nuclear envelope, whereas interaptin is not required for the localization of Sun-1, since it was accumulated in the nuclear envelope in the absence of interaptin. Surprisingly, Sun-1 mislocalized to the cytoplasm when interaptin and the interaptin KASH domain (GFP-IntCT, Rivero et al., 1998) were overexpressed, whereas basal expression levels of GFP-IntCT did not. These observations suggest a competitive localization of between Sun-1 and interaptin KASH domain in the nuclear envelope, probably by interaction with a common partner that may be quenched by high amounts of the KASH domain.



To test whether the KASH motif is required for the nuclear envelope targeting of interaptin and whether this motif competes with Sun-1, GFP-IntCT (Rivero et al., 1998) was truncated in the amino acids P-T (GFP-IntCT- Δ PT), alternatively the proline (1736) was mutated to alanine (GFP-IntCT-P/A). Intriguingly, GFP-IntCT- Δ PT and GFP-IntCT-P/A abrogated the targeting of the interaptin C-terminus to the nuclear envelope instead these proteins localized to the Golgi apparatus confirming that the final amino acids P-T as a functional KASH motif (Figure 18 and Figure 19). Taking into account that the endogenous Sun-1 and interaptin were localized to the nuclear envelope in GFP-IntCT- Δ PT and GFP-IntCT-P/A expressing cells, we suggest that Sun-1 competes with the KASH motif of interaptin in a dose-dependent manner, thus strengthening our hypothesis that Sun-1 and interaptin compete for the nuclear envelope localization.

The competition in *D. discoideum* contrasts with the findings that overexpression of the KASH domain from *C. elegans* Anc-1 and UNC-83, *D. melanogaster* Klarsicht and mammalian Nesprin-1 did not mislocalize their appropriate SUN domain proteins (Starr and Han, 2002; McGee et al., 2006; Guo et al., 2005; Grady et al., 2005; Zhang et al., 2001). Further, our observations conflicts with the common model proposed which says that SUN domain proteins of worm and mammals bind directly or indirectly to the KASH domain proteins in the nuclear envelope during nuclear positioning and migration (Starr and Han, 2002; Starr and Fischer, 2005; Wilhelmsen et al., 2006; Tzur et al., 2006).

With respect to our observations that the interaptin-deficient and overexpressing mutants do not exhibit nuclear positioning defects, we suggest that Sun-1 and interaptin may be involved in two independent mechanisms for the nuclear positioning in *D. discoideum*, which are capable to substitute their functions mutually: in the absence of interaptin, Sun-1 may interact with other KASH domain proteins in the nuclear envelope to establish nuclear positioning compensating the loss of interaptin, whereas overexpression of interaptin shifted the equilibrium to the interaptin-mediated nuclear positioning leading to mislocalization of Sun-1 from the nuclear envelope. The possibility of alternate mechanisms for nuclear positioning in



D. discoideum underscores the importance to define the nuclear position as postulated for worms, flies and mammals.

4.6 The N-terminus of Sun-1 confers INM localization

As demonstrated by the chromatin immunoprecipitation experiments, the endogenous Sun-1 may bind to chromatin (Figure 14); with respect of the topology determined by proteinase K protection assays (Figure 14), the N-terminus may be responsible for this interaction. To elucidate the function of the chromatin association, the Sun-1 N-terminus was replaced by a GFP tag (GFP- Δ NSun-1) and expressed in AX2 cells (Figure 20). GFP- Δ NSun-1 was localized at the nuclear envelope suggesting that the N-terminus is not essential for the nuclear envelope targeting. It might well be that the ER retention signal uniquely found in Sun-1 of *D. discoideum* confers nuclear envelope localization of GFP- Δ NSun-1.

As SUN domain proteins described so far and Sun-1 in *D. discoideum* do not possess any INM-specific signals (Lee et al., 2002; Fridkin et al., 2004; Hodzic et al., 2004; Padmakumar et al., 2005; Crisp et al., 2006) their INM localization may occur as proposed in the “Diffusion-Retention” model suggesting that INM proteins diffuse freely along the rER and nuclear pore membranes into the INM where they are retained by stable interactions with the nuclear lamina, chromatin or both (Ellenberg et al., 1997; Ohba et al., 2004; Ostlund et al., 1999; Smith and Blobel, 1993; Worman and Courvalin, 2000). The intriguing accumulation of GFP- Δ NSun-1 in the ONM as verified by electron microscopy using immunogold labeling as well as the selective digitonin permeabilization prior to immunofluorescence stainings proved that GFP- Δ NSun-1 exhibits the identical topology as suggested for the endogenous Sun-1 and that the truncation of the N-terminus prevents the INM localization (Figure 22 and Figure 23).



In conclusion, the endogenous Sun-1 may be retained in the INM by interaction with chromatin whereas GFP- Δ NSun-1 is not. The few immunogold particles observed in the INM may result from the diffusion of GFP- Δ NSun-1 into the INM or from the incorporation of GFP- Δ NSun-1 into a dimeric and oligomeric complex with the endogenous Sun-1 which is subsequently escorted into the INM and retained there. As matefin in *C. elegans* and mammalian Sun-1 and Sun-2 localize to the INM when lamins are depleted (Crisp et al., 2006; Fridkin et al., 2004; Haque et al., 2006; Hasan et al., 2006; Padmakumar et al., 2005) we propose that SUN domain proteins of higher eukaryotes may also engage chromatin binding for INM retention.

4.6.1 GFP- Δ NSun-1 affects the nuclear shape

Loss of GFP- Δ NSun-1 in the INM was frequently accompanied with dramatic changes in the nuclear morphology and an increase of the nuclear and cell volume in approximately 10% of cells (visual inspect, Figure 20). In these huge cells containing enlarged nuclei, we noticed nuclear envelope blebs that may result from a separation of the INM and ONM as observed in the sequentially digitonin/Triton X-100 permeabilized cells and electron microscopy. Interestingly, similar results were reported for mammalian cells devoid of both Sun-1 and Sun-2 (Crisp et al., 2006). However, the blebs were limited to some sites of the nuclear envelope implying that the effect of GFP- Δ NSun-1 on the nuclear morphology may be partially compensated by the endogenous Sun-1. As some separation of the INM and ONM was also observed in electron microscopy on nuclei isolated from wildtype AX2 cells (data not shown), further evaluations of the frequency are required to rule out the probability of experimental artifacts.

In concordance to the mislocalization of Sun-1 in the interaptin mutants, analysis of interaptin in GFP- Δ NSun-1 expressing cells confirmed the competition of these proteins for the nuclear envelope localization in a



dose-dependent manner, as interaptin was detected in the nuclear envelope of cells with a low level of GFP- Δ NSun-1, whereas the rim-like pattern of interaptin was abolished when GFP- Δ NSun-1 was overexpressed (Figure 24E-H). Occasionally, we noticed a protrusion emerging from the nuclear envelope of GFP- Δ NSun-1 expressing cells exhibiting a regular cell size comparable to that of wildtype AX2 cells (Figure 24). Paradoxically, the nuclear envelope protrusions were partially recognized by the mAb against Sun-1 (K55-460-1) but not at the tip of this protrusion, which may be due to the sensitivity of the antibodies. Another possibility is that the conformation or affinity of GFP- Δ NSun-1 dimers and/or oligomers in the tip of the protrusions may be distinct from those composed of the endogenous Sun-1 leading to inaccessibility for the antibodies. Collectively, nuclear envelope protrusions were not found in wildtype AX2 cells, the interaptin mutants and in GFP- Δ NSun-1 cells interaptin was absent from the whole protrusion, indicating that this phenotype is specific for the GFP- Δ NSun-1 expression and interaptin did not participate in the formation of these structures.

However, Zyg-12, a KASH domain protein in *C. elegans*, interacts with matefin/Sun-1 to provide the nucleus-centrosome attachment during embryonic development. Mutations in *zyg-12* are lethal for the embryos due to the centrosome disconnection that causes chromosome segregation defects (Fridkin et al., 2004; Malone et al., 2003). Likewise, Sun-1 may probably interact with a centrosome-attached KASH domain protein in the nuclear envelope to juxtapose the nucleus and centrosome. Accumulation of GFP- Δ NSun-1 in the ONM may bypass the connection to this centrosome linker, consequently causing the formation of nuclear envelope protrusions. Thus, finding a homolog of Zyg-12 is the key to prove a Sun-1-mediated connection to the centrosome.



4.6.2 GFP- Δ Sun-1 causes centrosome amplification

As the nuclear envelope protrusions in GFP- Δ Sun-1 cells seemed to be connected to a defined cellular element we set out to identify whether they are attached to the centrosomes. Indeed, the protrusions were oriented towards the centrosomes and colocalized with the pericentriolar material (Figure 24I-L). The formation of these protrusions caused a distal position of the nucleus to the centrosome in regular-sized cells, contrasting with the juxtaposition of the nucleus and centrosome in wildtype AX2 cells (Figure 25). Regardless of the nucleus-centrosome distance the number of nuclei correlated with that of the centrosomes in regular-sized GFP- Δ Sun-1 cells and wildtype AX2 cells implying that a physical connection regulate a coordinated replication of these organelles.

Interestingly, in huge cells with misshapen nuclear morphologies centrosomes were frequently found with an increased number (up to eight per cell) and were misplaced in the cell periphery instead of a central position as in wildtype cells (Figure 25). As nuclear envelope protrusions were absent in these huge cells, an imbalance of nucleus and centrosome number may be a consequence of the dissociation of nucleus-centrosome connection (Figure 26). Although *Dictyostelium* performs a closed mitosis that does not require a mitotic spindle formation, the nucleus-centrosome proximity is important for proper chromosome segregation and chromosome stability as demonstrated by an increase in aneuploidy in GFP- Δ Sun-1 expressing cells, which was not compensated by the endogenous Sun-1. Notably, aneuploidy in GFP- Δ Sun-1 expressing cells seemed to correlate with a retarded single cell growth and development (data not shown) demonstrating that an alteration of cell proliferation and apoptosis may be due to the loss of chromosomes. However, the extent and significance of the delayed growth and development need to be evaluated in the future.

When addressed the important aspect whether an increased nucleus-centrosome distance affects nuclear migration in living cells, both the huge and the regular-sized nuclei were not affected in their intracellular



motility, but their morphology was abnormal during the movement (Figure 28). In contrast, the nuclei of GFP-IntCT cells remained their rounded shape during intracellular translocation in the absence of interaptin in the nuclear envelope, thus demonstrating that interaptin may play a role in nuclear positioning, but not directly involved in nuclear migration (Figure 27). Apparently, the nuclei experienced dramatic deformations and failed to withstand the mechanical force transduced from the cytoskeleton implying that GFP- Δ NSun-1 expression may impair the nuclear stiffness or nuclear resistance to mechanical stress.

Our findings agreed well with the neoplastic characteristics of malignant tumors, in which centrosome amplification was always associated with aneuploidy (Boveri, 1914; Fukasawa, 2005; Hollander and Fornace, 2002; McKusick, 1985; Nigg, 2006; Zhu et al., 2005). To date, the mechanisms for centrosome amplification is not completely understood, but the most prevalent possibilities are (1) centrosome overduplication: A consequence of dissociation of the DNA replication cycles and the centrosome duplication combined with the loss of a centrosome-intrinsic inhibition of reduplication (Iarmarcovai et al., 2006). The well-characterized transcription factors Rb and p53 regulate the centrosome duplication by transcriptional repression of their appropriate downstream targets cyclin A and p21^{Cip/waf1} (Mantel et al., 1999; Meraldi et al., 1999; Tarapore et al., 2001). (2) Centriole *de novo* genesis: A mechanism related to overduplication favored by the absence of “template” centrioles, which may kinetically dominate the duplication machinery. In particular, *de novo* centriole generation as occurring in specialized multiciliated epithelia was mimicked by removal of centrioles in cultured cells using laser ablation or microsurgery (Khodjakov et al., 2002; La Terra et al., 2005; Shang et al., 2005). (3) Division failure: This theory suggest a dysfunction of mitotic progression and impaired DNA/chromatin metabolism could give rise to abortive mitosis with centrosome amplification as a secondary consequence that was reported for aneuploid breast cancers overexpressing of the mitotic kinase Aurora A (Ewart-Toland et al., 2003; Meraldi et al., 2004; Storchova et al., 2006).



In addition to these theories, we speculate that the physical attachment and the nucleus-centrosome proximity may coordinate the nuclear and centrosome replication in a concerted fashion and that Sun-1 in association with further centrosome-specific proteins of the ONM may provide the centrosome attachment in *D. discoideum*. Furthermore, we suggest that the nucleus-centrosome proximity may be important for the shuttling of regulatory cell cycle proteins between these organelles, given the evidences that nuclear proteins (p53, Orc2, Ocr6, RAD51) localize to and function at the centrosome (Daboussi et al., 2005; Prasanth et al., 2004; Prasanth et al., 2002; Tarapore et al., 2001), reversely, the centrosome protein centrin does so in the nucleus (Araki et al., 2001; Keryer et al., 2003).

Finally, SUN domain proteins are not only involved in the mechanical connection of the nucleus to the cytoskeleton. More diverse functions in cellular processes are attributed to these proteins, such as organization of the chromosomes, physiological influences on the fat metabolism, apoptosis and germline maturation (Chikashige et al., 2006; Fridkin et al., 2004; Greer and Brunet, 2005; Horvitz and Sulston, 1980). In addition to an alternate chromatin-mediated retention of Sun-1 in the INM, we propose that (1) interaction of Sun-1 with chromatin support the stiffness of the nucleus during intracellular migration; (2) Simultaneously, Sun-1 may provide binding sites for centrosome-linkers tethering the nucleus and centrosome in close proximity; (3) The nucleus-centrosome proximity in turn contribute to a central cytoplasmic position of the centrosome as well as chromosome stability and accuracy of chromosome segregation.



4.7 Proposed model for the function of Sun-1 in *D. discoideum*

Taken together, our data suggest that Sun-1 may form dimers or higher oligomers *in vivo*, which may be retained in the INM by binding to chromatin. The combined data of the proteinase K protection assay, the immunofluorescence and the electron microscopy experiments suggest that Sun-1 adopts the membrane topology of the type II integral proteins, thus the N-terminus is likely to interact with chromatin. The Sun-1 C-terminus projects into the perinuclear space, probably to interact directly or indirectly with a centrosome-specific linker to constitute the close proximity of nucleus and centrosome; Alternatively, Sun-1 may bind indirectly to interaptin to position the nucleus on F-actin (Figure 29A).

Truncation of the Sun-1 N-terminus abrogates the INM localization of GFP- Δ NSun-1. To some extent, low amount of GFP- Δ NSun-1 can be escorted in a complex with the endogenous Sun-1 to the INM whereas the majority of GFP- Δ NSun-1 accumulates in the ONM and counteracts the connection of the centrosome linker with the endogenous Sun-1 resulting in the formation of protrusions emerging from the nuclear envelope (Figure 29B). Subsequently, increase in nucleus-centrosome distance may lead to loss of the centrosome connection promoting the centrosome amplification and genome instability such as aneuploidy.

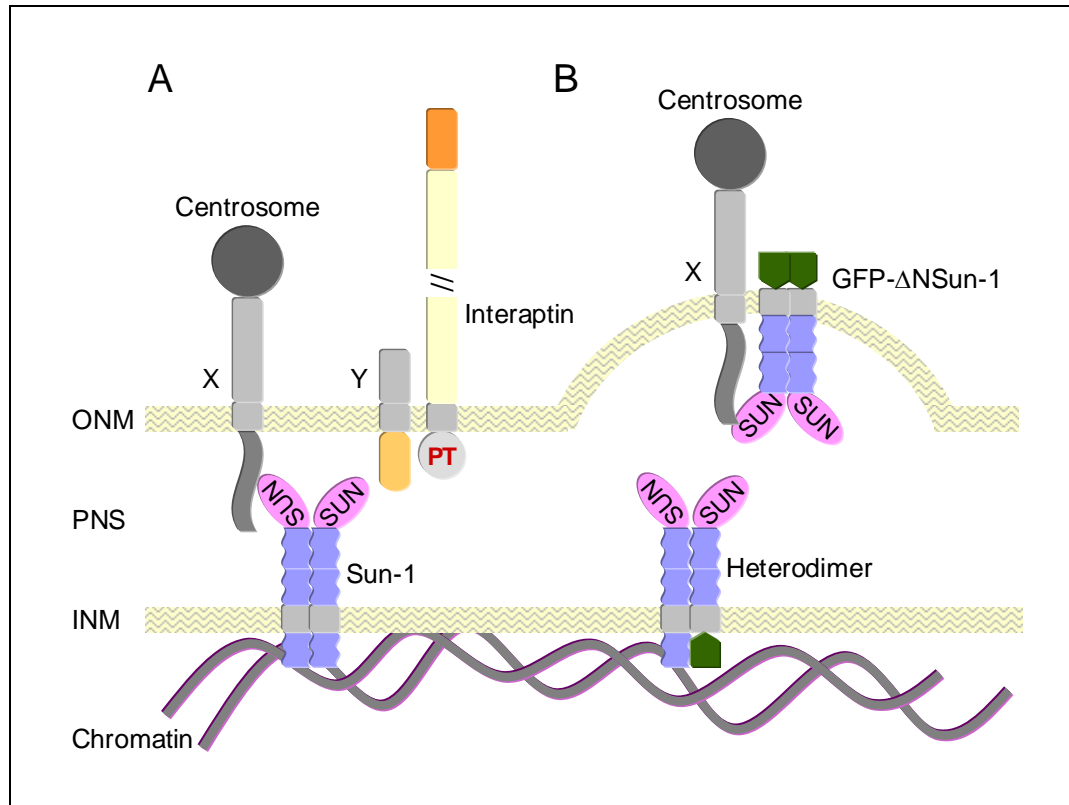


Figure 29: Proposed model for the function of Sun-1 in the INM. **A.** Sun-1 dimers may interact with chromatin to be retained in the INM. The SUN domain of Sun-1 may form a complex with centrosome linker proteins of the ONM (X) in the perinuclear space (PNS) to juxtapose the nucleus to the centrosome. Furthermore, Sun-1 may connect the nucleus to F-actin by indirect interaction with the interaptin KASH motif (PT) via a linker (Y). **B.** Truncation of the Sun-1 N-terminus abolished the INM retention of GFP- Δ NSun-1 that accumulated in the ONM. GFP- Δ NSun-1 can bypass the connection between the endogenous Sun-1 and the centrosome interaction of the SUN domain with the centrosome linker (X) leading to the formation of nuclear envelope protrusions and an increase in nucleus-centrosome distance. Loss of the nucleus-centrosome proximity results in aneuploidy caused by chromosome instability.



5 Summary

In worms, flies and mammals, the nucleus is attached to the cytoskeleton by binding of the SUN domain proteins to the KASH domain proteins in the outer nuclear membrane that connects the nucleus to either F-actin or microtubules. The association of the SUN domain proteins with both the nuclear lamina and the KASH domain proteins is attributed as a molecular bridging complex required for intracellular positioning and migration of the nucleus.

In this study, we investigated the role of Sun-1 and interaptin, a SUN and a KASH domain protein in *Dictyostelium discoideum* in nuclear positioning. In marked contrast to the model proposed for higher eukaryotes, Sun-1 and interaptin localized to the nuclear envelope in a competitive fashion, which may be due to a competitive binding to a yet unknown partner. Distinct from the higher eukaryotes, which engage the nuclear lamina for INM retention of the SUN domain proteins, an alternative mechanism may be considered for *D. discoideum* that lacks lamins. We provided evidence that Sun-1 can be immobilized in the INM by binding to chromatin probably via its N-terminus. The association of Sun-1 with chromatin may not only contribute to the formation of a bridging complex, but also control the juxtaposition of the nucleus and centrosome, as the truncation of the Sun-1 N-terminus disconnected the nucleus and the centrosome. Consequently, the disconnection may lead to chromosome instability as indicated by: (1) Nuclear envelope deformations (2) Enlargement of the nuclear and cell size (3) Tendencies for aneuploidy and (4) Amplification of the centrosome number. These data suggest that Sun-1 may regulate the nuclear shape, chromosome stability and the connection of the nuclei to the centrosomes.



6 Zusammenfassung

Untersuchungen in den eukaryotischen Modellen, Wurm, Fruchtfliege und Säuger, haben gezeigt, daß zwei konservierte Familien von Kernmembranproteinen für die definierte Position und die Translokation des Zellkerns innerhalb einer Zelle verantwortlich sind. Die Familie der KASH-Domänen Proteine sind vorwiegend in der äußeren Kernmembran verankert, wobei ihre N-Termini mit Zytoskelettstrukturen interagieren. Die zweite Familie, die SUN-Domänen Proteine, sind durch Bindung an die Kernlamina in der inneren Kernmembran verankert. Beide Vertreter dieser Familie strecken ihre C-Termini in das perinukläre Lumen zwischen der inneren und der äußeren Kernmembran und interagieren mit einander, wodurch der Zellkern an Actinfilamenten sowie Intermediärfilamenten befestigt und/oder entlang den Mikrotubuli transportiert werden kann.

Um die Verankerung und den intrazellulären Transport des Zellkerns in *D. discoideum* aufzuklären haben wir die Funktion der Proteine Sun-1 und Interaptin untersucht, die eine SUN- bzw. ein KASH-Domäne enthalten. Im Gegensatz zu den Tiermodellen haben wir eine kompetitive Lokalisation von Sun-1 und interaptin gezeigt, die vermutlich auf eine Bindung an einen unbekanntem gemeinsamen Interaktionspartner zurückzuführen ist. Da *D. discoideum* keine Kernlamina enthält, müssen die Proteine der inneren Kernmembran über einen Alternativmechanismus spezifisch dorthin dirigiert werden. Unsere Versuche haben gezeigt, daß die Interaktion von Sun-1 mit DNA die spezifische Lokalisation bestimmt, wobei der N-Terminus vermutlich essentiell ist, weil Sun-1 mit deletiertem N-Terminus in der äußeren Kernmembran verbleibt. Ähnlich wie in Invertebraten und Vertebraten bildet Sun-1 Dimere und höhere Oligomere *in vivo* und stellt eine Verbindung mit weiteren noch unbekanntem Proteinen zum Zentrosom her, welche sowohl die Distanz und eine koordinierte Zytokinese des Zellkern und Duplikation der Zentrosomen bestimmt, wodurch die Morphologie der Kernmembran und des Zytoplasmas sowie die Stabilität der Chromosomen und Zentrosomen erhalten wird.



7 References

- Apel, E.D., R.M. Lewis, R.M. Grady, and J.R. Sanes. 2000. Syne-1, a dystrophin- and Klarsicht-related protein associated with synaptic nuclei at the neuromuscular junction. *J Biol Chem.* 275:31986-95.
- Araki, M., C. Masutani, M. Takemura, A. Uchida, K. Sugasawa, J. Kondoh, Y. Ohkuma, and F. Hanaoka. 2001. Centrosome protein centrin 2/caltractin 1 is part of the xeroderma pigmentosum group C complex that initiates global genome nucleotide excision repair. *J Biol Chem.* 276:18665-72.
- Bogan, A.A., and K.S. Thorn. 1998. Anatomy of hot spots in protein interfaces. *J Mol Biol.* 280:1-9.
- Boveri, T. The Origin of Malignant Tumours. (1914) [English translation by M. Boveri (1929), Baillière, Tindall & Cox].
- Brinda, K.V., and S. Vishveshwara. 2005. Oligomeric protein structure networks: insights into protein-protein interactions. *BMC Bioinformatics.* 6:296.
- Chikashige, Y., C. Tsutsumi, M. Yamane, K. Okamasa, T. Haraguchi, and Y. Hiraoka. 2006. Meiotic proteins bqt1 and bqt2 tether telomeres to form the bouquet arrangement of chromosomes. *Cell.* 125:59-69.
- Crisp, M., Q. Liu, K. Roux, J.B. Rattner, C. Shanahan, B. Burke, P.D. Stahl, and D. Hodzic. 2006. Coupling of the nucleus and cytoplasm: role of the LINC complex. *J Cell Biol.* 172:41-53.
- Daboussi, F., J. Thacker, and B.S. Lopez. 2005. Genetic interactions between RAD51 and its paralogues for centrosome fragmentation and ploidy control, independently of the sensitivity to genotoxic stresses. *Oncogene.* 24:3691-6.
- Dreger, M., L. Bengtsson, T. Schoneberg, H. Otto, and F. Hucho. 2001. Nuclear envelope proteomics: novel integral membrane proteins of the inner nuclear membrane. *Proc Natl Acad Sci U S A.* 98:11943-8.
- Eichinger, L., J.A. Pachebat, G. Glockner, M.A. Rajandream, R. Suggang, M. Berriman, J. Song, R. Olsen, K. Szafranski, Q. Xu, B. Tunggal, S. Kummerfeld, M. Madera, B.A. Konfortov, F. Rivero, A.T. Bankier, R. Lehmann, N. Hamlin, R. Davies, P. Gaudet, P. Fey, K. Pilcher, G. Chen, D. Saunders, E. Sodergren, P. Davis, A. Kerhornou, X. Nie, N. Hall, C. Anjard, L. Hemphill, N. Bason, P. Farbrother, B. Desany, E. Just, T. Morio, R. Rost, C. Churcher, J. Cooper, S. Haydock, N. van Driessche, A. Cronin, I. Goodhead, D. Muzny, T. Mourier, A. Pain, M. Lu, D. Harper, R. Lindsay, H. Hauser, K. James, M. Quiles, M. Madan Babu, T. Saito, C. Buchrieser, A. Wardroper, M. Felder, M. Thangavelu, D. Johnson, A. Knights, H. Loulseged, K. Mungall, K. Oliver, C. Price, M.A. Quail, H. Urushihara, J. Hernandez, E. Rabinowitsch, D. Steffen, M. Sanders, J. Ma, Y. Kohara, S. Sharp, M. Simmonds, S. Spiegler, A. Tivey, S. Sugano, B. White, D. Walker, J. Woodward, T. Winckler, Y. Tanaka, G. Shaulsky, M. Schleicher, G. Weinstock, A. Rosenthal, E.C. Cox, R.L. Chisholm, R. Gibbs, W.F. Loomis, M. Platzer, R.R. Kay, J. Williams, P.H. Dear, A.A. Noegel, B. Barrell, and A. Kuspa. 2005. The genome of the social amoeba *Dictyostelium discoideum*. *Nature.* 435:43-57.
- Ellenberg, J., E.D. Siggia, J.E. Moreira, C.L. Smith, J.F. Presley, H.J. Worman, and J. Lippincott-Schwartz. 1997. Nuclear membrane dynamics and reassembly in living cells: targeting of an inner nuclear membrane protein in interphase and mitosis. *J Cell Biol.* 138:1193-206.
- Ewart-Toland, A., P. Briassouli, J.P. de Koning, J.H. Mao, J. Yuan, F. Chan, L. MacCarthy-Morrogh, B.A. Ponder, H. Nagase, J. Burn, S. Ball, M. Almeida, S. Linardopoulos, and A. Balmain. 2003. Identification of Stk6/STK15 as a candidate low-penetrance tumor-susceptibility gene in mouse and human. *Nat Genet.* 34:403-12.
- Fischer, J.A., S. Acosta, A. Kenny, C. Cater, C. Robinson, and J. Hook. 2004. *Drosophila* klarsicht has distinct subcellular localization domains for nuclear envelope and microtubule localization in the eye. *Genetics.* 168:1385-93.
- Fischer-Vize, J.A., and K.L. Mosley. 1994. Marbles mutants: uncoupling cell determination and nuclear migration in the developing *Drosophila* eye. *Development.* 120:2609-18.



- Franke, W.W., U. Scheer, G. Krohne, and E.D. Jarasch. 1981. The nuclear envelope and the architecture of the nuclear periphery. *J Cell Biol.* 91:39s-50s.
- Fridkin, A., E. Mills, A. Margalit, E. Neufeld, K.K. Lee, N. Feinstein, M. Cohen, K.L. Wilson, and Y. Gruenbaum. 2004. Matefin, a *Caenorhabditis elegans* germ line-specific SUN-domain nuclear membrane protein, is essential for early embryonic and germ cell development. *Proc Natl Acad Sci U S A.* 101:6987-92.
- Fukasawa, K. 2005. Centrosome amplification, chromosome instability and cancer development. *Cancer Lett.* 230:6-19.
- Gerace, L., and B. Burke. 1988. Functional organization of the nuclear envelope. *Annu Rev Cell Biol.* 4:335-74.
- Gough, L.L., J. Fan, S. Chu, S. Winnick, and K.A. Beck. 2003. Golgi localization of Syne-1. *Mol Biol Cell.* 14:2410-24.
- Grady, R.M., D.A. Starr, G.L. Ackerman, J.R. Sanes, and M. Han. 2005. Syne proteins anchor muscle nuclei at the neuromuscular junction. *Proc Natl Acad Sci U S A.* 102:4359-64.
- Greer, E.L., and A. Brunet. 2005. FOXO transcription factors at the interface between longevity and tumor suppression. *Oncogene.* 24:7410-25.
- Gruenbaum, Y., A. Margalit, R.D. Goldman, D.K. Shumaker, and K.L. Wilson. 2005. The nuclear lamina comes of age. *Nat Rev Mol Cell Biol.* 6:21-31.
- Guo, Y., S. Jangi, and M.A. Welte. 2005. Organelle-specific control of intracellular transport: distinctly targeted isoforms of the regulator Klar. *Mol Biol Cell.* 16:1406-16.
- Hagan, I., and M. Yanagida. 1995. The product of the spindle formation gene *sad1+* associates with the fission yeast spindle pole body and is essential for viability. *J Cell Biol.* 129:1033-47.
- Hanahan, D. 1983. Studies on transformation of *Escherichia coli* with plasmids. *J Mol Biol.* 166:557-80.
- Haque, F., D.J. Lloyd, D.T. Smallwood, C.L. Dent, C.M. Shanahan, A.M. Fry, R.C. Trembath, and S. Shackleton. 2006. SUN1 interacts with nuclear lamin A and cytoplasmic nesprins to provide a physical connection between the nuclear lamina and the cytoskeleton. *Mol Cell Biol.* 26:3738-51.
- Hasan, S., S. Guttinger, P. Muhlhauser, F. Anderegg, S. Burgler, and U. Kutay. 2006. Nuclear envelope localization of human UNC84A does not require nuclear lamins. *FEBS Lett.* 580:1263-8.
- Hedgecock, E.M., and J.N. Thomson. 1982. A gene required for nuclear and mitochondrial attachment in the nematode *Caenorhabditis elegans*. *Cell.* 30:321-30.
- Hodzic, D.M., D.B. Yeater, L. Bengtsson, H. Otto, and P.D. Stahl. 2004. Sun2 is a novel mammalian inner nuclear membrane protein. *J Biol Chem.* 279:25805-12.
- Hollander, M.C., and A.J. Fornace, Jr. 2002. Genomic instability, centrosome amplification, cell cycle checkpoints and Gadd45a. *Oncogene.* 21:6228-33.
- Holmer, L., and H.J. Worman. 2001. Inner nuclear membrane proteins: functions and targeting. *Cell Mol Life Sci.* 58:1741-7.
- Horton, H.R., Moran, L.A., Ochs, R.S., Rawn, D.J., Scrimgeour K.G. (2001). Principles of Biochemistry. 3rd Edition
- Horvitz, H.R., and J.E. Sulston. 1980. Isolation and genetic characterization of cell-lineage mutants of the nematode *Caenorhabditis elegans*. *Genetics.* 96:435-54.
- Iarmarcovai, G., A. Botta, and T. Orsiere. 2006. Number of centromeric signals in micronuclei and mechanisms of aneuploidy. *Toxicol Lett.* 166:1-10.
- Jaspersen, S.L., A.E. Martin, G. Glazko, T.H. Giddings, Jr., G. Morgan, A. Mushegian, and M. Winey. 2006. The Sad1-UNC-84 homology domain in Mps3 interacts with Mps2 to connect the spindle pole body with the nuclear envelope. *J Cell Biol.* 174:665-75.
- Keryer, G., B. Di Fiore, C. Celati, K.F. Lehtreck, M. Mogensen, A. Delouvee, P. Lavia, M. Bornens, and A.M. Tassin. 2003. Part of Ran is associated with AKAP450 at the centrosome: involvement in microtubule-organizing activity. *Mol Biol Cell.* 14:4260-71.
- Khodjakov, A., C.L. Rieder, G. Sluder, G. Cassels, O. Sibon, and C.L. Wang. 2002. De novo formation of centrosomes in vertebrate cells arrested during S phase. *J Cell Biol.* 158:1171-81.
- La Terra, S., C.N. English, P. Hergert, B.F. McEwen, G. Sluder, and A. Khodjakov. 2005. The de novo centriole assembly pathway in HeLa cells: cell cycle progression and centriole assembly/maturation. *J Cell Biol.* 168:713-22.



- Lee, K.K., D. Starr, M. Cohen, J. Liu, M. Han, K.L. Wilson, and Y. Gruenbaum. 2002. Lamin-dependent localization of UNC-84, a protein required for nuclear migration in *Caenorhabditis elegans*. *Mol Biol Cell*. 13:892-901.
- Lippincott-Schwartz, J., T.H. Roberts, and K. Hirschberg. 2000. Secretory protein trafficking and organelle dynamics in living cells. *Annu Rev Cell Dev Biol*. 16:557-89.
- Malone, C.J., W.D. Fixsen, H.R. Horvitz, and M. Han. 1999. UNC-84 localizes to the nuclear envelope and is required for nuclear migration and anchoring during *C. elegans* development. *Development*. 126:3171-81.
- Malone, C.J., L. Misner, N. Le Bot, M.C. Tsai, J.M. Campbell, J. Ahringer, and J.G. White. 2003. The *C. elegans* hook protein, ZYG-12, mediates the essential attachment between the centrosome and nucleus. *Cell*. 115:825-36.
- Mantel, C., S.E. Braun, S. Reid, O. Henegariu, L. Liu, G. Hangoc, and H.E. Broxmeyer. 1999. p21(cip-1/waf-1) deficiency causes deformed nuclear architecture, centriole overduplication, polyploidy, and relaxed microtubule damage checkpoints in human hematopoietic cells. *Blood*. 93:1390-8.
- McGee, M.D., R. Rillo, A.S. Anderson, and D.A. Starr. 2006. UNC-83 IS a KASH protein required for nuclear migration and is recruited to the outer nuclear membrane by a physical interaction with the SUN protein UNC-84. *Mol Biol Cell*. 17:1790-801.
- McKusick, V.A. 1985. Marcella O'Grady Boveri (1865-1950) and the chromosome theory of cancer. *J Med Genet*. 22:431-40.
- Meraldi, P., R. Honda, and E.A. Nigg. 2004. Aurora kinases link chromosome segregation and cell division to cancer susceptibility. *Curr Opin Genet Dev*. 14:29-36.
- Meraldi, P., J. Lukas, A.M. Fry, J. Bartek, and E.A. Nigg. 1999. Centrosome duplication in mammalian somatic cells requires E2F and Cdk2-cyclin A. *Nat Cell Biol*. 1:88-93.
- Mislow, J.M., M.S. Kim, D.B. Davis, and E.M. McNally. 2002. Myne-1, a spectrin repeat transmembrane protein of the myocyte inner nuclear membrane, interacts with lamin A/C. *J Cell Sci*. 115:61-70.
- Monnat, J., U. Hacker, H. Geissler, R. Rauchenberger, E.M. Neuhaus, M. Maniak, and T. Soldati. 1997. Dictyostelium discoideum protein disulfide isomerase, an endoplasmic reticulum resident enzyme lacking a KDEL-type retrieval signal. *FEBS Lett*. 418:357-62.
- Morris, N.R. 2000. Nuclear migration. From fungi to the mammalian brain. *J Cell Biol*. 148:1097-101.
- Newport, J.W., and D.J. Forbes. 1987. The nucleus: structure, function, and dynamics. *Annu Rev Biochem*. 56:535-65.
- Nigg, E.A. 2006. Origins and consequences of centrosome aberrations in human cancers. *Int J Cancer*. 119:2717-23.
- Niwa, O., M. Shimanuki, and F. Miki. 2000. Telomere-led bouquet formation facilitates homologous chromosome pairing and restricts ectopic interaction in fission yeast meiosis. *Embo J*. 19:3831-40.
- Noegel, A.A., R. Blau-Wasser, H. Sultana, R. Muller, L. Israel, M. Schleicher, H. Patel, and C.J. Weijer. 2004. The cyclase-associated protein CAP as regulator of cell polarity and cAMP signaling in Dictyostelium. *Mol Biol Cell*. 15:934-45.
- Ohba, T., E.C. Schirmer, T. Nishimoto, and L. Gerace. 2004. Energy- and temperature-dependent transport of integral proteins to the inner nuclear membrane via the nuclear pore. *J Cell Biol*. 167:1051-62.
- Ostlund, C., J. Ellenberg, E. Hallberg, J. Lippincott-Schwartz, and H.J. Worman. 1999. Intracellular trafficking of emerin, the Emery-Dreifuss muscular dystrophy protein. *J Cell Sci*. 112 (Pt 11):1709-19.
- Padmakumar, V.C., T. Libotte, W. Lu, H. Zaim, S. Abraham, A.A. Noegel, J. Gotzmann, R. Foisner, and I. Karakesisoglou. 2005. The inner nuclear membrane protein Sun1 mediates the anchorage of Nesprin-2 to the nuclear envelope. *J Cell Sci*. 118:3419-30.
- Patterson, K., A.B. Molofsky, C. Robinson, S. Acosta, C. Cater, and J.A. Fischer. 2004. The functions of Klarsicht and nuclear lamin in developmentally regulated nuclear migrations of photoreceptor cells in the *Drosophila* eye. *Mol Biol Cell*. 15:600-10.
- Piperno, G., and M.T. Fuller. 1985. Monoclonal antibodies specific for an acetylated form of alpha-tubulin recognize the antigen in cilia and flagella from a variety of organisms. *J Cell Biol*. 101:2085-94.



- Prasanth, S.G., K.V. Prasanth, K. Siddiqui, D.L. Spector, and B. Stillman. 2004. Human Orc2 localizes to centrosomes, centromeres and heterochromatin during chromosome inheritance. *Embo J.* 23:2651-63.
- Prasanth, S.G., K.V. Prasanth, and B. Stillman. 2002. Orc6 involved in DNA replication, chromosome segregation, and cytokinesis. *Science.* 297:1026-31.
- Reinsch, S., and P. Gonczy. 1998. Mechanisms of nuclear positioning. *J Cell Sci.* 111 (Pt 16):2283-95.
- Rivero, F., A. Kuspa, R. Brokamp, M. Matzner, and A.A. Noegel. 1998. Interaptin, an actin-binding protein of the alpha-actinin superfamily in Dictyostelium discoideum, is developmentally and cAMP-regulated and associates with intracellular membrane compartments. *J Cell Biol.* 142:735-50.
- Rosenberg-Hasson, Y., M. Renert-Pasca, and T. Volk. 1996. A Drosophila dystrophin-related protein, MSP-300, is required for embryonic muscle morphogenesis. *Mech Dev.* 60:83-94.
- Shang, Y., C.C. Tsao, and M.A. Gorovsky. 2005. Mutational analyses reveal a novel function of the nucleotide-binding domain of gamma-tubulin in the regulation of basal body biogenesis. *J Cell Biol.* 171:1035-44.
- Simpson, P.A., J.A. Spudich, and P. Parham. 1984. Monoclonal antibodies prepared against Dictyostelium actin: characterization and interactions with actin. *J Cell Biol.* 99:287-95.
- Siu, C.H., T.J. Harris, J. Wang, and E. Wong. 2004. Regulation of cell-cell adhesion during Dictyostelium development. *Semin Cell Dev Biol.* 15:633-41.
- Smith, S., and G. Blobel. 1993. The first membrane spanning region of the lamin B receptor is sufficient for sorting to the inner nuclear membrane. *J Cell Biol.* 120:631-7.
- Soullam, B., and H.J. Worman. 1993. The amino-terminal domain of the lamin B receptor is a nuclear envelope targeting signal. *J Cell Biol.* 120:1093-100.
- Soullam, B., and H.J. Worman. 1995. Signals and structural features involved in integral membrane protein targeting to the inner nuclear membrane. *J Cell Biol.* 130:15-27.
- Starr, D.A., and M. Han. 2002. Role of ANC-1 in tethering nuclei to the actin cytoskeleton. *Science.* 298:406-9.
- Starr, D.A., and M. Han. 2005. A genetic approach to study the role of nuclear envelope components in nuclear positioning. *Novartis Found Symp.* 264:208-19; discussion 219-230.
- Starr, D.A., G.J. Hermann, C.J. Malone, W. Fixsen, J.R. Priess, H.R. Horvitz, and M. Han. 2001. unc-83 encodes a novel component of the nuclear envelope and is essential for proper nuclear migration. *Development.* 128:5039-50.
- Storchova, Z., A. Breneman, J. Cande, J. Dunn, K. Burbank, E. O'Toole, and D. Pellman. 2006. Genome-wide genetic analysis of polyploidy in yeast. *Nature.* 443:541-7.
- Sulston, J.E., and H.R. Horvitz. 1981. Abnormal cell lineages in mutants of the nematode *Caenorhabditis elegans*. *Dev Biol.* 82:41-55.
- Tarapore, P., H.F. Horn, Y. Tokuyama, and K. Fukasawa. 2001. Direct regulation of the centrosome duplication cycle by the p53-p21Waf1/Cip1 pathway. *Oncogene.* 20:3173-84.
- Tzur, Y.B., K.L. Wilson, and Y. Gruenbaum. 2006. SUN-domain proteins: 'Velcro' that links the nucleoskeleton to the cytoskeleton. *Nat Rev Mol Cell Biol.* 7:782-8.
- Volk, T. 1992. A new member of the spectrin superfamily may participate in the formation of embryonic muscle attachments in Drosophila. *Development.* 116:721-30.
- Walenta, J.H., A.J. Didier, X. Liu, and H. Kramer. 2001. The Golgi-associated hook3 protein is a member of a novel family of microtubule-binding proteins. *J Cell Biol.* 152:923-34.
- Wallraff, E., M. Schleicher, M. Modersitzki, D. Rieger, G. Isenberg, and G. Gerisch. 1986. Selection of Dictyostelium mutants defective in cytoskeletal proteins: use of an antibody that binds to the ends of alpha-actinin rods. *Embo J.* 5:61-7.
- Warren, D.T., Q. Zhang, P.L. Weissberg, and C.M. Shanahan. 2005. Nesprins: intracellular scaffolds that maintain cell architecture and coordinate cell function? *Expert Rev Mol Med.* 7:1-15.
- Watson, M.L. 1955. The nuclear envelope; its structure and relation to cytoplasmic membranes. *J Biophys Biochem Cytol.* 1:257-70.
- Wilhelmsen, K., M. Ketema, H. Truong, and A. Sonnenberg. 2006. KASH-domain proteins in nuclear migration, anchorage and other processes. *J Cell Sci.* 119:5021-9.



- Wilhelmsen, K., S.H. Litjens, I. Kuikman, N. Tshimbalanga, H. Janssen, I. van den Bout, K. Raymond, and A. Sonnenberg. 2005. Nesprin-3, a novel outer nuclear membrane protein, associates with the cytoskeletal linker protein plectin. *J Cell Biol.* 171:799-810.
- Williams, K.L., and P.C. Newell. 1976. A genetic study of aggregation in the cellular slime mould *Dictyostelium discoideum* using complementation analysis. *Genetics.* 82:287-307.
- Worman, H.J., and J.C. Courvalin. 2000. The inner nuclear membrane. *J Membr Biol.* 177:1-11.
- Yu, J., D.A. Starr, X. Wu, S.M. Parkhurst, Y. Zhuang, T. Xu, R. Xu, and M. Han. 2006. The KASH domain protein MSP-300 plays an essential role in nuclear anchoring during *Drosophila* oogenesis. *Dev Biol.* 289:336-45.
- Zhang, Q., C. Ragnauth, M.J. Greener, C.M. Shanahan, and R.G. Roberts. 2002. The nesprins are giant actin-binding proteins, orthologous to *Drosophila melanogaster* muscle protein MSP-300. *Genomics.* 80:473-81.
- Zhang, Q., J.N. Skepper, F. Yang, J.D. Davies, L. Hegyi, R.G. Roberts, P.L. Weissberg, J.A. Ellis, and C.M. Shanahan. 2001. Nesprins: a novel family of spectrin-repeat-containing proteins that localize to the nuclear membrane in multiple tissues. *J Cell Sci.* 114:4485-98.
- Zhen, Y.Y., T. Libotte, M. Munck, A.A. Noegel, and E. Korenbaum. 2002. NUANCE, a giant protein connecting the nucleus and actin cytoskeleton. *J Cell Sci.* 115:3207-22.
- Zhu, J., E.C. Beattie, Y. Yang, H.J. Wang, J.Y. Seo, and L.X. Yang. 2005. Centrosome impairments and consequent cytokinesis defects are possible mechanisms of taxane drugs. *Anticancer Res.* 25:1919-25.



8 Table of figures

FIGURE 1: COMPOSITION OF THE NUCLEAR ENVELOPE IN EUKARYOTIC CELLS.	1
FIGURE 2: PROPOSED MODEL FOR NUCLEAR POSITIONING AND MIGRATION.	4
FIGURE 3: PHYLOGENY OF SUN DOMAIN PROTEINS (JASPERSEN ET AL., 2006).	9
FIGURE 4: DEVELOPMENT OF <i>D. DISCOIDEUM</i> FROM SINGLE-CELL AMEBA INTO THE MULTICELLULAR FRUITING BODIES (COURTESY OF M. GRIMSON, R. BLANTON, TEXAS TECH UNIVERSITY).	12
FIGURE 5: PRIMARY STRUCTURE OF SUN-1 AND SUN-2 IN <i>D. DISCOIDEUM</i>	28
FIGURE 6: SEQUENCE HOMOLOGY OF SUN DOMAINS OF <i>D. DISCOIDEUM</i> SUN-1, HUMAN SUN-1, <i>S. POMBE</i> SAD1, <i>C. ELEGANS</i> SUN-1 AND UNC-84, <i>D. DISCOIDEUM</i> SUN-2, <i>S. CEREVISIAE</i> SLP1P, <i>S. POMBE</i> SLP1P, <i>D. MELANOGASTER</i> Q7YU09 AND <i>O. SATIVA</i> Q8LJA6.	30
FIGURE 7: GENERATION OF MONOCLONAL ANTIBODIES AGAINST SUN-1.	31
FIGURE 8: SCREENINGS OF MONOCLONAL ANTIBODIES AGAINST SUN-1.	33
FIGURE 9: LOCALIZATION OF SUN-1 TO THE NUCLEAR COMPARTMENT.	35
FIGURE 10: SUN-1 IS A PUTATIVE INTEGRAL NUCLEAR MEMBRANE PROTEIN.	37
FIGURE 11: RECOMBINANT SUNCT1 FORMS OLIGOMERS IN VITRO.	39
FIGURE 12: PULLDOWN EXPERIMENT USING GST-SUNCT1.	42
FIGURE 13: THE C-TERMINUS OF SUN-1 IS LOCATED IN THE PERINUCLEAR SPACE (PNS).	44
FIGURE 14: CHROMATIN IMMUNOPRECIPITATION (CHIP)..	46
FIGURE 15: MULTIPLE ALIGNMENTS OF C-TERMINAL TAIL SEQUENCES OF INTERAPTIN AND KASH DOMAIN PROTEINS.	48
FIGURE 16: SUN-1 AND INTERAPTIN ARE INDEPENDENTLY EXPRESSED IN AX2.	50
FIGURE 17: SUBCELLULAR LOCALIZATION OF SUN-1 IN AX2 CELLS	52
FIGURE 18: LOCALIZATION OF KASH MOTIF MUTANTS IN AX2 CELLS.	54
FIGURE 19: KASH DOMAIN OF INTERAPTIN IS CAPABLE TO DISPLACE THE ENDOGENOUS SUN-1 FROM THE NUCLEAR ENVELOPE.	56
FIGURE 20: GFP- Δ SUN-1 CAUSED NUCLEAR ENVELOPE DEFORMATIONS.	58
FIGURE 21: GFP- Δ SUN-1 CELLS EXHIBITED ANEUPLOIDY.	60
FIGURE 22: GFP- Δ SUN-1 WAS ACCUMULATED IN THE ONM.	63
FIGURE 23: ELECTRON MICROGRAPH OF A NUCLEUS ISOLATED FROM GFP- Δ SUN1 EXPRESSING CELLS.	64
FIGURE 24: GFP- Δ SUN-1 CELLS FORM NUCLEAR ENVELOPE PROTRUSIONS DISASSOCIATING THE NUCLEUS-CENTROSOME PROXIMITY.	67
FIGURE 25: GFP- Δ SUN-1 EXPRESSION ABROGATED THE PROXIMITY BETWEEN THE NUCLEUS AND CENTROSOME.	69
FIGURE 26: IMBALANCE OF NUCLEUS AND CENTROSOME RATIO.	71
FIGURE 27: LIVE-CELL IMAGING OF GFP-INTCT EXPRESSING CELLS.	73
FIGURE 28: NUCLEI IN GFP- Δ SUN-1 CELLS EXPERIENCE HIGHER MECHANICAL STRESS DURING INTRACELLULAR MOVEMENT.	74
FIGURE 29: PROPOSED MODEL FOR THE FUNCTION OF SUN-1 IN THE INM.	92



9 Appendix

General abbreviations

%	Percent
°	Degree
∅	Diameter
A	Ampere or nucleotide Adenosine
aa	Amino acid(s)
Amp	Ampicilline
APS	Ammonium persulfate
Aqua dest.	<i>Aqua destillata</i> , distilled water
ATP	Adenosine triphosphat
bp	Base pair(s)
BSA	Bovine serum albumine
C	Celsius or nucleotide Cytosine
ca.	Circa, approximately
CIP	Calf intestine alkaline phosphatase
cm	centimeter
DMEM	Dulbecco's Modified Eagle Medium
DMSO	Dimethylsulfoxide
DNA	Deoxyribonucleic acid
dNTP	Desoxyribonucleotidetriphosphat
DTT	Dithiothreitol
<i>E. coli</i>	<i>Escherichia coli</i>
EDTA	Ethylen-Diamine-Tetra-acetate
rER	Rough endoplasmatic retikulum
EtBr	Ethidiumbromide
EtOH	Ethanol
FCS	Fetal calf serum)
G	Glycine or nucleotide guanosin
g	Gramm
<i>g</i>	Relative centrifugation force
GFP	Green fluorescence protein of <i>Aequorea victoria</i>
hr	Hour(s)
HEPES	N-(2-Hydroxyethyl)piperazin-N'-2-ethansulfonsäure
INM	Inner nuclear membrane
KASH	<u>K</u> larsicht/ <u>A</u> nc-1/ <u>S</u> yne homology
kDa	Isopropyl-β-D-thiogalaktopyranoside
kb	Kilo base
kDa	Kilo dalton
λ	Wave length
M	Molar
mAb	Monoclonal antibody
MDa	Megadalton
min	Minute



µg	Microgramm
ml	Milliliter
µm	Micrometer
µl	Microliter
mM	Millimolar
mRNA	Messenger Ribonucleic acid
NE	Nuclear envelope
ng	Nanogramm
nm	Nanometer
ONM	Outer nuclear membrane
ORF	Open reading frame
ori	Origine of replication
pAb	Polyclonal antibody
PAGE	Polyacrylamide gel electrophoresis
PBS	Phosphat buffered saline
PCR	Polymerase chain reaction
PNS	Perinuclear space
RNA	Ribonucleic acid
rpm	Rounds per minute
RT	Room temperature
SDS	Sodium dodecyl sulfate
sec	Second
SUN	<u>Sad1/UNC-84</u> homology
TAE	Tris-Acetate-EDTA
<i>Taq</i>	<i>Thermus aquaticus</i>
TBE	Tris-Borate-EDTA
TE	Tris-EDTA
TEMED	N,N,N',N'-Tetramethyl-ethylendiamin
Tris	Trishydroxyaminomethan
U	Unit
UV	Ultraviolet light
V	Volt
v/v	Volume per volume
w/v	Weight per volume
X-Gal	5-Bromo-4-chlor-3-indolyl-β-D-galactopyranoside

Eidesstattliche Erklärung

Hiermit erkläre ich, daß die von mir vorgelegte Dissertation selbständig angefertigt, die benutzten Quellen und Hilfsmittel vollständig angegeben und die Stellen der Arbeit, einschließlich Tabellen und Abbildungen, die anderen Werke im Wortlaut oder dem Sinn nach entnommen sind, in jedem Einzelfall als Entlehnung kenntlich gemacht habe; zudem, daß diese Dissertation noch keiner anderen Fakultät oder Universität zur Prüfung vorgelegen hat; daß sie noch nicht veröffentlicht ist und ich eine Veröffentlichung vor Abschluß des Promotionsverfahrens nicht vornehmen werde.

Die Bestimmungen der Promotionsordnung sind mir bekannt. Die von mir vorgelegte Dissertation ist von Frau Prof. Dr. Angelika A. Noegel betreut worden.

Köln, den 14. Feb. 2007 **Huajiang Xiong**

Curriculum vitae

Personal details

Name Huajiang Xiong
Date of Birth June 30th 1977,
Place of birth Chang Chun, V.R. China
Nationality Chinese
Current address Bruesseler Strasse 43, 50674 Cologne, Germany
eMail deinehu@yahoo.de

Scientific education

PhD studies

Oct 2006 – Feb 2007 Faculty of Mathematics and Natural Science,
University of Cologne,
Supervisor: Prof Dr Angelika A. Noegel
Center for Biochemistry, Medical Faculty, Joseph-
Stelman-Str. 52, D50931 Cologne, Germany

Sept 2003 – Sept 2006 PhD fellowship funded by “International Graduate
School in Genetics and Functional Genomics”,
University of Cologne, Germany
Title: Sun-1, a regulator of the nuclear shape in *D.*
discoideum
Supervisor: Prof Dr Angelika A. Noegel

Diploma studies

Sept 2000 – Mar 2003 Diploma thesis in Biology (equivalent to M.Sc.)
Johann Wolfgang Goethe University,
Frankfurt/Main, Germany
Title: Generation of expression vectors for
secretory multimeric peptides inhibiting HIV-1
fusion with target cells (A)
Supervisors: Prof Dr Anna Starzinski-Powitz, Dr
Ursula Dietrich, Prof Dr Dorothee M. von Laer

June 2000 – July 2000 Diploma exams in Biology
Johann Wolfgang Goethe University,
Frankfurt/Main, Germany
Principle subjects:
Genetics (A), Plant physiology (A), Cell and
developmental Biology (A)

Sept 1998 – June 2000 Basics in Biology
Johann Wolfgang Goethe University,
Frankfurt/Main, Germany

Languages Chinese, German, English, French, Latin

Lebenslauf

Name Huajiang Xiong
Geburtsdatum 30. Juni 1977
Geburtsort Chang Chun, V.R. China
Nationalität Chinesisch
Aktuelle Adresse Bruesseler Strasse 43, 50674 Cologne, Germany
eMail deinehu@yahoo.de

Bildung

Promotionsstudium

Okt 2006 – Feb 2007 Mathematisch-naturwissenschaftliche Fakultät,
Universität zu Köln,
Betreuerin: Prof. Dr. Angelika A. Noegel

Sept 2003 – Sept 2006 Stipendiatin der "International Graduate School in
Genetics and Functional Genomics", Universität zu
Köln
Titel: Sun-1, a regulator of the nuclear shape in *D.*
discoideum
Betreuerin: Prof. Dr. Angelika A. Noegel
Zentrum für Biochemie, Medizinische Fakultät,
Joseph-Stelman-Str. 52, D50931Cologne

Diplomstudium

Sept 2000 – März 2003 Diplomarbeit in Biologie
Johann Wolfgang Goethe Universität,
Frankfurt/Main
Titel: Herstellung von Expressionsvektoren für
secretorische multimere Peptide zur Inhibitiion von
HIV-1 Fusion mit Zielzellen (Note 1.1)
Betreuerinnen: Prof. Dr. Anna Starzinski-Powitz,
Dr. Ursula Dietrich, Prof. Dr. Dorothee M. von Laer

Juni 2000 – Juli 2000 Diplomprüfungen
Johann Wolfgang Goethe Universität,
Frankfurt/Main
Hauptfächer:
Genetik (1.0), Pflanzenphysiologie (1.3), Zell- und
Entwicklungsbiologie (1.0)

Sept 1998 – Juni 2000 Grundstudium Biologie (Diplom)
Johann Wolfgang Goethe Universität,
Frankfurt/Main

Sprachkenntnisse Chinesisch, Deutsch, Englisch, Französisch, Latein